Cheiron School, SPring-8, Japan
October 2, 2014

Studies on atoms and molecules using synchrotron radiation and free electron lasers

Kiyoshi Ueda
Institute of multidisciplinary research for advanced materials
Tohoku University, Sendai 980-8577, Japan

Introduction of myself

Prof. Kiyoshi Ueda
at
Tohoku University（Sendai）
Institute of multidisciplinary research for advanced materials

Leading
a research group for electron and molecular dynamics

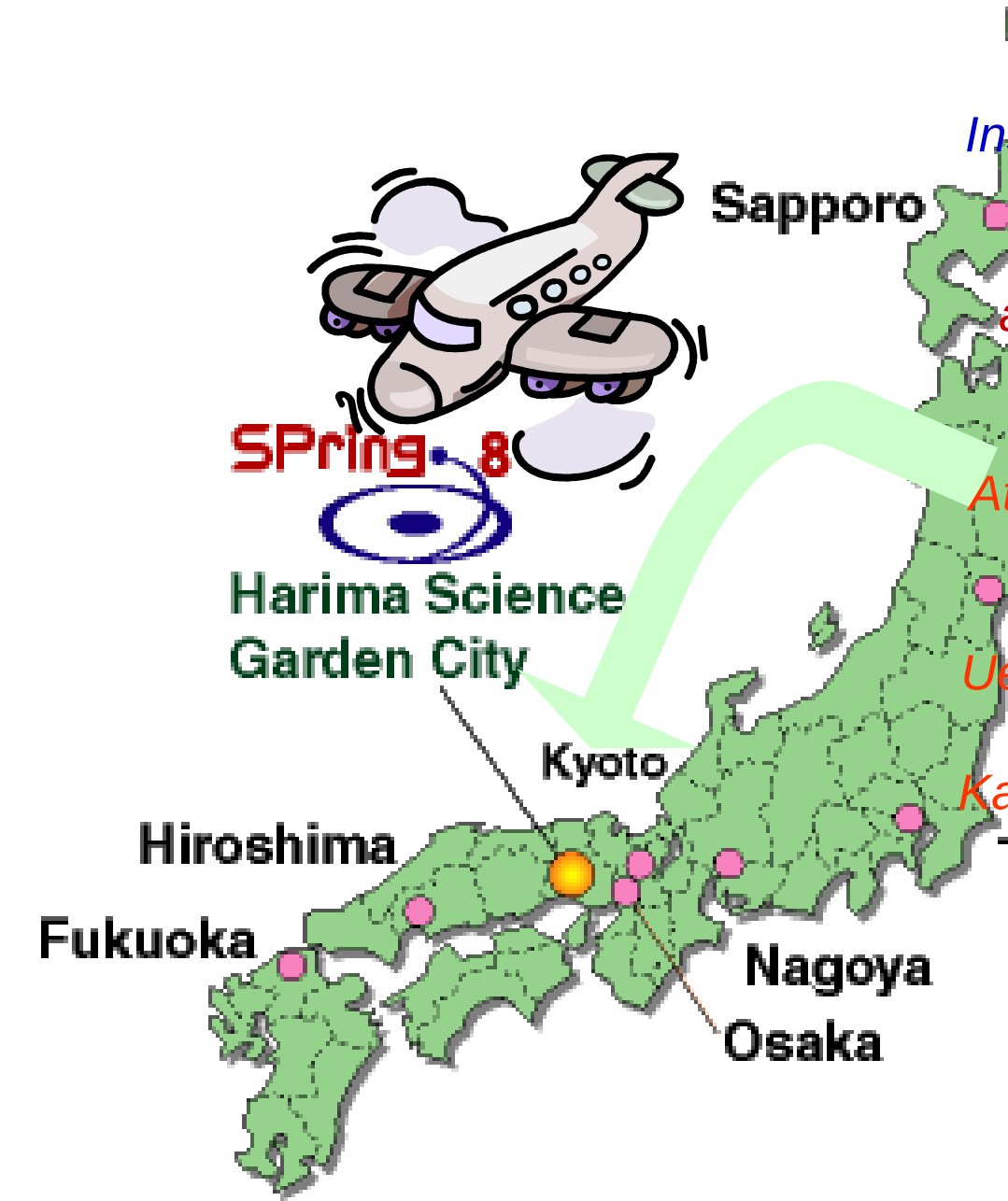

Atomic and molecular science using Synchrotron Radiation
Ueda, JPB 36, R1 (2003);
Ueda & Eland, JPB 38, S839 (2005);
Ueda, JPSJ 75, 032001 (2006);
Kabachnik et al. PR 451, 155 (2007).

Application of the SR-based experimental techniques to laser experiments
(femtosecond laser and FEL)

Outline

1. Introduction to quantum world

2. Atomic resonant photoemission spectroscopy

- Introduction to the quantum interference

3. Vibrationally-resolved core-level photoelectron spectroscopy

- Adiabatic approximation and Franck-Condon analysis

- Young's double-slit experiments

4. Multiple-ion momentum imaging

- Snapshots of molecular deformation within a few fs

5. Electron-ion momentum imaging

- Molecular-frame photoelectron angular distributions

6. Interatomic Coulombic decay

7. Characteristic properties of free electron lasers

8. Atomic multi-photon processes by FEL: from EUV to X

Photoelectric effect

When matter is shined by the light, electron is emitted from the surface.

(i) Frequency of the light needs to be larger than ν_0.
(ii) Kinetic energy of the electron is determined by the frequency of the light.
(iii) Number of electrons is proportional to the intensity of the light.

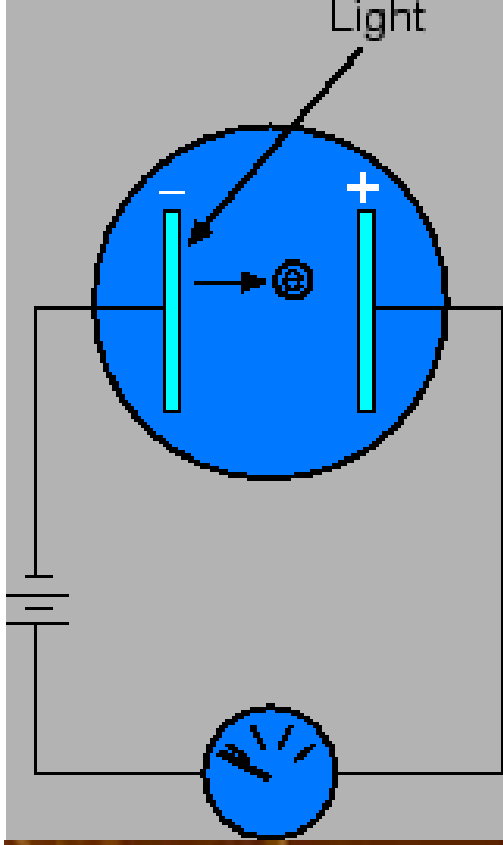

Einstein's explanation

Light at frequency of ν is considered to be a group of particles (photons) and each photon has energy $h\nu$.
An electron gets the energy $h\nu$ when it absorb one photon.
The electron in the matter is bound. For the electron to be emitted from the matter, the electron needs to receive the energy more than the work function *W.*
Then the kinetic energy *KE* of the emitted electron can be given as $KE = h\nu - W$.

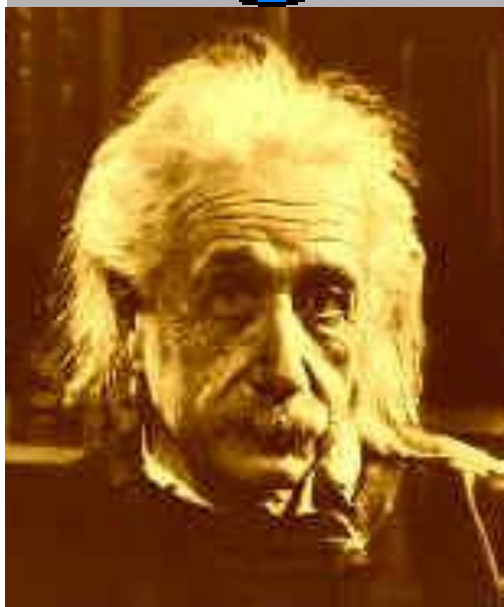

Photoelectron spectroscopy (UPS, XPS)

Precision measurements for kinetic energies of photoelectrons emitted via Einstein's photoelectric effects

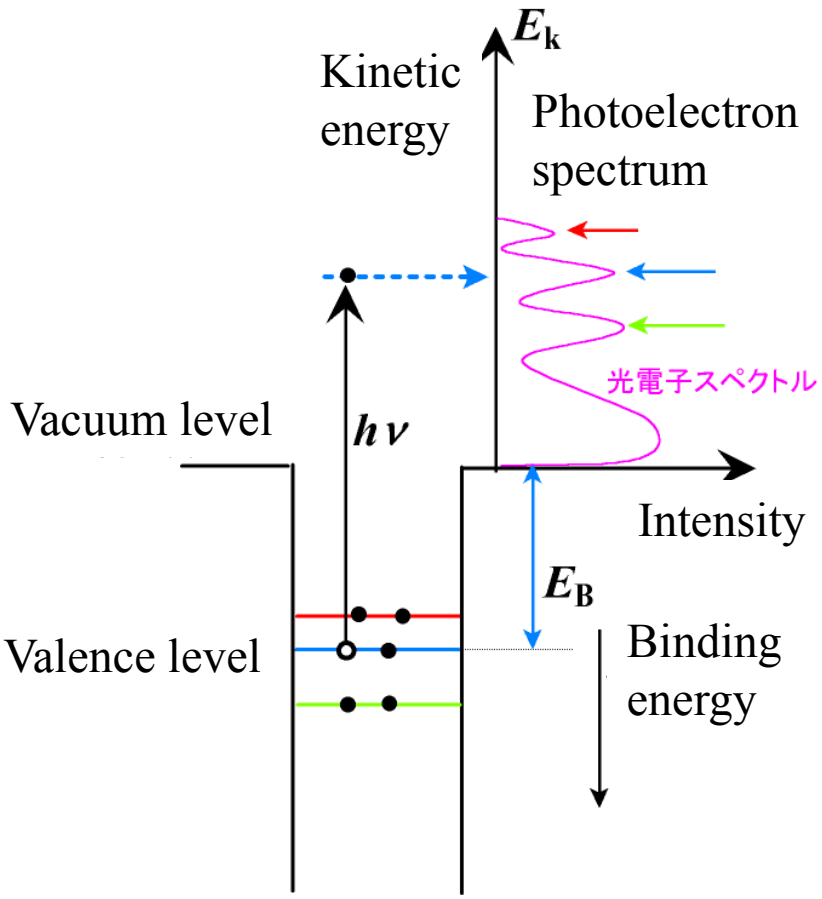

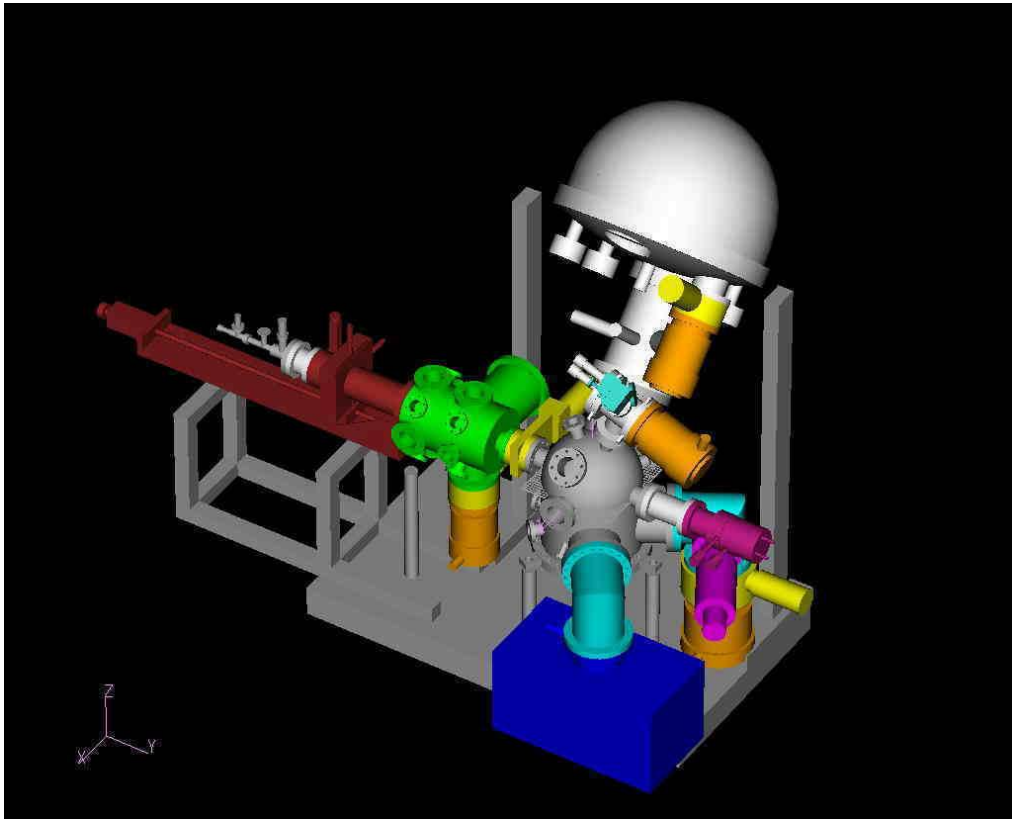

Balmer and Rydberg formulae

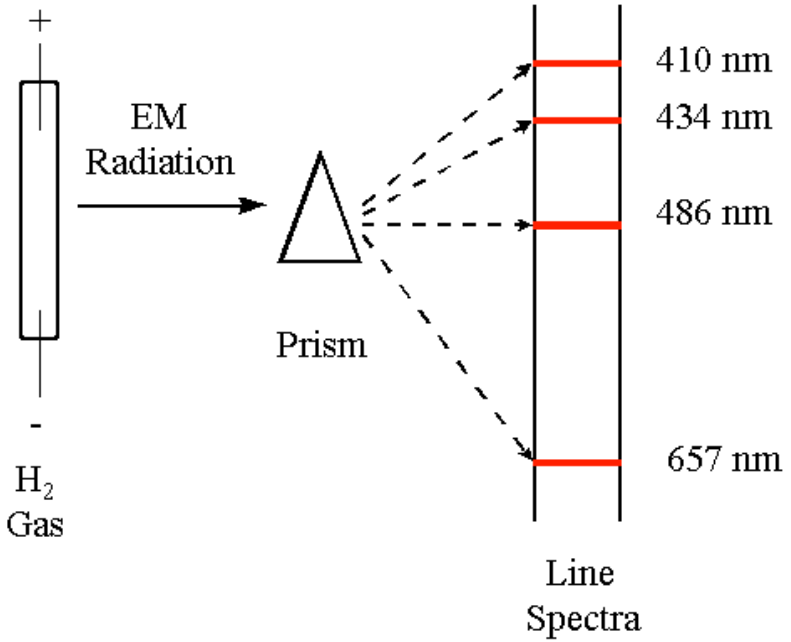

Hydrogen Spectrum: Balmer series

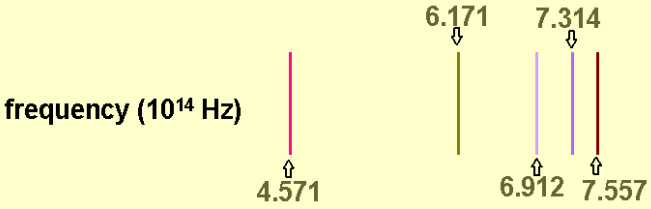

Balmer Formula: $\nu = \nu_0 \left((1/n^2) - (1/m^2) \right)$

$32.91 \left(1/4 - 1/9 \right) = 4.571$

$32.91 \left(1/4 - 1/16 \right) = 6.171$

$32.91 \left(1/4 - 1/25 \right) = 6.911$

$32.91 \left(1/4 - 1/36 \right) = 7.313$

$32.91 \left(1/4 - 1/49 \right) = 7.556$

IT WORKS!

Balmer found beautiful regularity in the H spectrum!

Rydberg formula: $$\frac{\nu}{c} = \frac{1}{\lambda} = R\left(\frac{1}{n^2} - \frac{1}{n'^2} \right)$$

c, speed of light; λ, wavelength; *R*, Rydberg constant (*R* =109737.309 cm^{-1})

Bohr's atomic model

Electron orbits exist only when the classical orbits satisfy the following condition of quantization:

$$\int_0^{2\pi} p_\varphi \, \mathrm{d}\varphi = nh$$

φ, angle of rotation; $p_\varphi = m_e r^2 d\varphi / \mathrm{d}t$, angular momentum; r, radius; m_e, electron mass

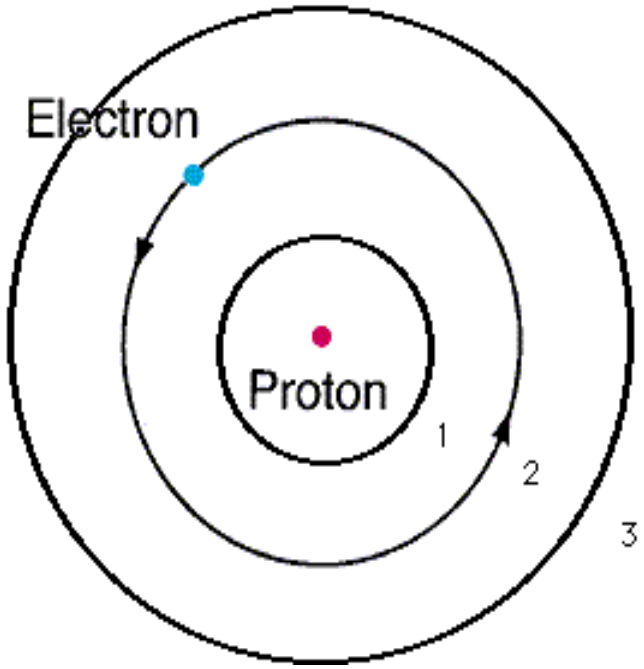

The electron binding energies are discrete:

$$\bar{E}_n = -hcR/n^2$$

De Broglie's matter wave and Bohr's model

$$Quantization\ :\ \int_0^{2\pi} p_\varphi \, \mathrm{d}\varphi = nh$$

$\lambda = h/p$ $\qquad$ $2\pi r_n = n\lambda = nh/p = nh/mv$

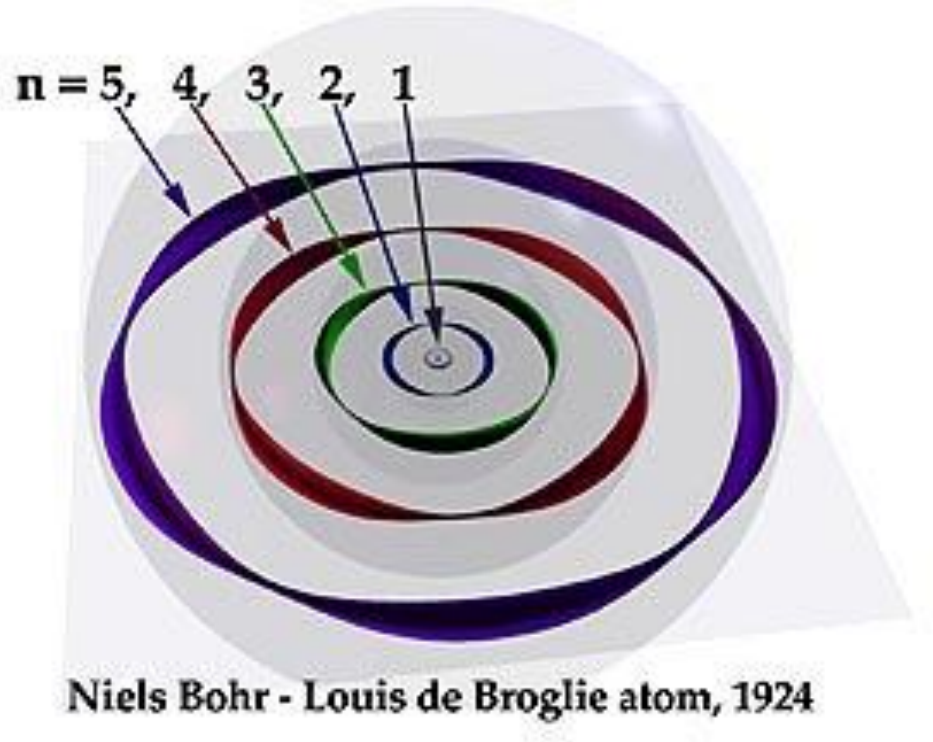

Niels Bohr - Louis de Broglie atom, 1924

Schrödinger equation of H atom (in atomic units)

$$H\Psi(r) = E\Psi(r)$$

$$H = T + U(r)$$ Hamiltonian

$$T = \frac{p^2}{2} = -\frac{1}{2}\frac{\partial^2}{\partial r^2}$$ kinetic energy

$$p = i\frac{\partial}{\partial r}$$ momentum

$$U(r) = -\frac{1}{r}$$ potential energy

$$E_n = -\frac{1}{2n^2}$$

Ψ: wave function
complex number (with phase!)

Atomic and molecular science now

Target: single atom or molecule; size: ~ 1 Å (= 0.1 nm = 10^{-10} m)

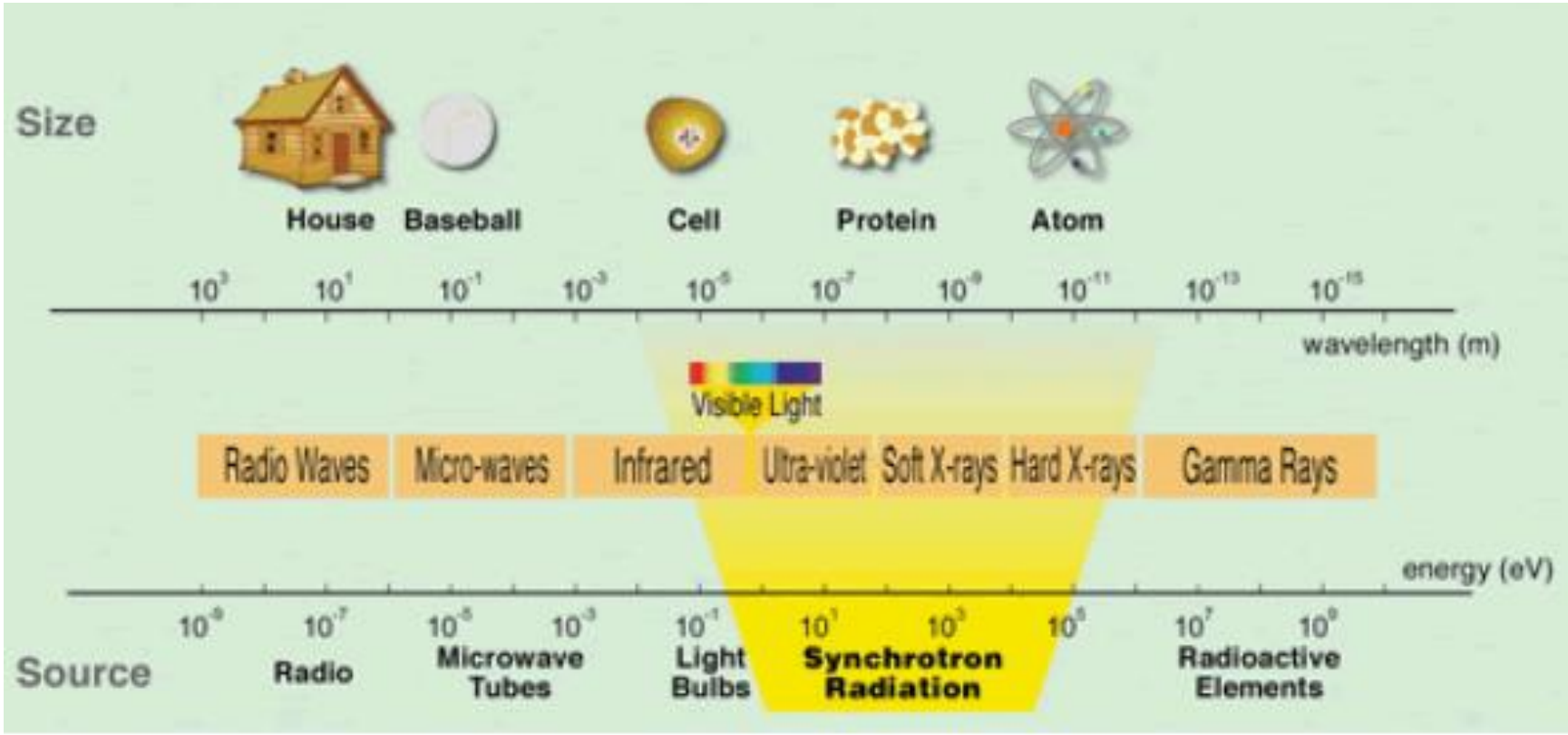

How to use synchrotron radiation to study atoms and molecules

We use monochromatic synchrotron radiation to excite atoms and molecules and to study their electronic structures as well as electron and nuclear dynamics in the excited states.

A single photon should be absorbed by a single atom or molecule first!

What photon energies to be used

Electron binding energies (eV) *Vacuum ultraviolet light!*

Element	K 1s	L_1 2s	L_2 $2p_{1/2}$	L_3 $2p_{3/2}$
1 H	13.6			
2 He	24.6*			
3 Li	54.7*			
4 Be	111.5*			
5 B	188*			
6 C	284.2*			
7 N	409.9*	37.3*		
8 O	543.1*	41.6*		
9 F	696.7*			
10 Ne	870.2*	48.5*	21.7*	21.6*

The experiments need to be in the vacuum!

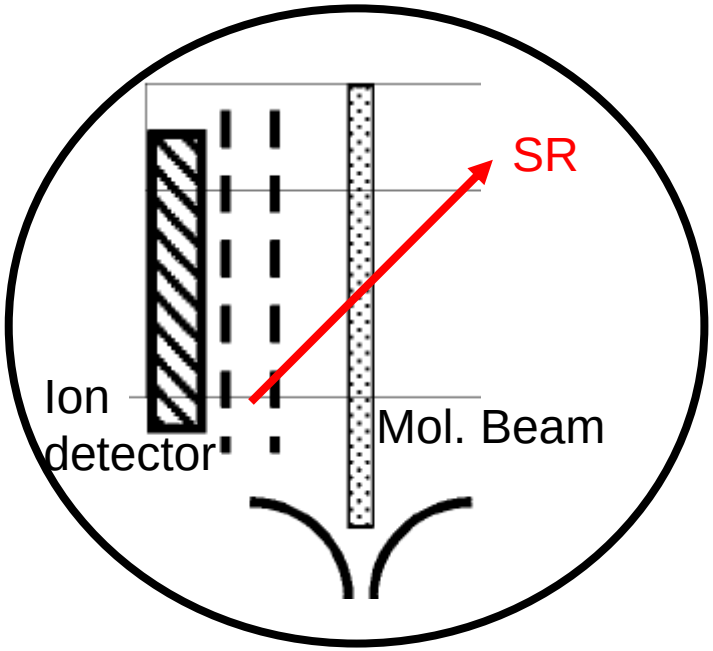

The easiest experiment: ion yield spectroscopy

SPring-8 BL27SU

Figure-8 undulator

- Linearly polarized light
- Horizontal polarization (1st)
- Vertical polarization (0.5th)

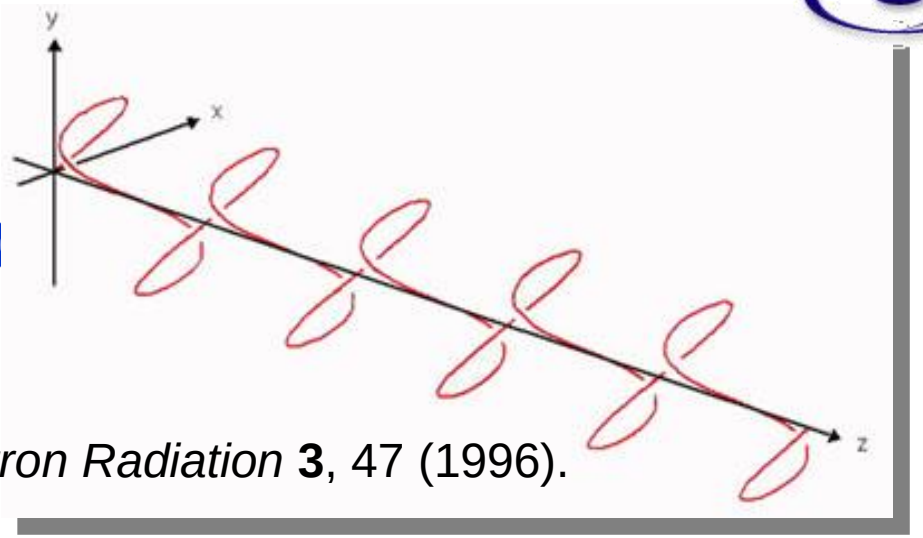

T. Tanaka and H. Kitamura, *J. Synchrotron Radiation* **3**, 47 (1996).

Soft X-ray monochromator

- Hettrick type: varied line spacing plane grating

Energy range	0.15 ~ 2.5 keV
Photon Flux	> 10^{11} photon/s
Energy resolution	10000 - 20000

H. Ohashi, Y. Tamenori, E. Ishiguro *et al*. *Nucl. Instr. Methods A* **467**, 533 (2001).

Ne 1s total ion yield spectrum

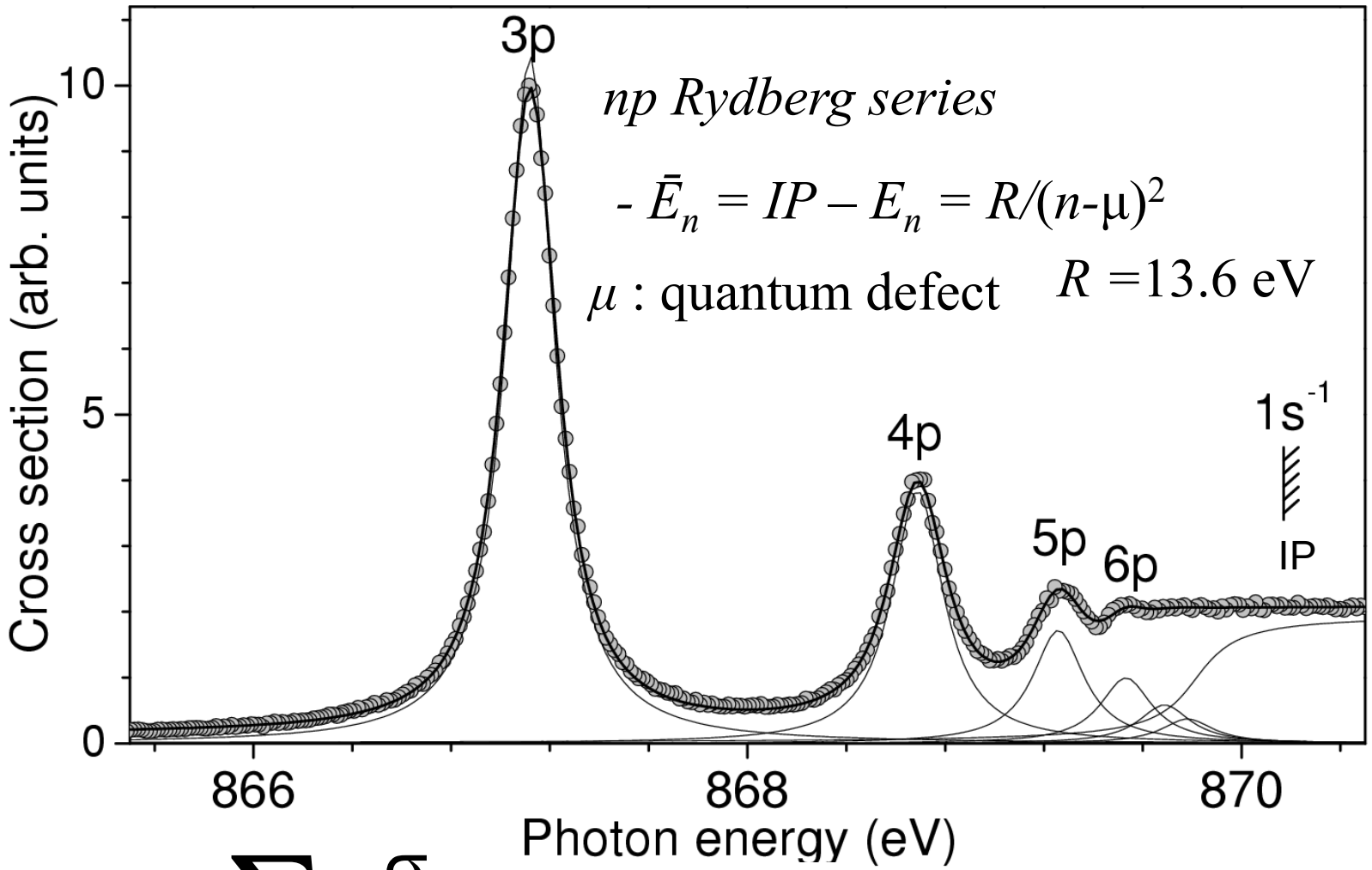

$$\sigma = \sigma_{dir} + \sum_n \frac{\sigma_n}{1+\varepsilon_n^2} + \sigma_{1s} \qquad \varepsilon = (h\nu\text{-}E_n)/(\Gamma_n/2)$$

$$\sigma_n \propto 1/(n-\mu)^3 \qquad \Gamma_n = \text{const!}$$

Auger decay and Auger electron spectroscopy

(a) Core ionization

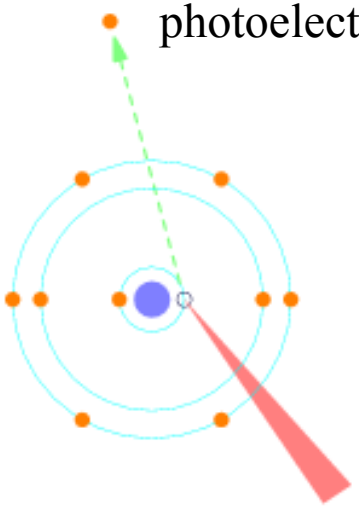

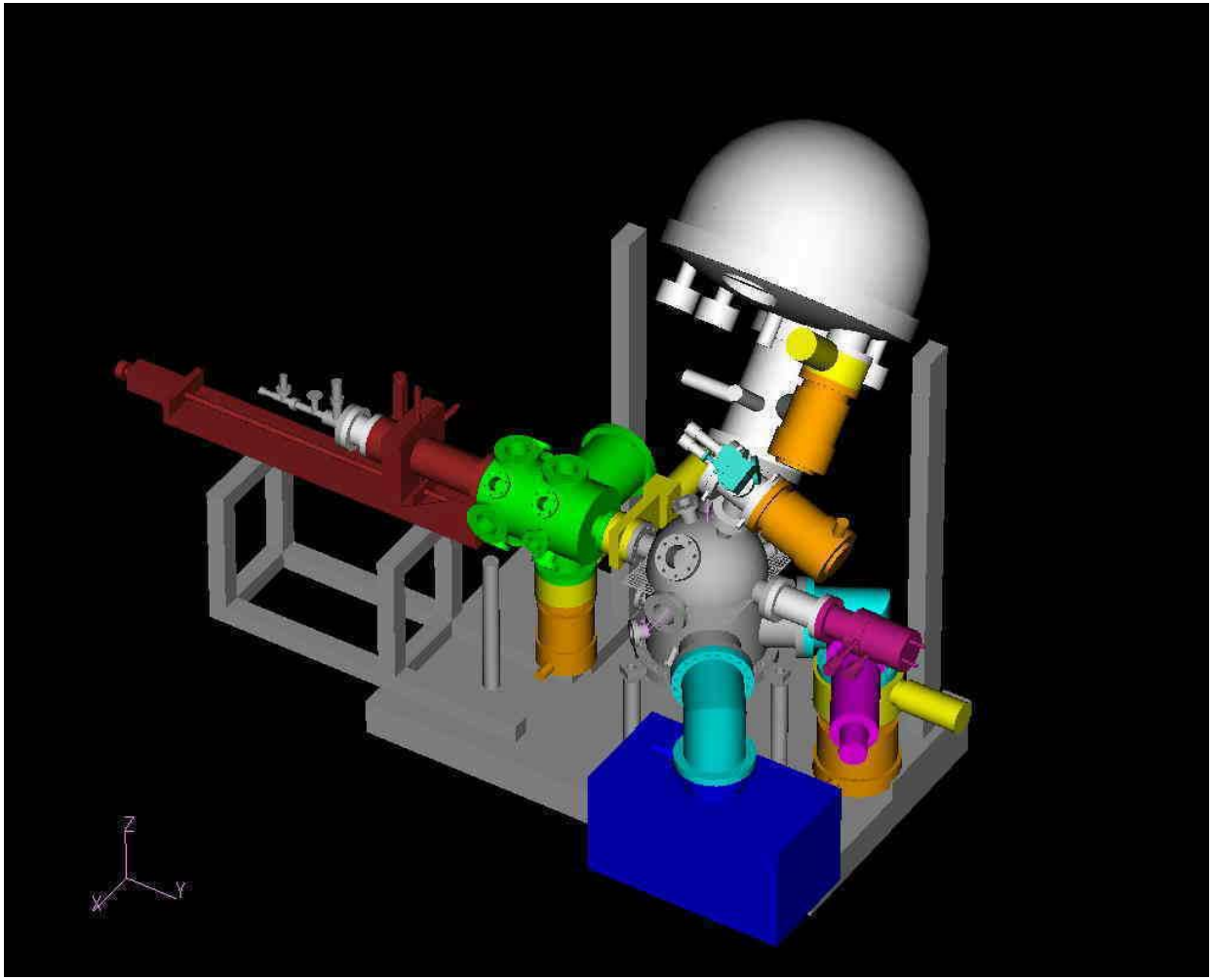

(b) Auger decay:

Core hole lifetime
defines the line width!

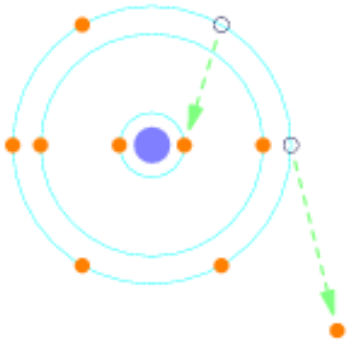

SES2002 analyzer

- Electrostatic hemispherical analyzer
  - Mean radius 200 mm
  - ΔE/PE=1/1600

  (66 meV at pass 100 eV)
  - **MCP+CCD camera**

  or MCP+Delay line anode

  - **Gas cell system**

  or Doppler-free molecular beam source

  Ueda *et al. PRL* . **90**, 153005 (2003)

  or effusive beam + momentum resolved ion spectrometer

  Prümper *et al.* PRA **71**, 052704, (2005).

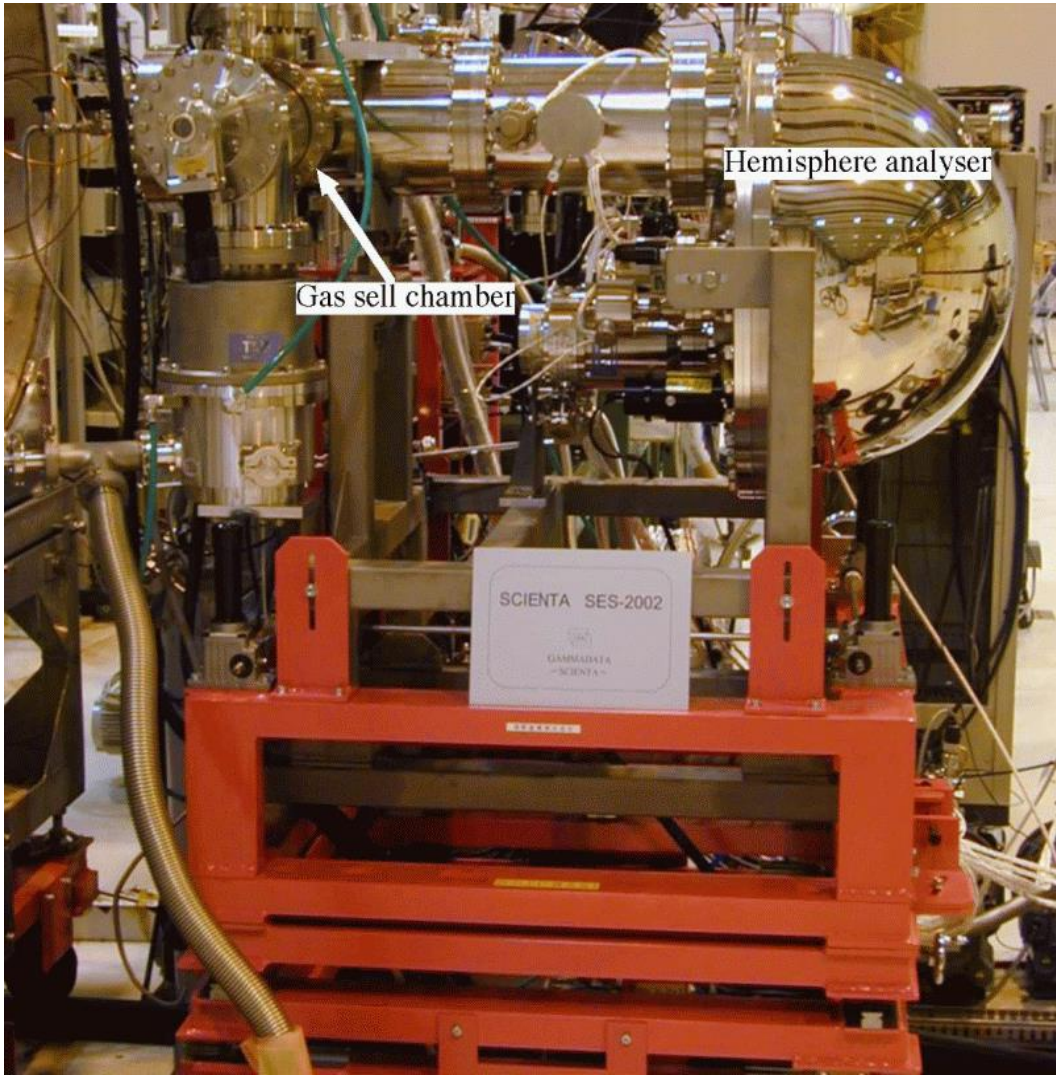

Angle-resolved resonant Auger spectra of Ne at 1s -> 3p excitation

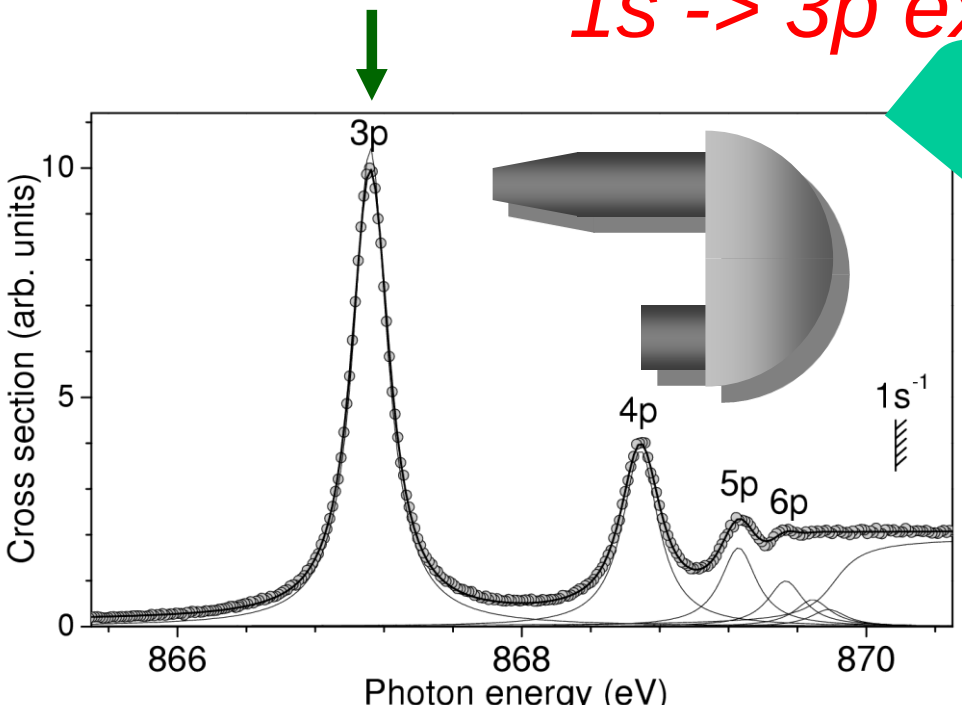

$$\frac{d\sigma}{d\theta} = \frac{\sigma}{4\pi}[1 + \beta P_2(\cos\theta)]$$

$$P_2(\cos\theta) = [3\cos\theta - 1]/2$$

β: asymmetry parameter

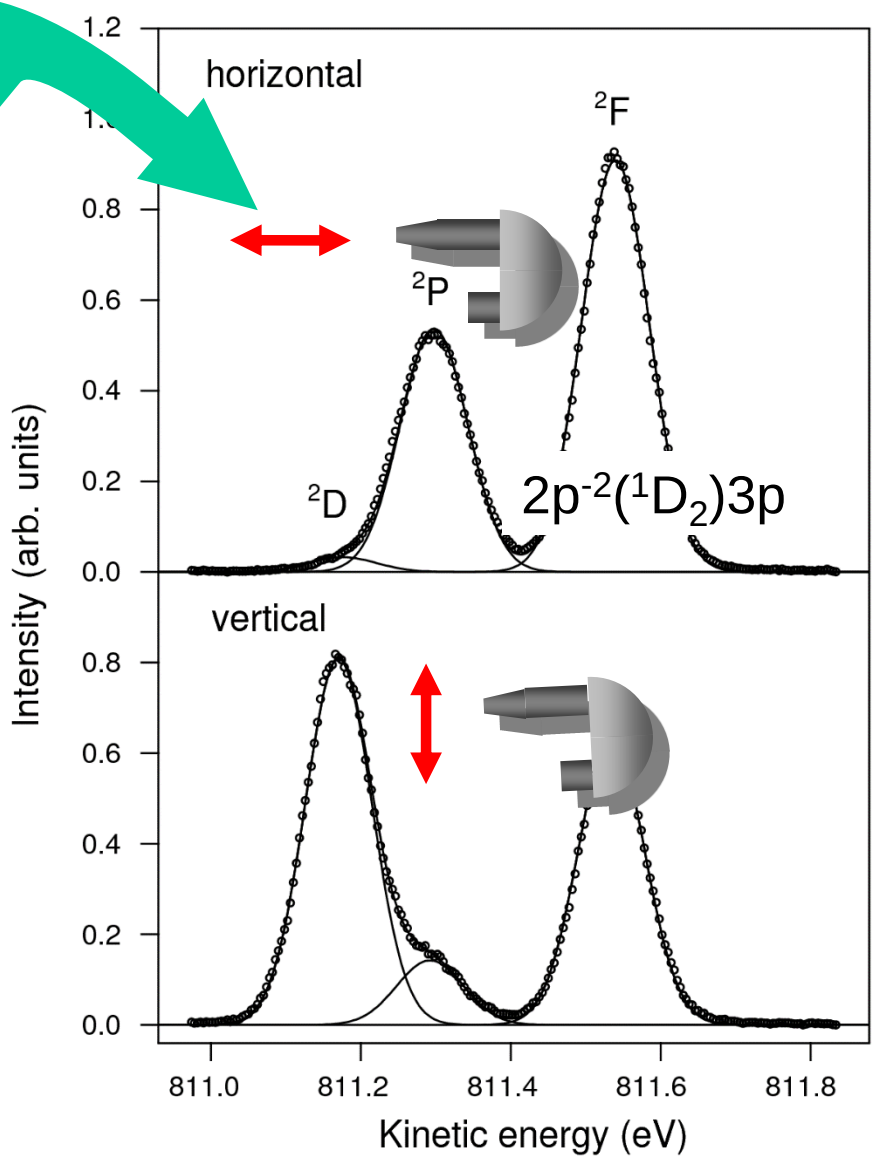

Measured angular distributions tell us how the angular momenta are coupled in the atom , allowing us the spectroscopic assignment !

Resonant Auger spectra of Ne "between" 1s -> 3p and 1s -> 4p excitations

$$\frac{d\sigma}{d\theta} = \frac{\sigma}{4\pi}[1 + \beta P_2(\cos\theta)] \qquad \sigma \propto I(0) + 2 \times I(90)$$

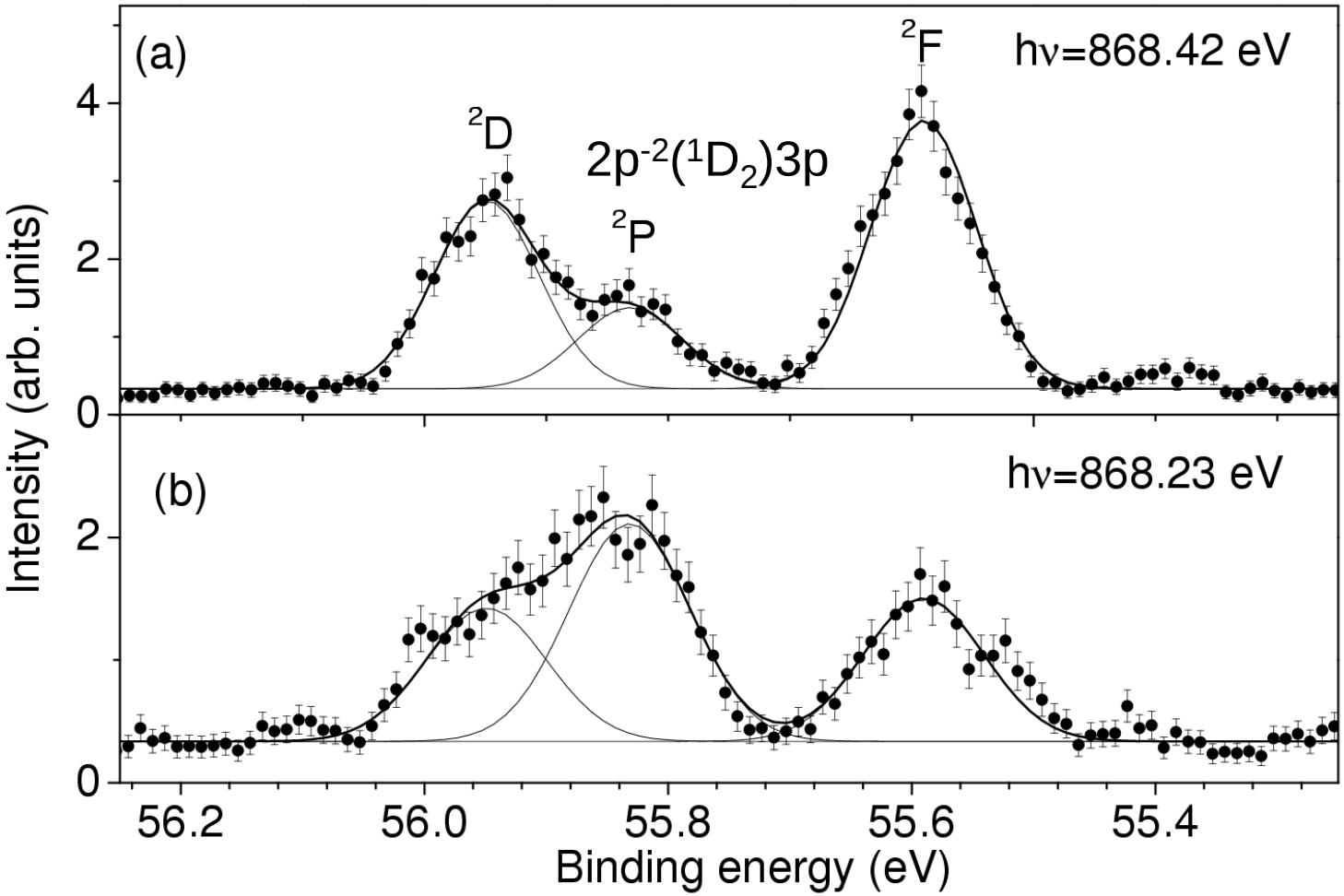

Interference effects between the two paths

$$A_\alpha = d_\alpha + \sum_n \frac{D_{n\alpha}}{i+\varepsilon_n}$$

$$\sigma_\alpha = |A_\alpha|^2$$

$$\varepsilon_n = (h\nu - E_n)/(\Gamma_n/2)$$

$$d_\alpha = \langle g|r|\alpha\rangle$$

$$D_{n\alpha} = \langle g|r|i_n\rangle\langle i_n|v|\alpha\rangle$$

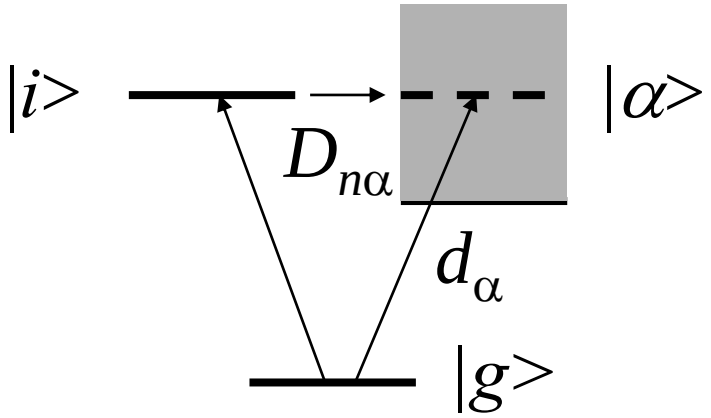

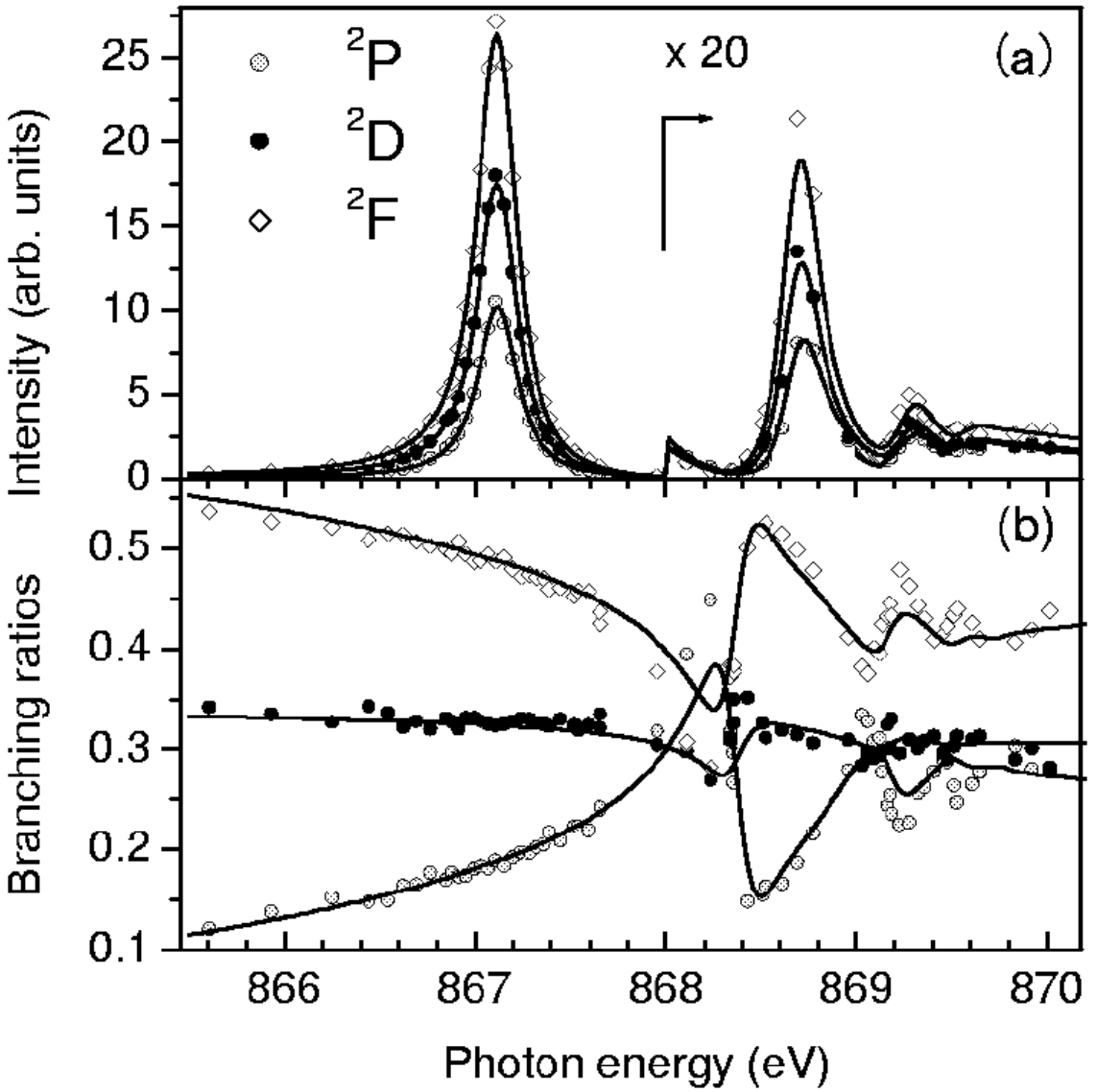

De Fanis *et al.* Phys. Rev. Lett. **89**, 023006 (2002).

Sendai City

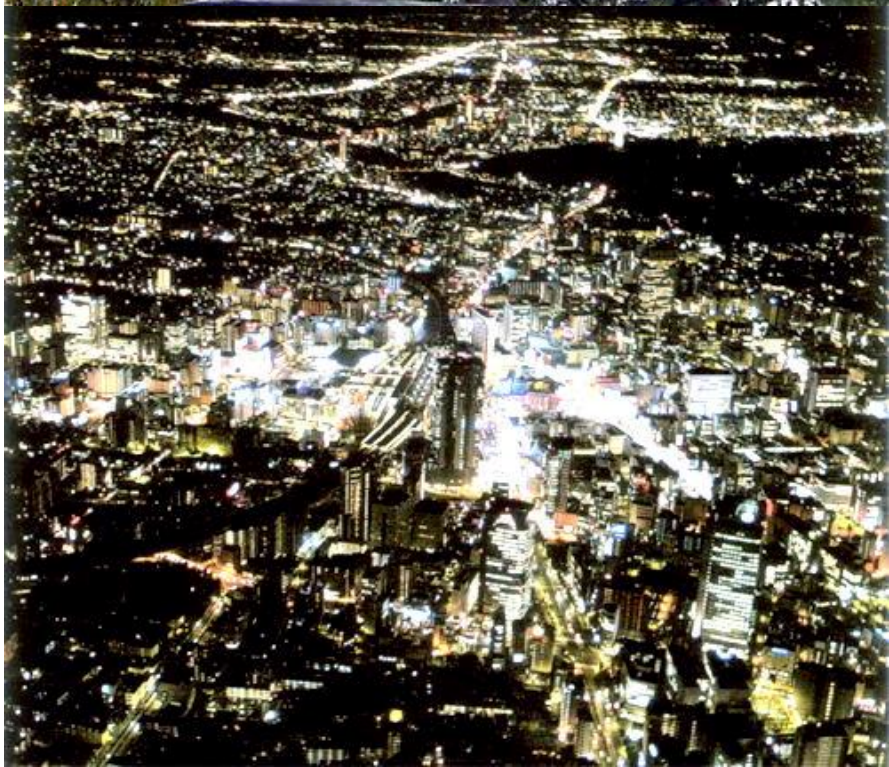

Introduction of molecular world

$$H\Psi(R,r) = E\Psi(R,r) \qquad H = T_R + T_r + V(r,R)$$

$$T_R = -\frac{\hbar}{2}\sum_k \frac{\partial^2}{M_k \partial R_k^2} \quad \text{KE of nucleus} \qquad T_r = -\frac{\hbar}{2m}\sum_j \frac{\partial^2}{\partial r_j^2} \quad \text{KE of electrons}$$

$$H = H_0 + T_R \qquad H_0 = T_r + V(r,R)$$

$$[H_0 - \varepsilon_n(R)]\varphi(R,r) = 0$$

$\varepsilon_n(R)$: adiabatic potential energy

$$\Psi(R,r) = \sum_n \Phi_n(R)\varphi_n(R,r)$$

$$[T_R + \varepsilon_m(R)]\Phi^0_{mv}(R) = E^0_{mv}\Phi^0_{mv}(R)$$

Nuclear motion is within the adiabatic potential energy surface!

Born-Oppenheimer approximation

Franck-Condon approximation for photoionization

$$\sigma^{+}_{iv'}(E) \sim \left| \int X^{*}_{iv'}(R) D_E(R) X_0(R) dR \right|^2$$

$X^{*}_{iv'}(R), X_0(R)$: Vibrational wavefunctions of ionic *iv'* and ground 0 states

$$D_E(R) = \int \varphi^{*}_{E}(r,R) r \varphi_{\text{core}}(r,R) \mathrm{d}r$$

$\varphi_E(r,R), \varphi_{\text{core}}(r,R)$: Electronic wavefunctions of the continuum *E* and core orbitals

Assume that the dipole moment $D_E(R)$ does not depend on R

$$\sigma^{+}_{iv'}(E) \sim \left| D_E(R_e) \right|^2 F(v'0)$$

$$F(v'0) = \left| \int X^{*}_{iv'}(R) X_0(R) \mathrm{d}R \right|^2$$ Franck-Condon factor

Vibrational intensity distribution in the photoelectron spectrum is determined by the Franck-Condon factors

Franck-Condon analysis based on harmonic approximation
Linear coupling model

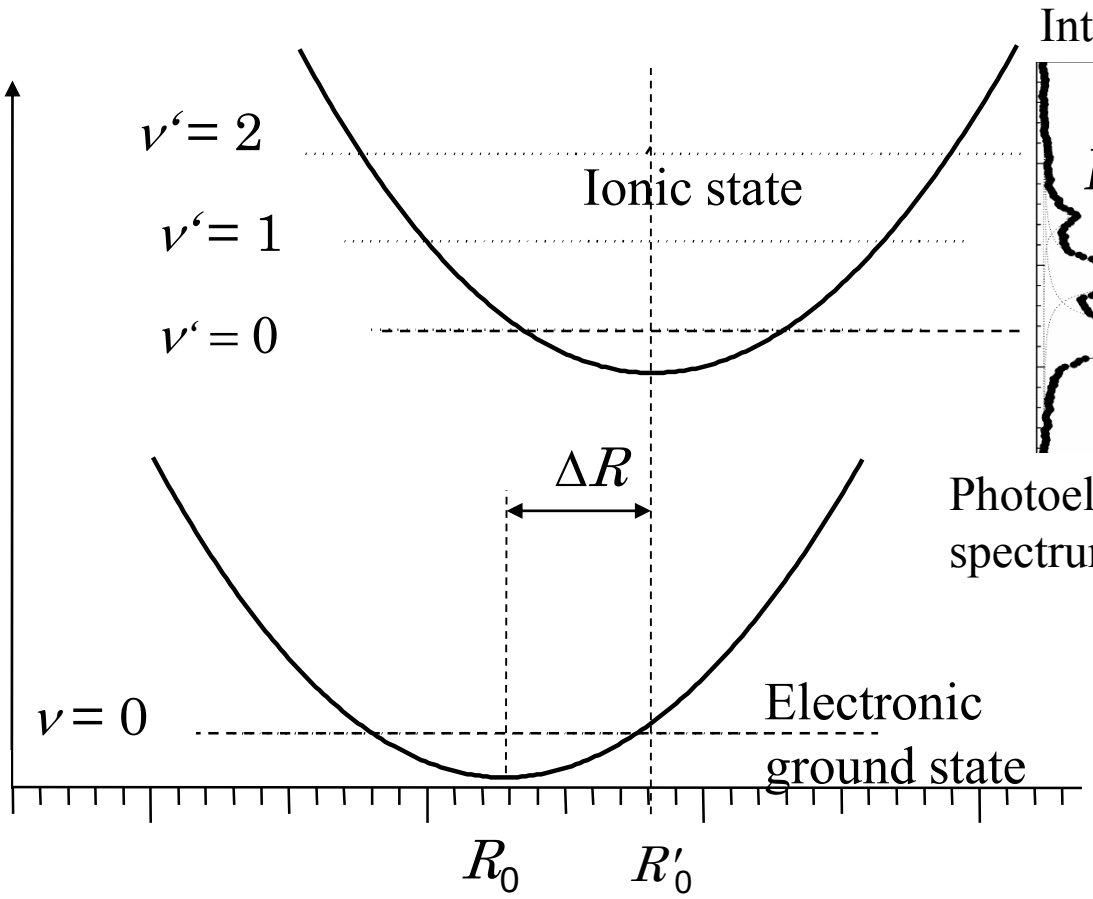

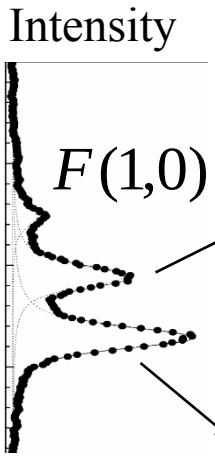

$$F(1,0) = \frac{\alpha(\Delta R)^2}{2}\exp\left(-\frac{\alpha(\Delta R)^2}{2}\right)$$

$$\alpha = \mu\omega/\hbar$$

$$F(0,0) = \exp\left(-\frac{\alpha(\Delta R)^2}{2}\right)$$

$$\frac{F(1,0)}{F(0,0)} = \frac{\alpha(\Delta R)^2}{2}$$

One can extract ΔR from photoelectron spectroscopy!

Franck-Condon analysis for the vibrational structure of the C 1s and O 1s mainlines of CO

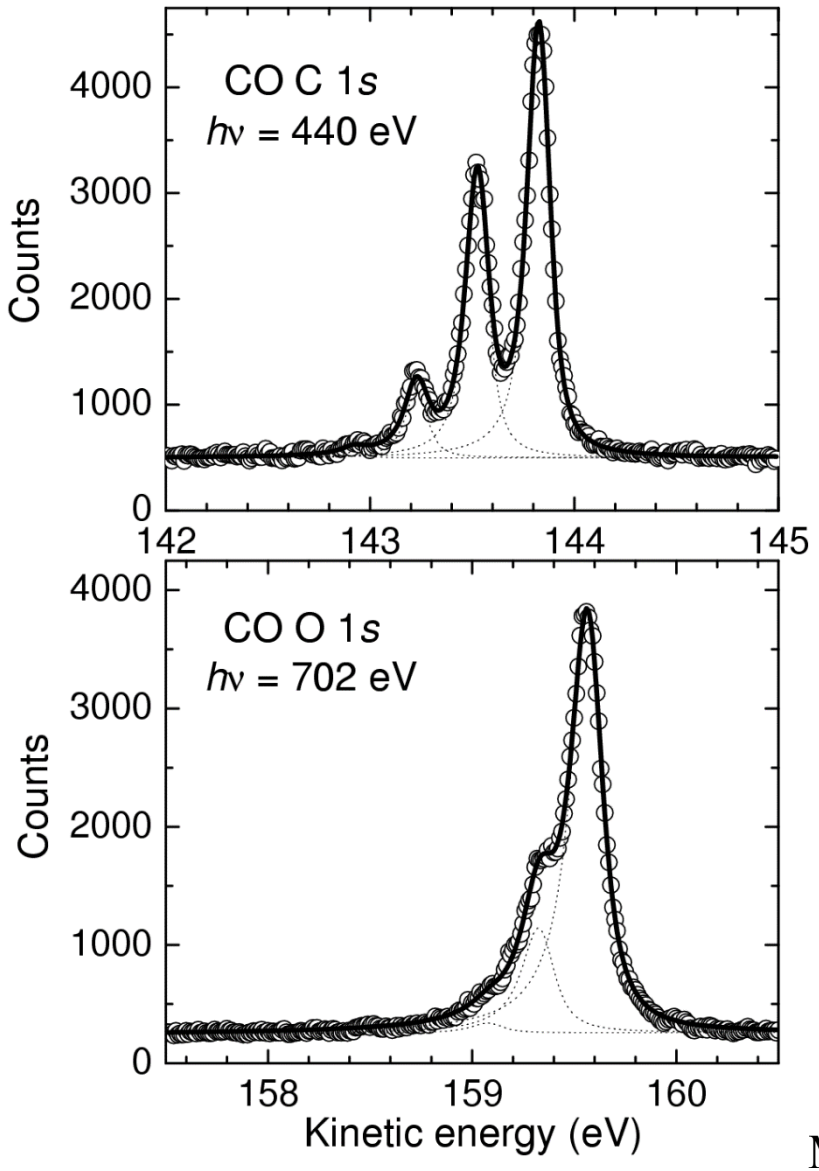

$I \sim |\langle \psi^{+}_{v} | \psi_0 \rangle|^2$: FC factor

ψ_0: v=0 vibrational wave function in the ground state

ψ^{+}_{v}: v-th vibrational wave function in the core-ionized state

Stable geometry of the core-ionized state extracted from the vibrational structure

	Exper.	Theory
C $1s^{-1}$		
ΔR_e (Å)	-0.051 (1)	-0.051
O $1s^{-1}$		
ΔR_e (Å)	0.037(2)	0.028

Matsumoto *et al.* Chem. Phys. Lett. **417**, 89-93 (2006).

Satellite spectrum in core-level photoemission in CO

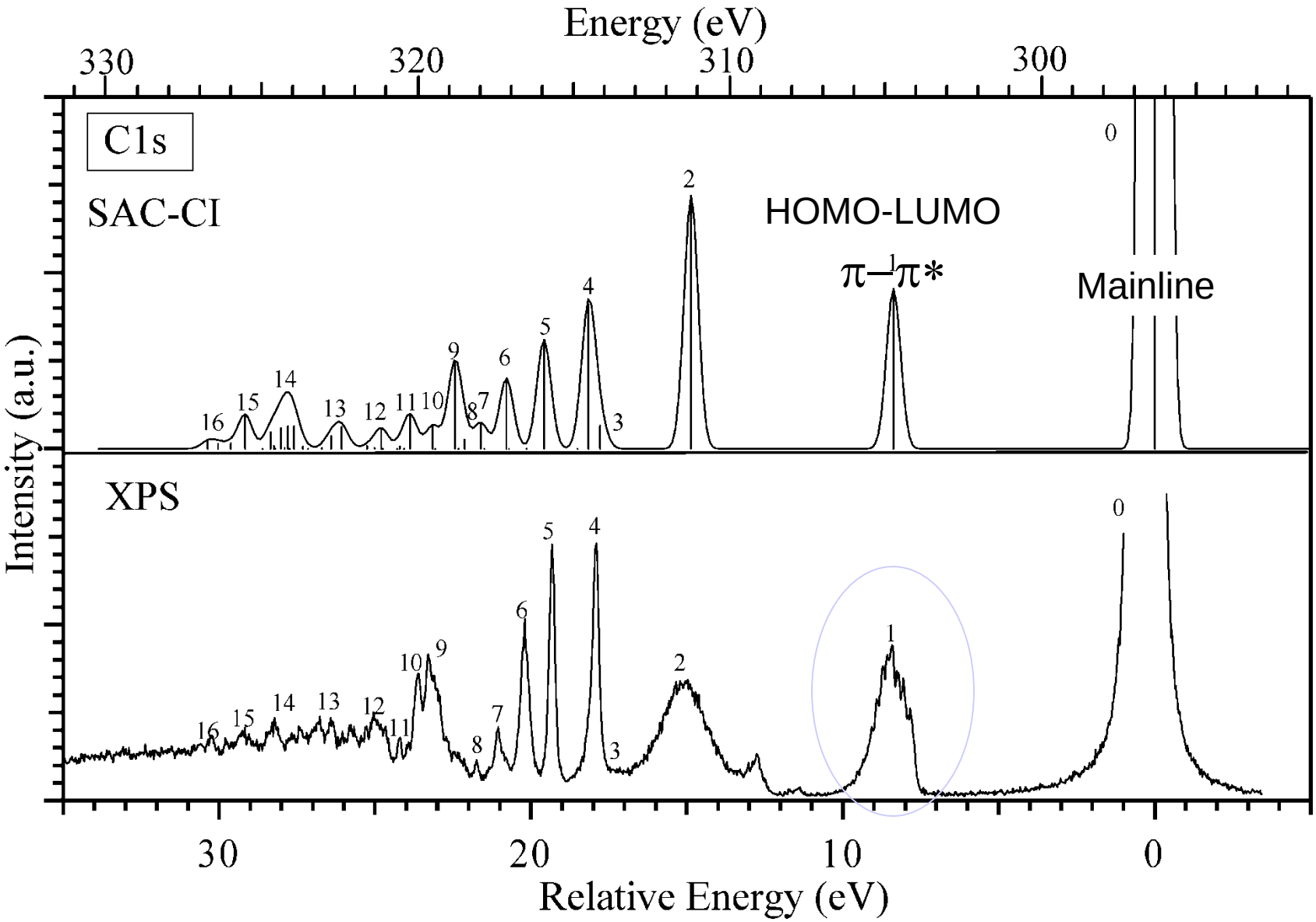

Ehara *et al.* J. Chem. Phys. **125**, 114304 (2006).

Franck-Condon analysis of the vibrational structure in the symmetry-resolved C 1s satellite bands of CO

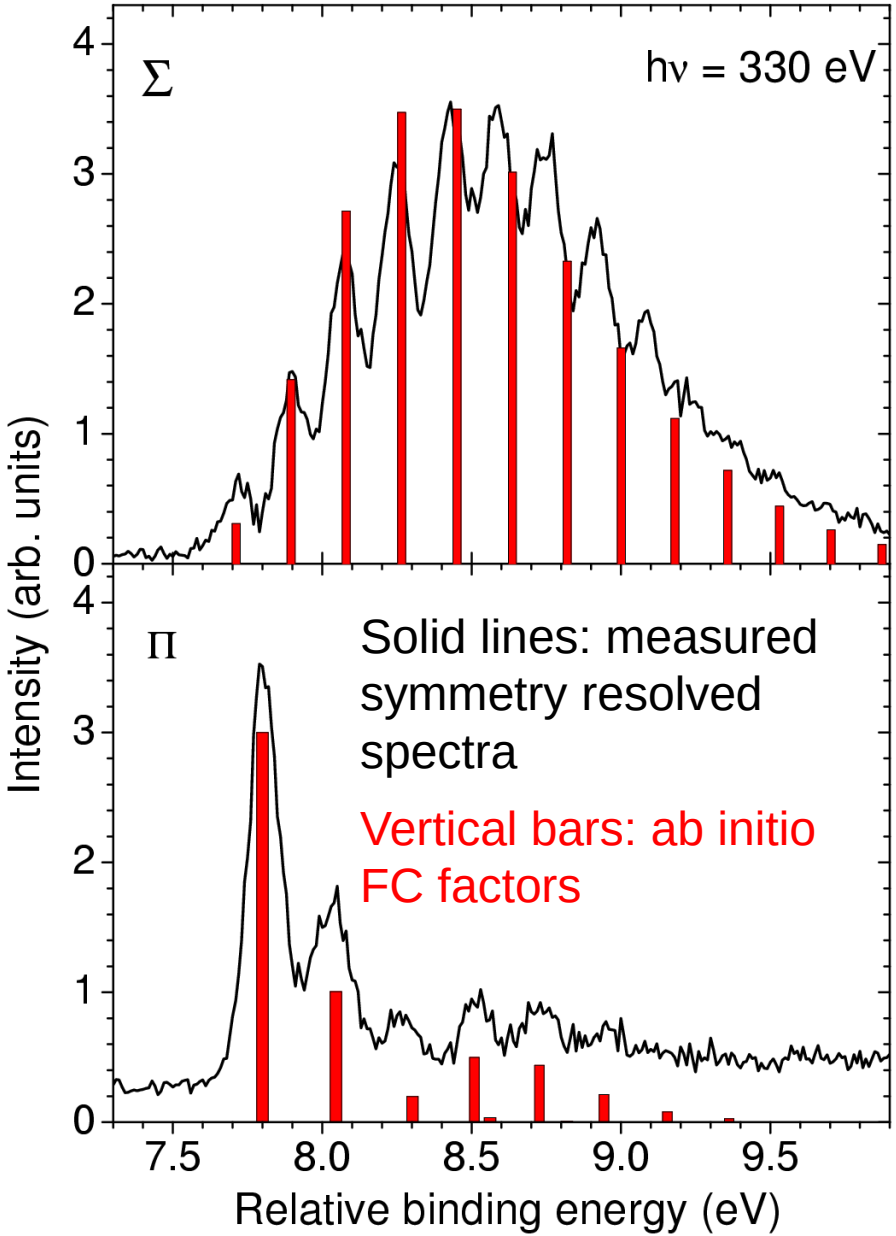

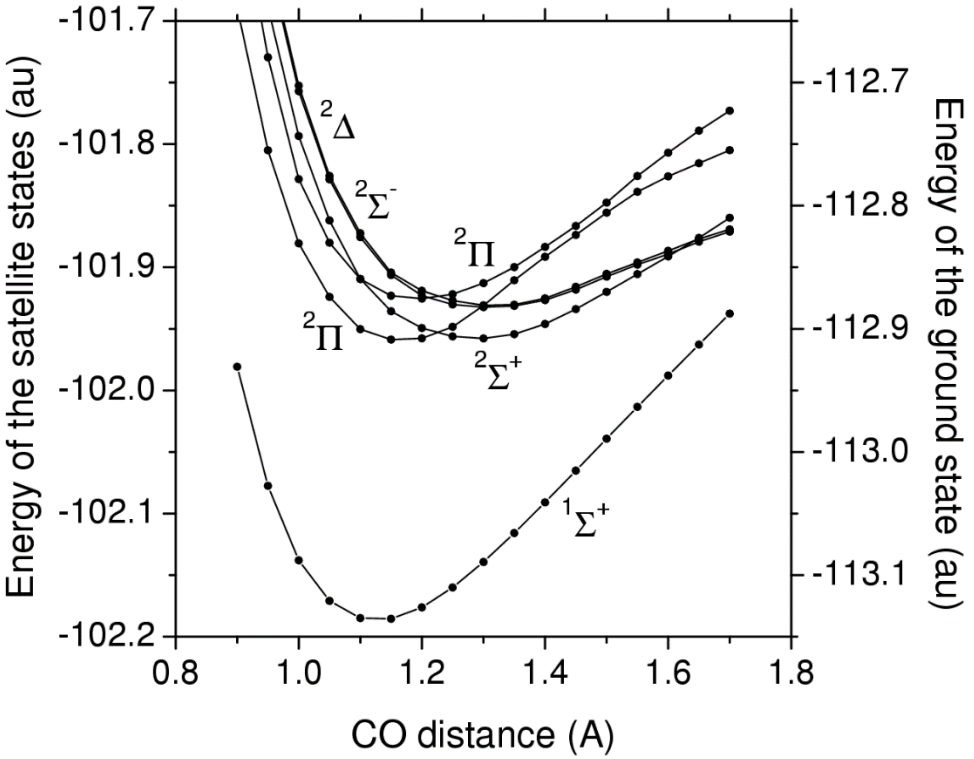

Ab initio potential curves

Ab initio FC factors reproduce the measured vibrational distributions.

Ueda *et al.,* Phys. Rev. Lett. **94**, 243004 (2005).

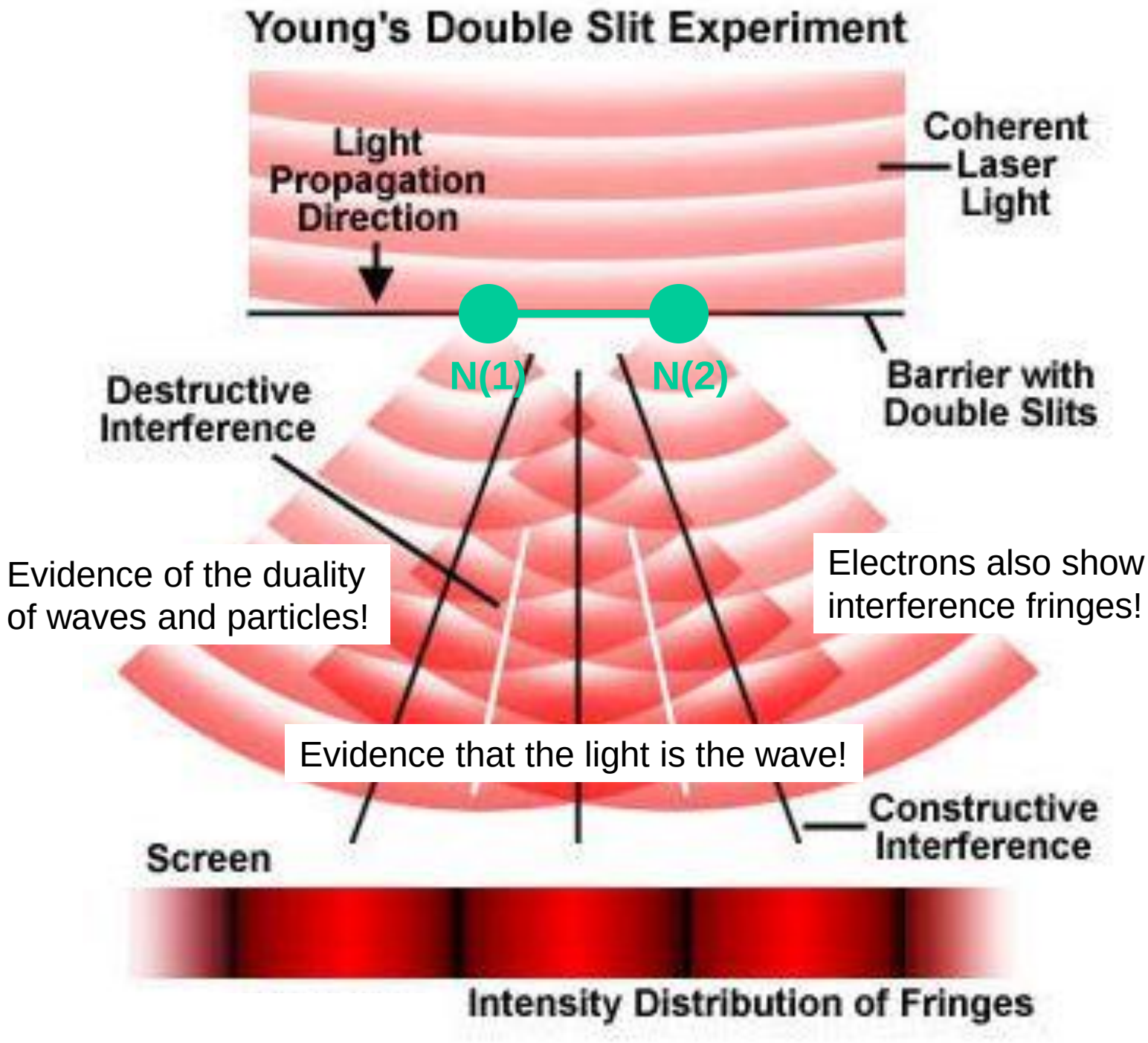
Young's Double Slit Experiment
Light Propagation Direction
Coherent Laser Light
N(1)
N(2)
Barrier with Double Slits
Destructive Interference
Evidence of the duality of waves and particles!
Electrons also show interference fringes!
Evidence that the light is the wave!
Constructive Interference
Screen
Intensity Distribution of Fringes

Franck-Condon analysis for the vibrational structure of the N 1s $1\sigma_u$ and $1\sigma_g$ mainlines of N_2

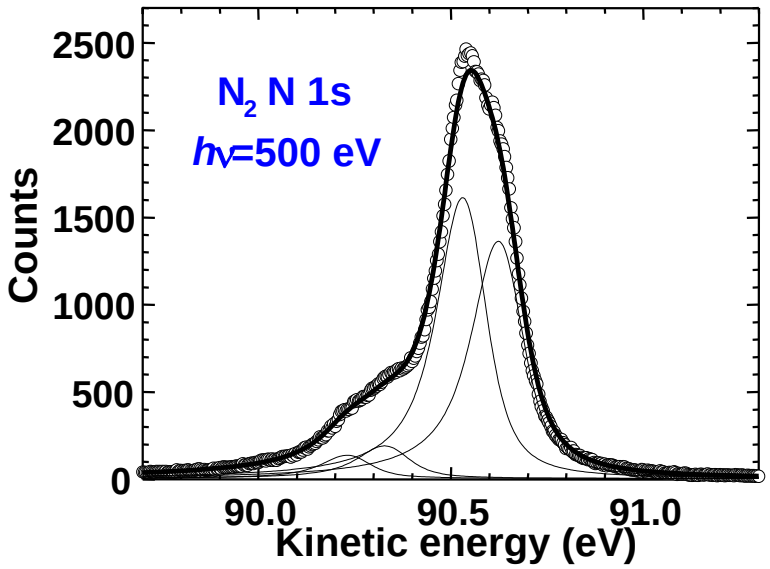

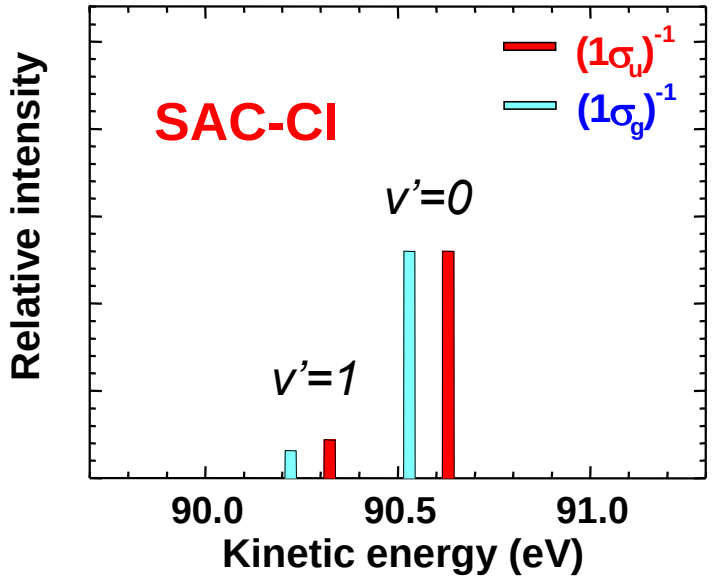

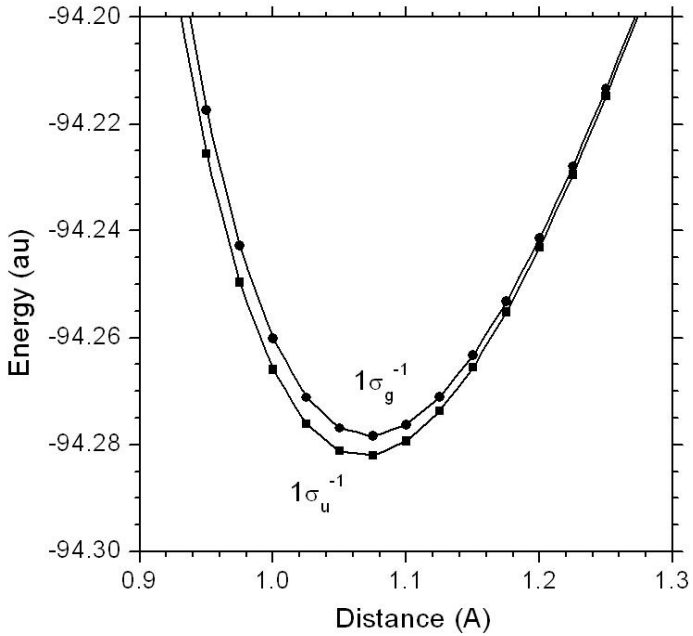

Equilibrium geometries of the core-ionized states extracted from the vibrational structure

	Exper.	Theory
N $1\sigma_u^{-1}$		
ΔR_e (Å)	-0.023(1)	-0.021
N $1\sigma_g^{-1}$		
ΔR_e (Å)	-0.018(1)	-0.017

Ehara *et al.* JCP **124**, 124311 (2006)

Cohen-Fano two-center interference

Two 1s ortibals in N_2 correspond to Young's double slits.

Molecular core-level ortibals: $1\sigma_{g,u} = \dfrac{1s_1 \pm 1s_2}{\sqrt{2}}$.

Core-level photoemission from fixed-in-space N_2:

$$\sigma_{g,u}(\omega) \propto \frac{1}{2}\left|e^{i\mathbf{k}\cdot\mathbf{R}_1} \pm e^{i\mathbf{k}\cdot\mathbf{R}_2}\right|^2 = 1 \pm \cos(\mathbf{k}\cdot\mathbf{R}) \ ,$$

Two center photoelectron wave — *Interference fringe*

where k: photoelectron momentum; R_1,R_2: position vectors of N (1) and N(2)

$\mathbf{R} = \mathbf{R}_1 - \mathbf{R}_2.$

Orientational average: Cohen-Fano formula

$$\sigma_{g,u}(\omega) = \sigma_0(\omega)\left[1 \pm \chi_{\mathrm{CF}}(k)\right] \ , \ \ \chi_{\mathrm{CF}}(k) = \frac{\sin kR}{kR}$$

Interference oscillatory structure becomes much smaller but remains!

H.D. Cohen and U. Fano, Phys. Rev. **150**, 30 (1966).

Ab initio N 1s $1\sigma_u$ and $1\sigma_g$ photoionization cross sections of N_2

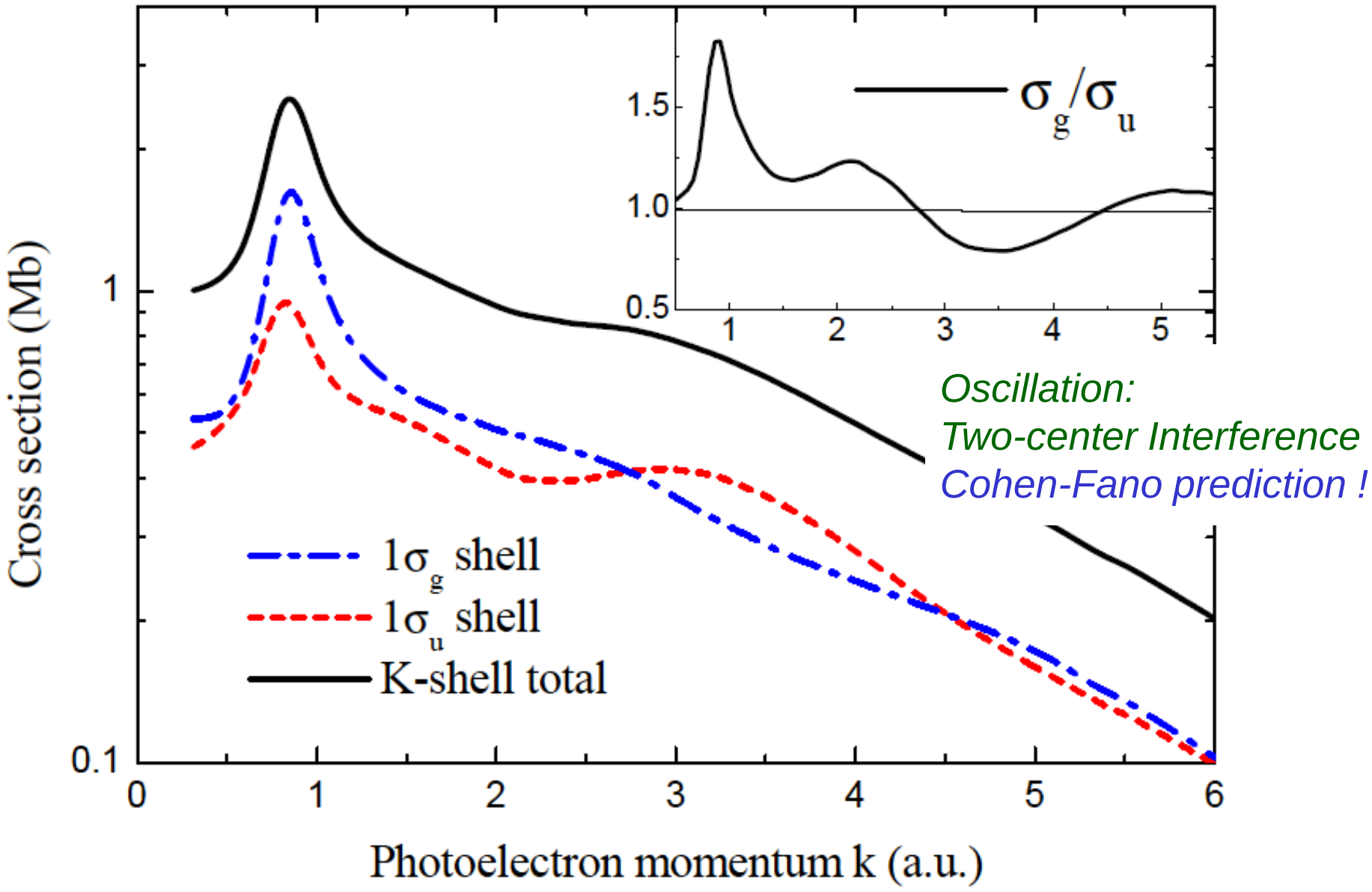

Semenov *et al.*, J. Phys. B: At. Mol. Opt. Phys. 39, L261 (2006)

σ_g/σ_u ratio: experiment vs ab initio and Cohen-Fano

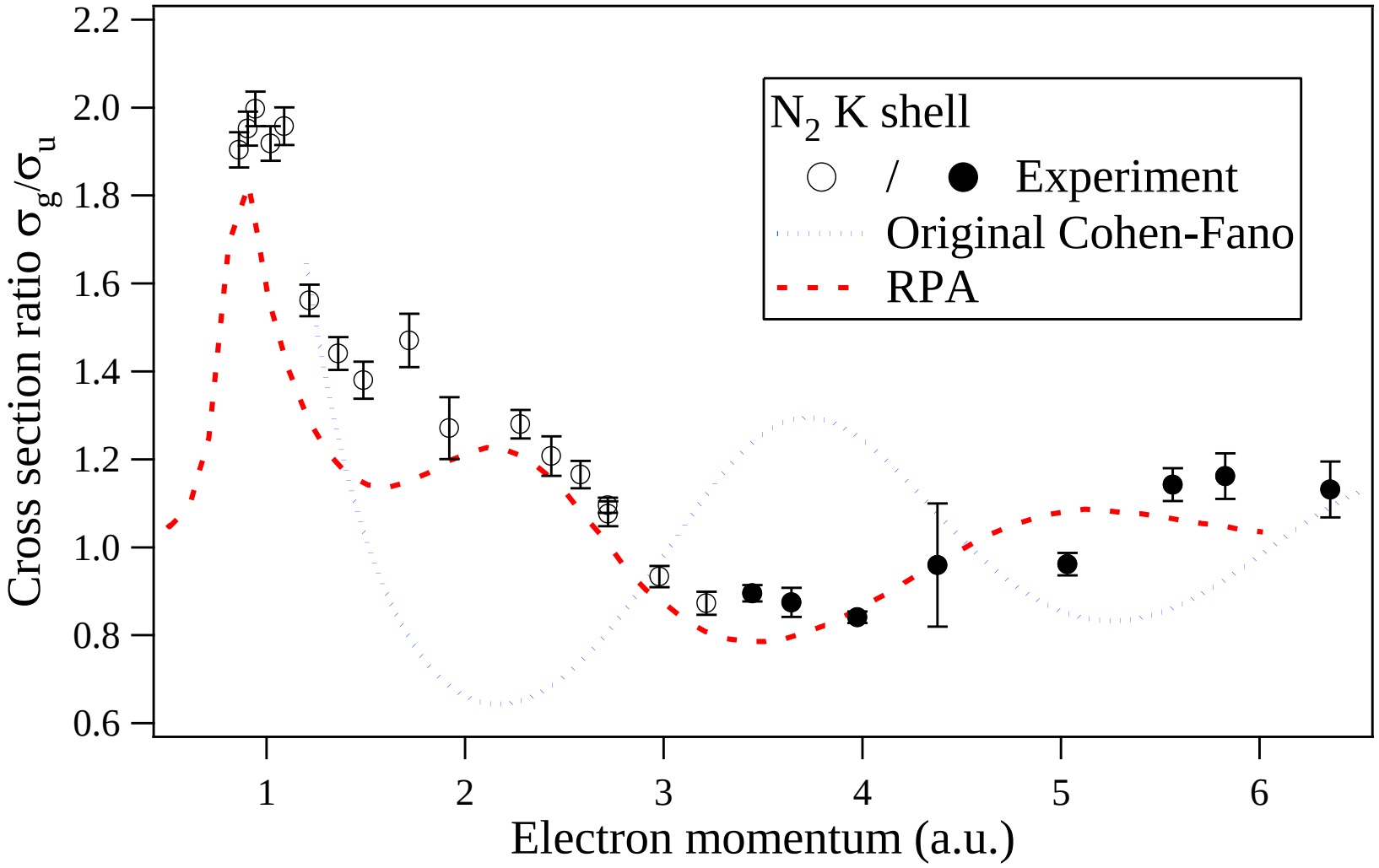

Both experimental and ab initio interference fringes shift from the prediction by Cohen-Fano formula!

Liu *et al.,* J. Phys. B. **39,** 4801-4817 (2006); JESRP **156-158**, 73-77 (2007).

Photoelectron scattering by the neighboring N atom

The amplitude of the photoelectron wave from one center:

$$\psi_1 = \underbrace{\hat{\mathbf{k}} e^{i\mathbf{k}\cdot\mathbf{R}_1}}_{A_1} + \underbrace{\hat{\mathbf{R}} \frac{e^{ikR}}{R} f(\vartheta) e^{i\mathbf{k}\cdot\mathbf{R}_2}}_{B_1} .$$

$$\psi_2 = A_2 + B_2$$

The amplitude of the photoelectron wave from two centers: $\psi_1 \pm \psi_2$

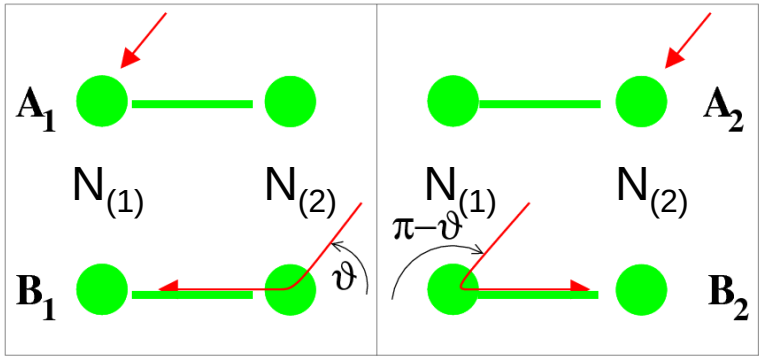

Cohen-Fano interference
A_1A_2 interference term

$$\chi_{CF}(k) = \frac{\sin kR}{kR}$$

The cross section~ $|\psi_1 \pm \psi_2|^2 = |(A_1+B_1) \pm (A_2+B_2)|^2$

$$\frac{\sigma_{g,u}(\omega)}{\sigma_0(\omega)} = 1 - \frac{1}{kR^2} \mathrm{Im}\left\{ f(\pi) e^{2i[kR+\delta_1(k)]} \right\} \pm \chi(k) ,$$

0

A_1B_1 and A_2B_2 one-center interference terms

$$\chi(k) = \frac{1}{kR} \sin\left[kR + 2\delta_1(k)\right]$$

δ_1(k): scattering phase

CF A_1A_2 interference term

A_1B_2 and A_2B_1 two-center interference terms !

Sendai
in summer

Tanabata festival

Multiple-ion coincidence imaging setup

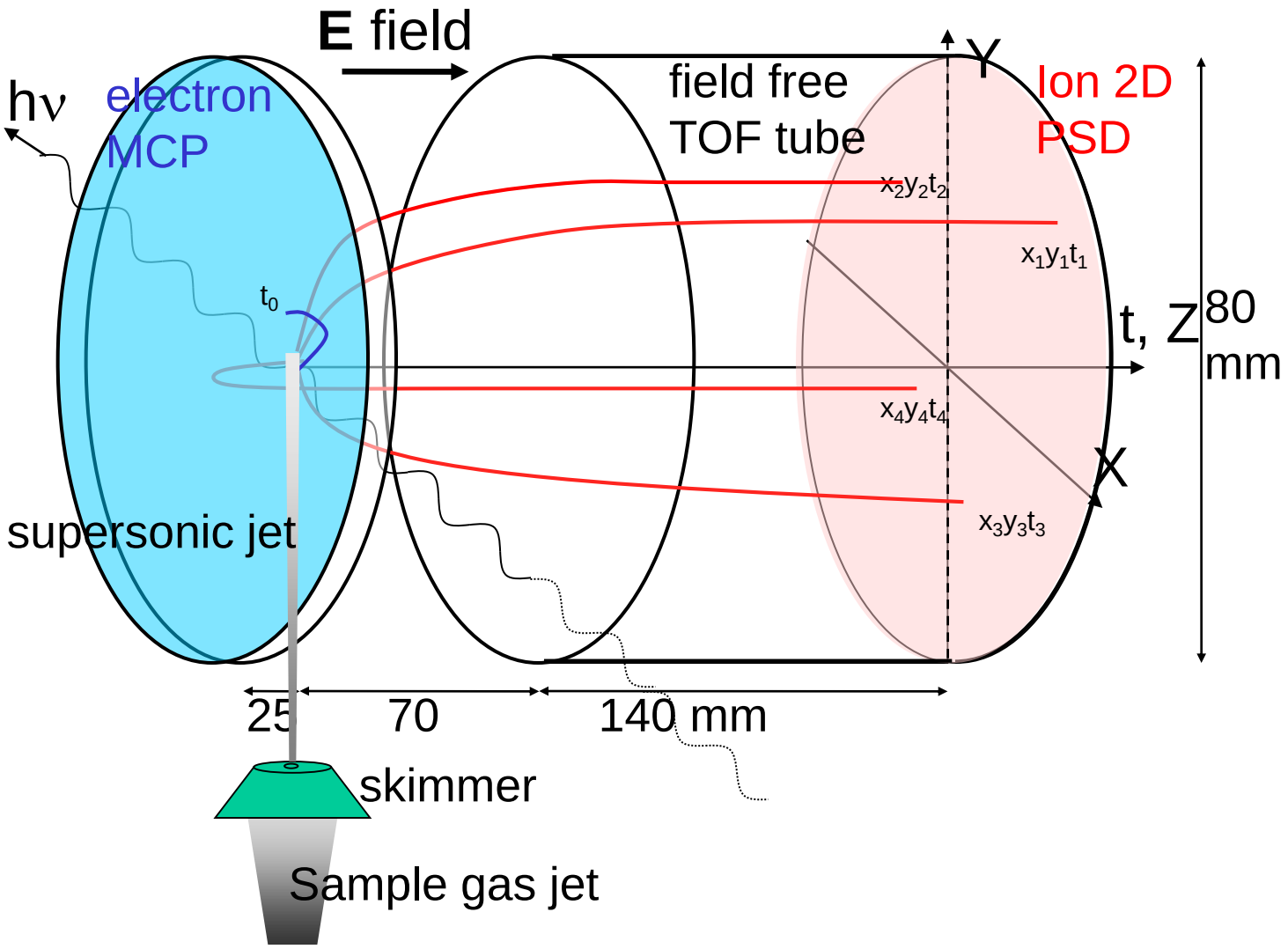

position & time of flight (x,y,t) → *3D momentum of each particle*

How to obtain 3D momentum

$$p_x = \frac{m(x - x_0)}{t}, \quad p_y = \frac{m(y - y_0)}{t}, \quad p_z = qE(t - t_0)$$

t: ion time-of-flight

t_0: ion TOF at rest

x, y: arrival position on the detector.

x_0, y_0 : initial position of the ion

m : ion mass

q: ion charge

E: electric field in the acceleration region

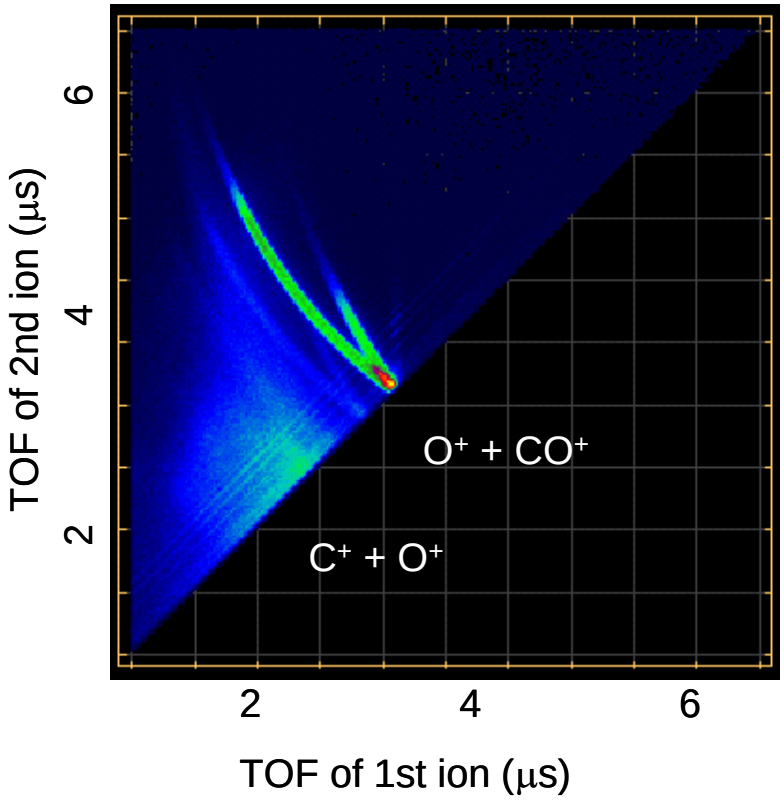

To be exact Pz becomes nonlinear → Iterative procedure

Total electron yield spectrum of CO_2 in the C1s excitation region

CO_2 ground state configuration:

$$\underbrace{1\sigma_g^2 1\sigma_u^2}_{\text{O1s}}\ \underbrace{2\sigma_g^2}_{\text{C1s}}\ \underbrace{3\sigma_g^2 2\sigma_u^2}_{\text{O2s}}\ \underbrace{4\sigma_g^2}_{\text{C2s}}$$

$$3\sigma_u^2 1\pi_u^4 1\pi_g^4(^1\Sigma_g^+);\ 2\pi_u^0 5\sigma_g^0 4\sigma_u^0$$

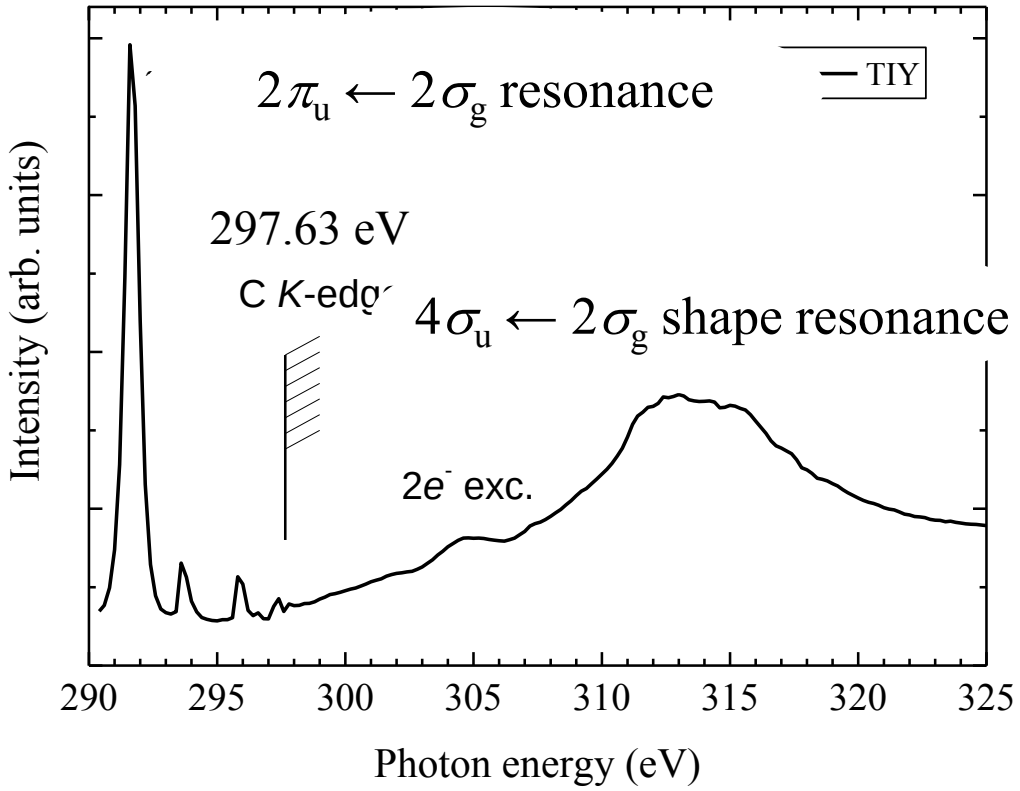

Renner-Teller splitting of CO_2

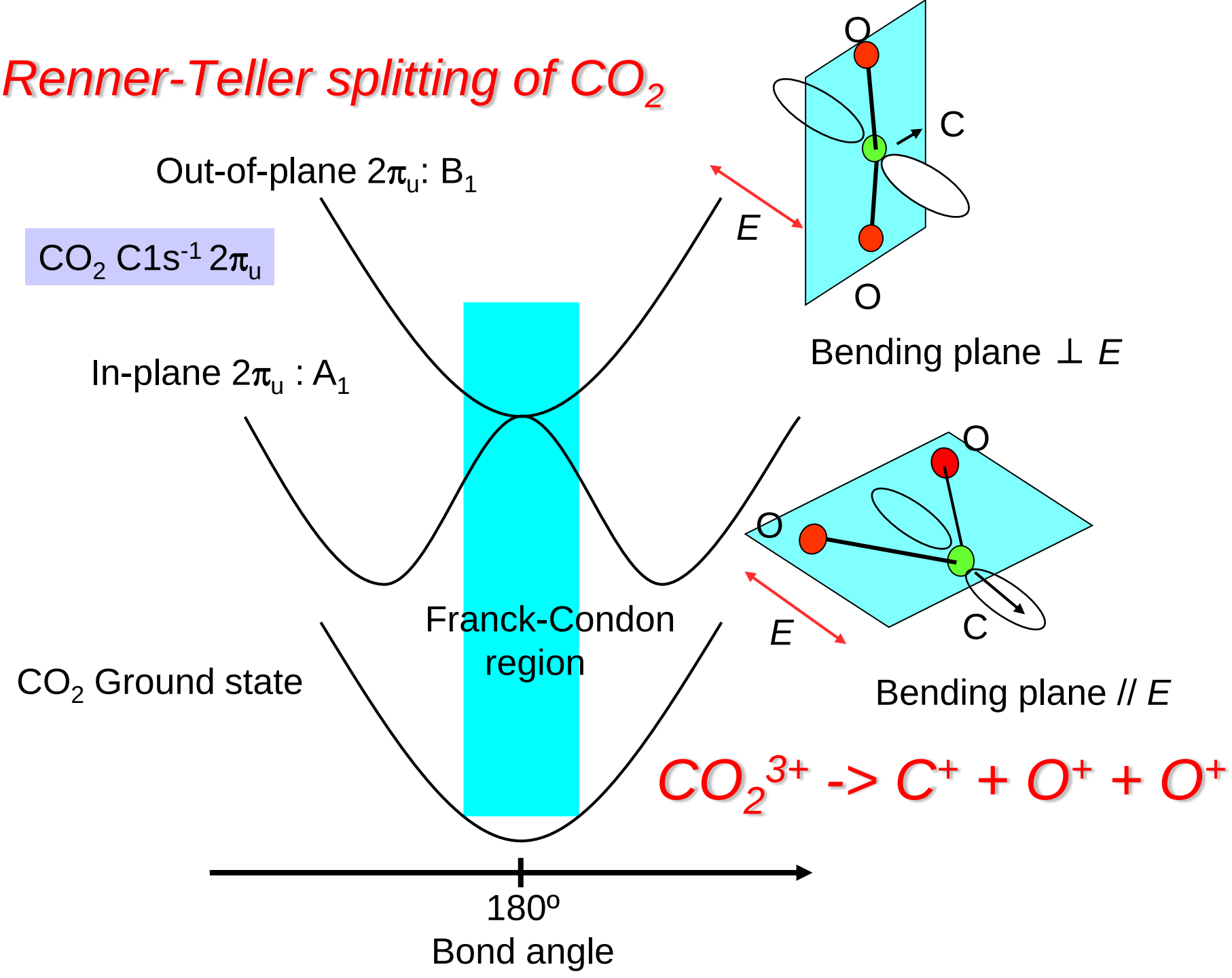

Snapshot of the bending motion in the core-exited state with a liftetime ~7 fs

Newton Diagram

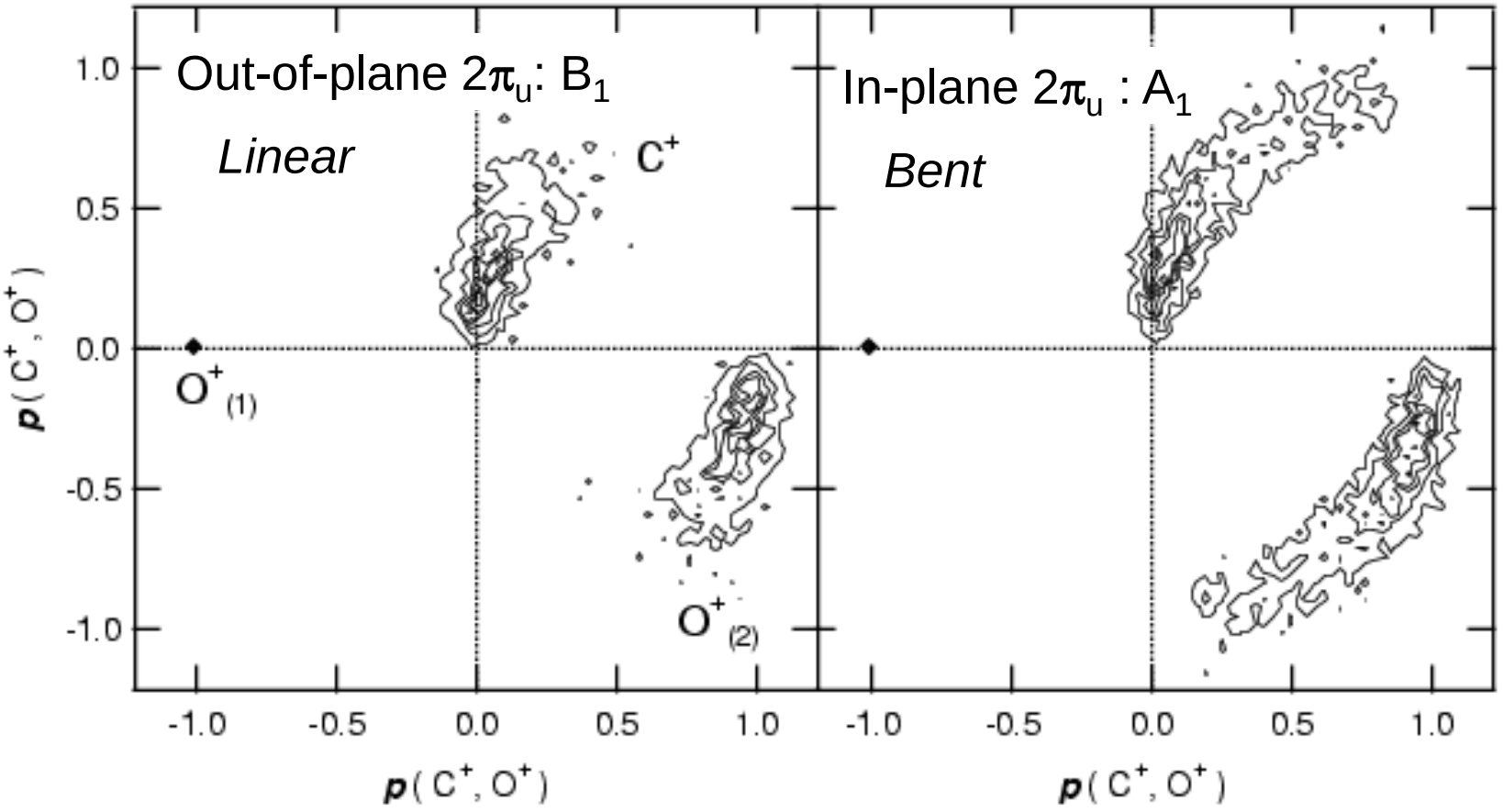

Muramatsu et al. Phys. Rev. Lett. 88, 133002 (2002).

Electron-ion coincidence momentum imaging

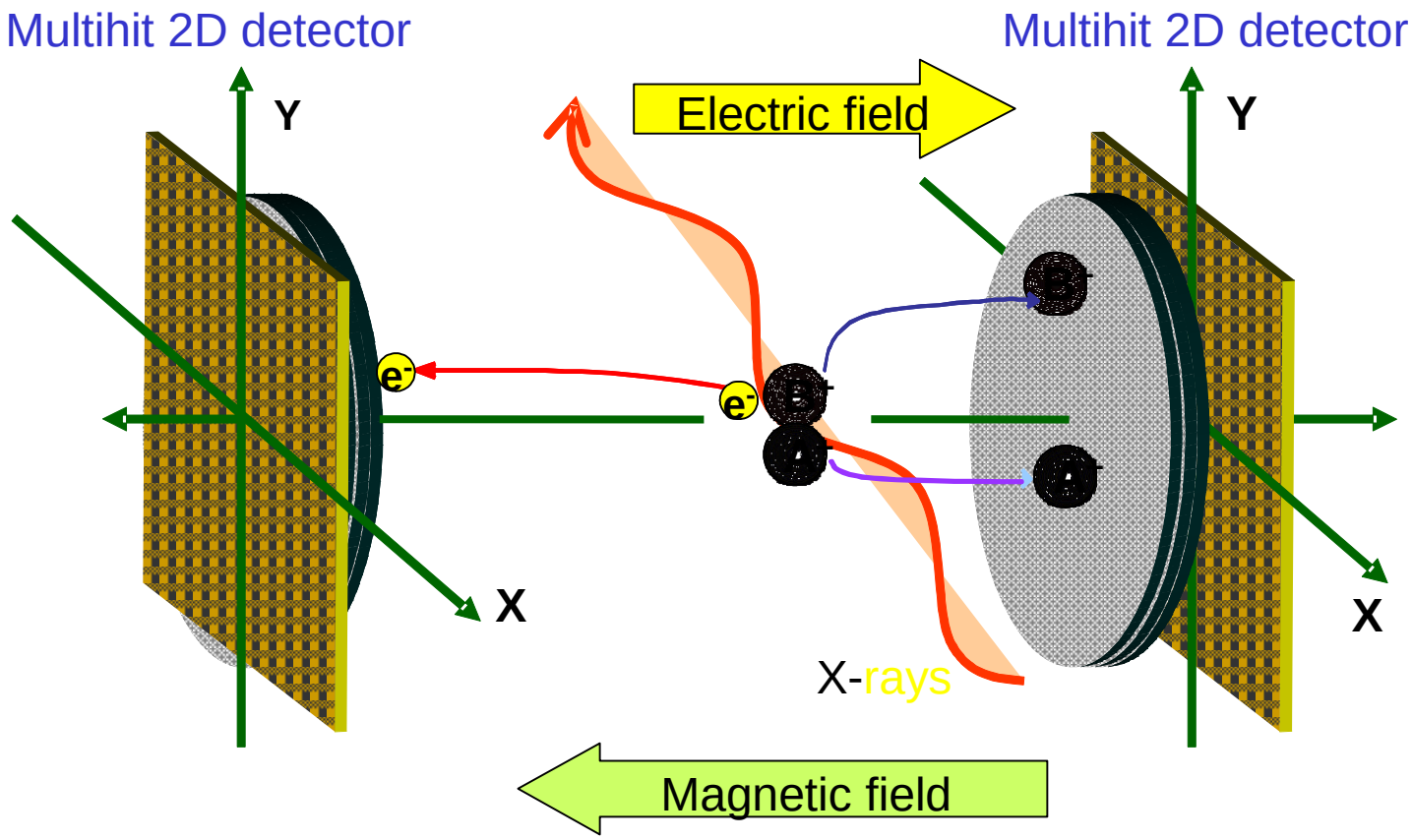

Ion-ion coincidence → *Molecular axis*

Ion momentum conservation → *Retrieval of the source point*

Electron-ion-ion coincidence → *Molecular-frame e^- angular distribution*

Towards photoelectron diffraction measurement

Total electron yield spectrum of CO_2 in the C1s ionization region

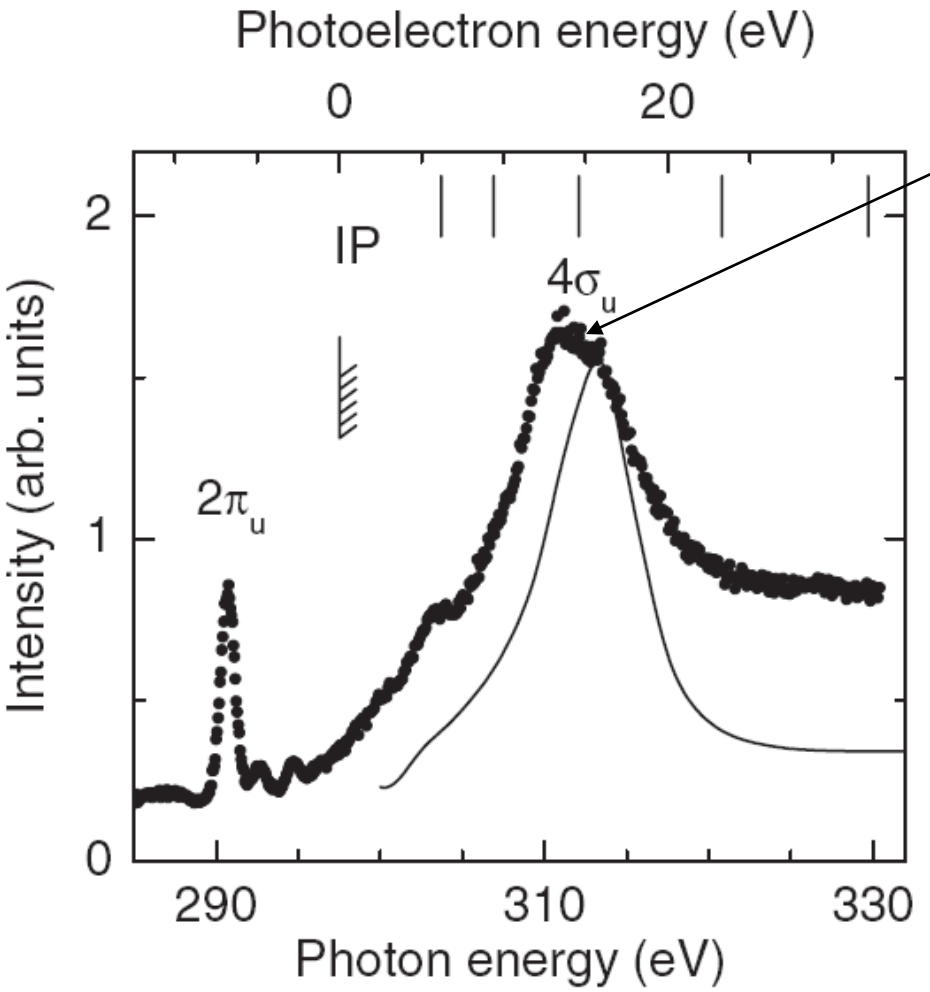

$4\sigma_u \leftarrow 2\sigma_g$ shape resonance

CO_2 ground state configuration:

$\underbrace{1\sigma_g^2 1\sigma_u^2}_{\text{O1s}}\ \underbrace{2\sigma_g^2}_{\text{C1s}}\ \underbrace{3\sigma_g^2 2\sigma_u^2}_{\text{O2s}}\ \underbrace{4\sigma_g^2}_{\text{C2s}}$

$3\sigma_u^2 1\pi_u^4 1\pi_g^4 (^1\Sigma_g^+);\ 2\pi_u^0 5\sigma_g^0 4\sigma_u^0$

C 1s threshold
297.63 eV

N. Saito *et al.*, J. Phys. B, **36** L25 (2003).

Reaction plane

Reaction plane ＝plane define by the E vector and molecular axis

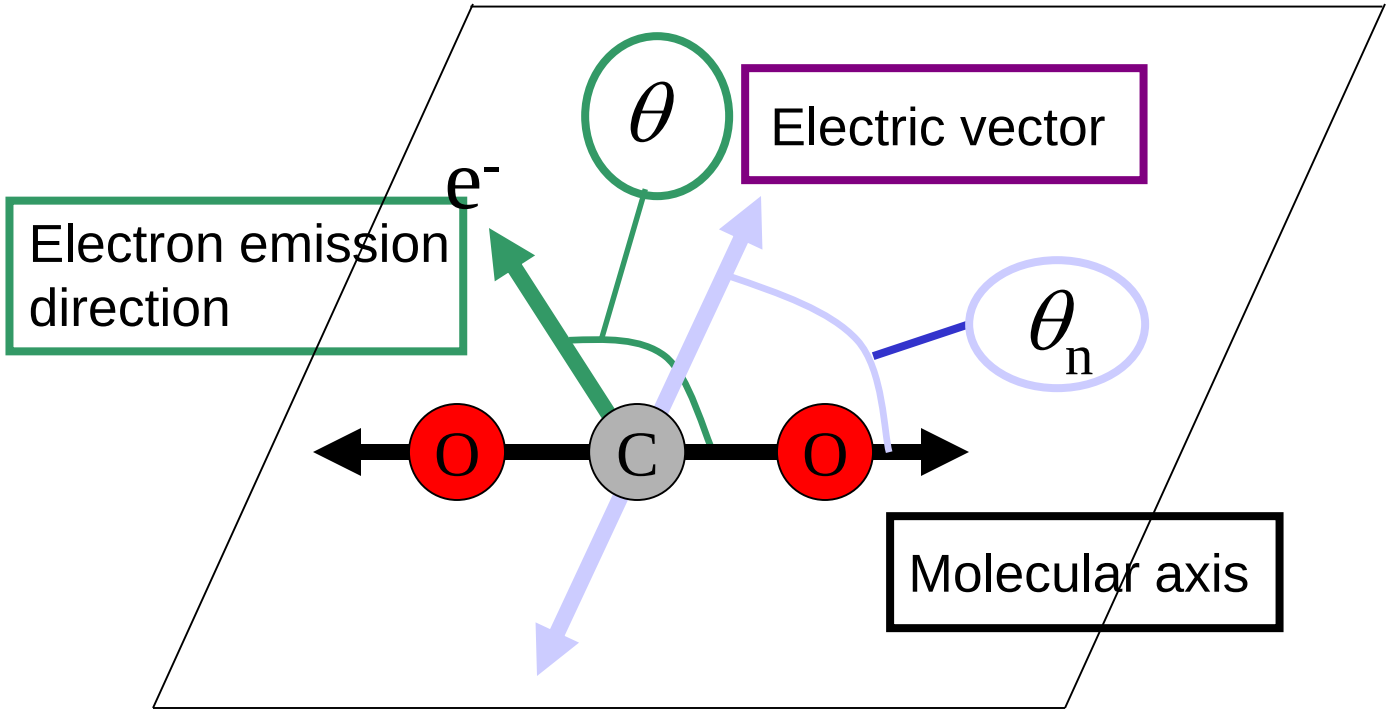

We focus on the electron emission within this reaction plane

C1s photoelectron diffraction (MFPAD) of CO_2: comparison between experiment and theory

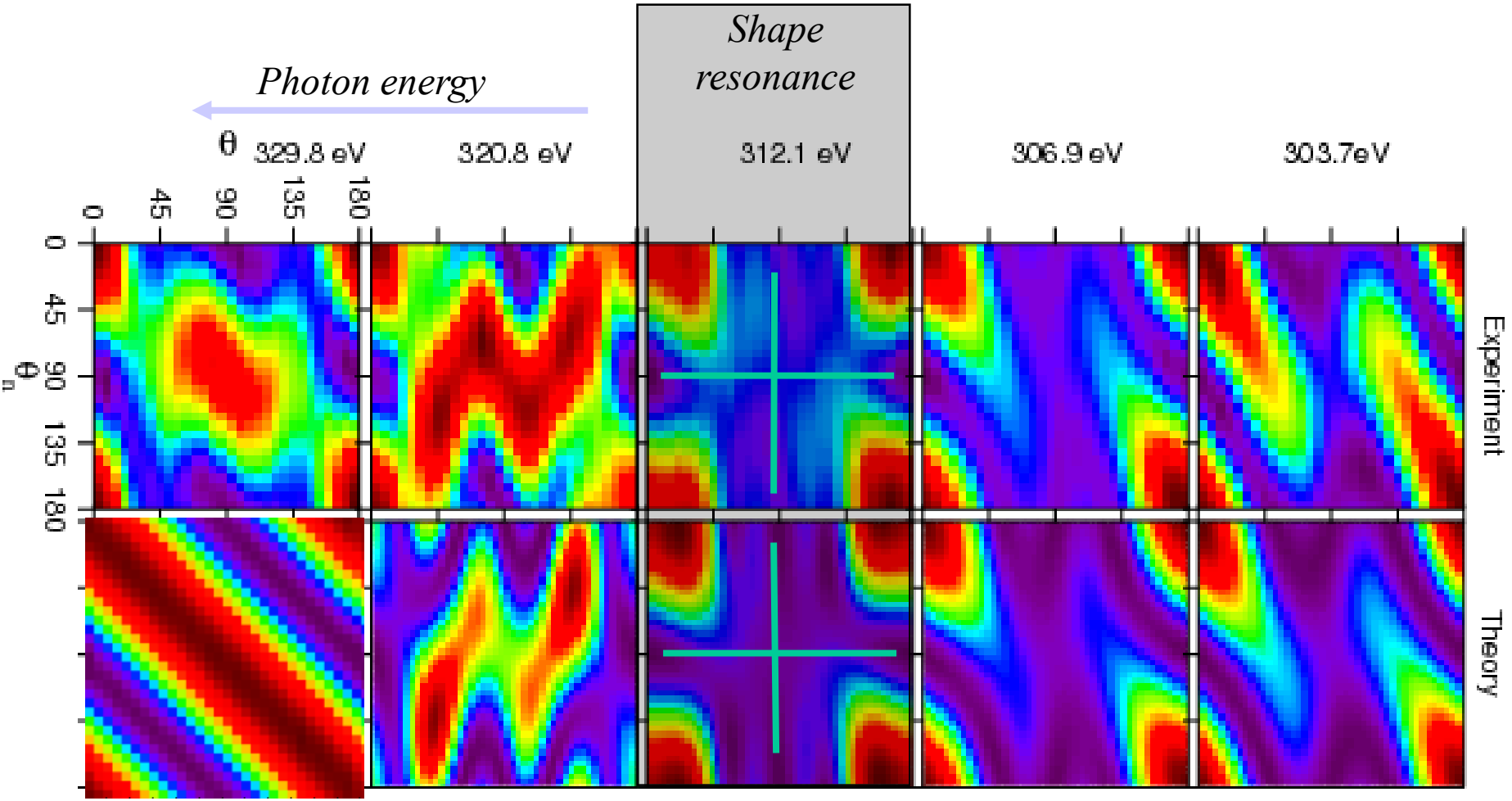

The general agreement between experiment and theory is reasonable.

At the shape resonance, the intensity drops at $\theta_n = 90°$ *i.e.* Σ-Σ *parallel transition. The intensity drops at* $\theta = 90°$, *i.e.,* σ_u *photoelectron wave !*

Near Sendai

Motsu-ji

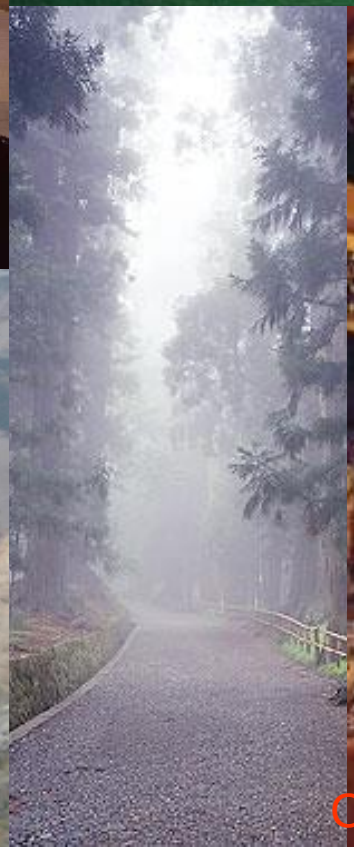

Chuson-ji

Auger vs Interatomic Coulombic Decay (ICD)

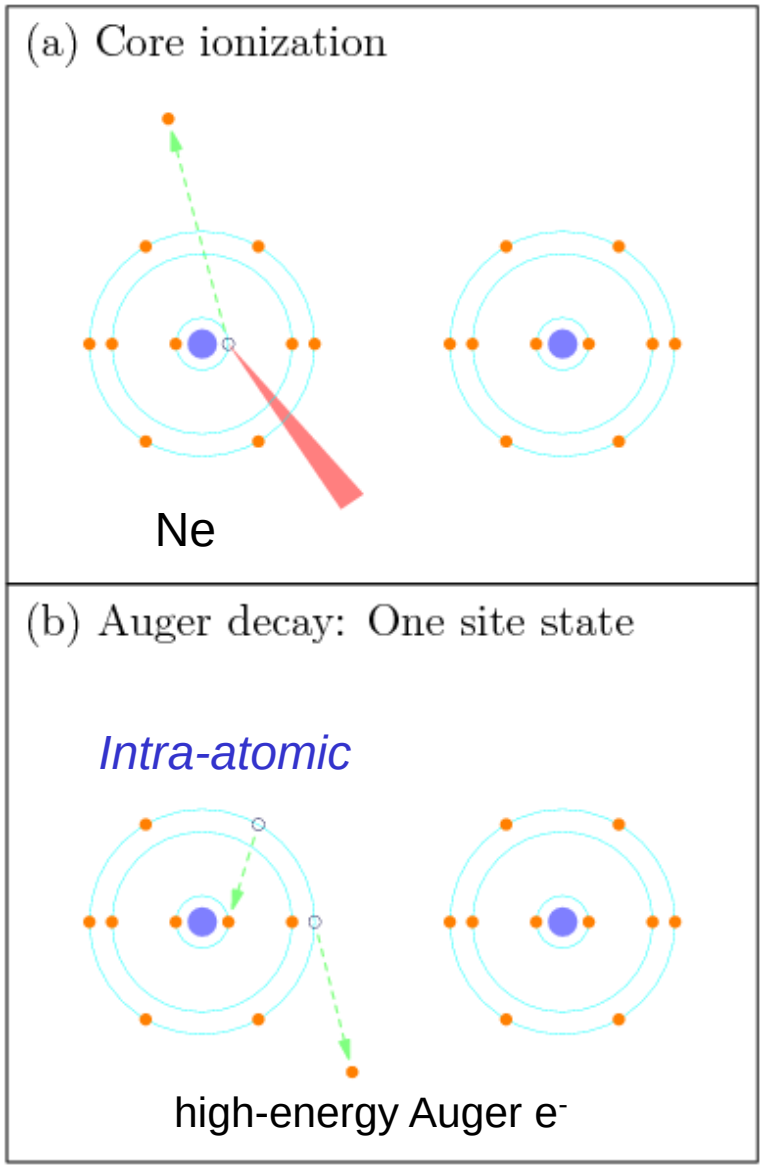

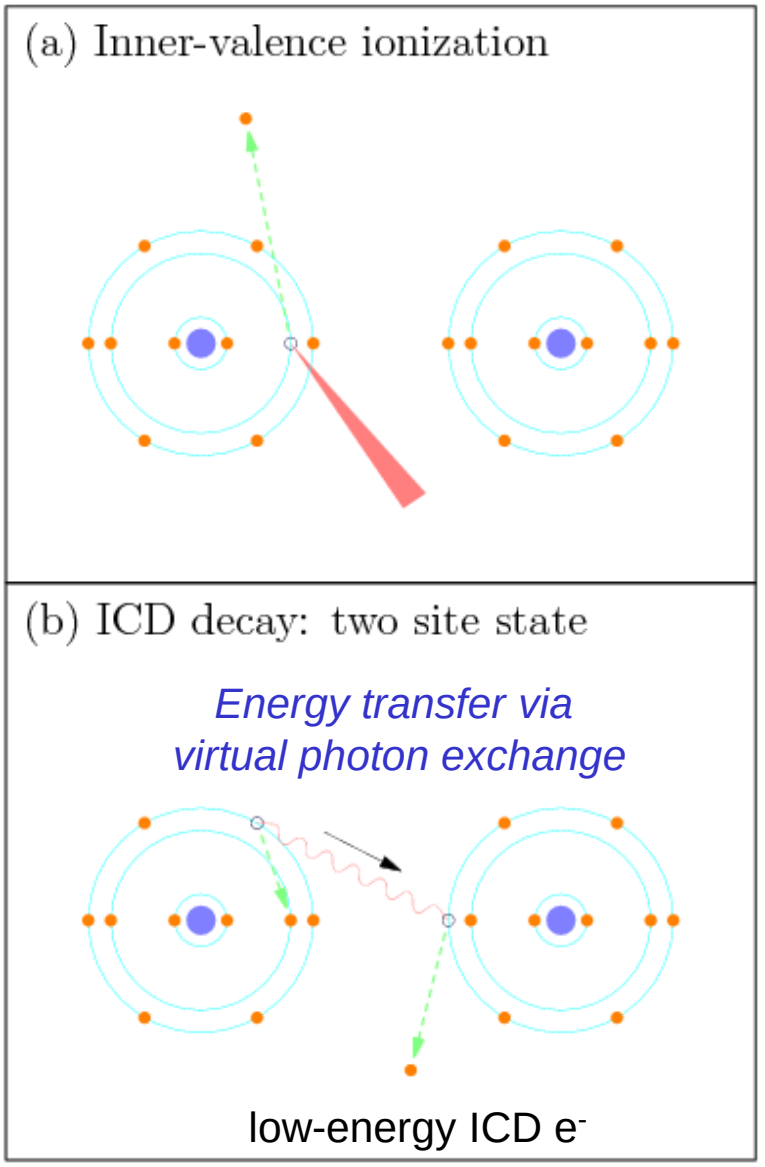

ICD rate is R dependent!

Why is ICD important?

ICD: electronic decay where the environment plays a role!

ICD takes place in van der Waals clusters, in hydrogen bonding clusters, in metallofullerenes, in bio-molecules in the living cell, etc

ICD is everywhere!

ICD is one of the key players in energy and charge transfer in these systems.

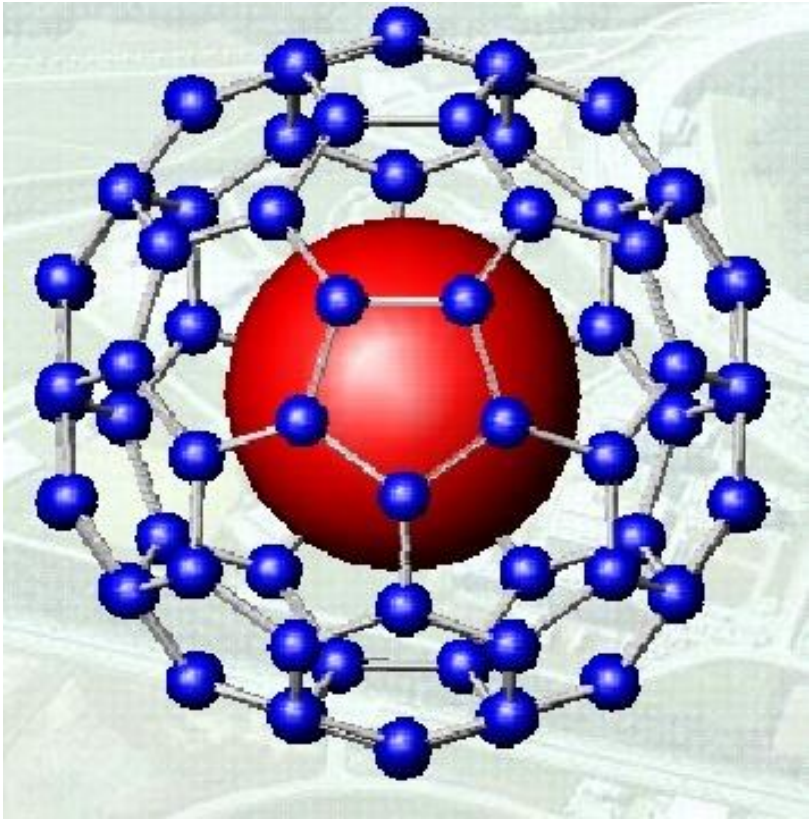

Metal atom in C_{60}

Interatomic Coulombic Decay (ICD)

Theoretical

First prediction - HF cluster:

L.S. Cederbaum, J. Zobeley, and F. Tarantelli, Phys. Rev. Lett. 79, 4778 (1997).

Prediction - Ne dimer:

R. Santra, J. Zobeley, L.S. Cederbaum *et al*., Phys. Rev. Lett. 85, 4490 (2000).

Experimental

First observation - Ne cluster:

U. Hergenhahn and coworkers, Phys.Rev. Lett. 90, 203401 (2003).

Cluster-size-dependent lifetime:

G. Öhrwall *et al*., Phys. Rev. Lett. 93, 173401 (2004).

Ne_2 e-ion-ion coincidence:

R. Dörner and coworkers, Phys. Rev. Lett. 93, 163401 (2004).

ICD after Auger decay in a rare-gas dimer

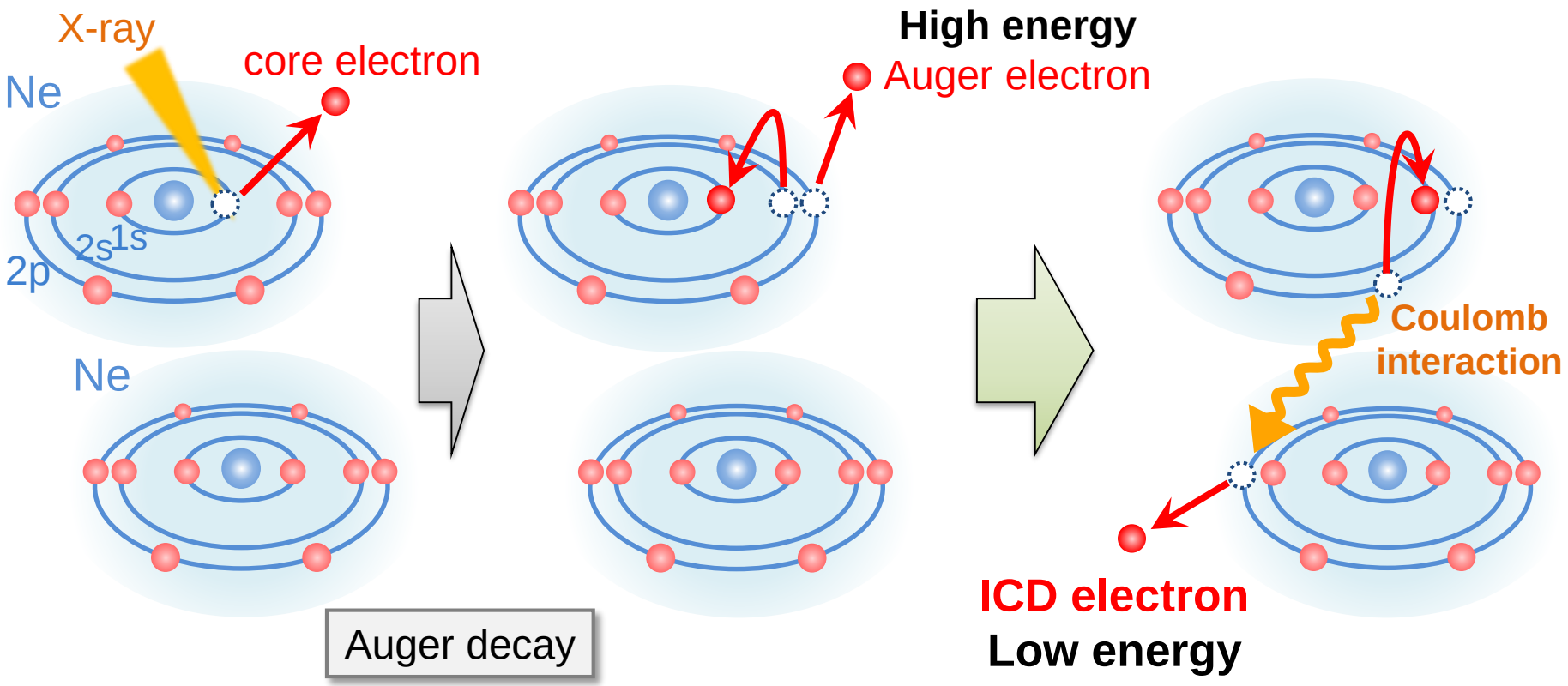

（ICD; Interatomic Coulombic Decay）

If an atom has an inner-valence hole,
the adjacent atom may be ionized via ICD

R. Santra and L. S. Cederbaum, Phys. Rev. Lett. **90**, 153401 (2003).

Why is ICD after Auger decay important?

Radiation damage caused in bio-molecules in the living cell

Radiation damage, caused by e.g., X-ray radiation, is initiated by core ionization.

Radiation damage is known to be caused by low energy electron collisions, not high energy Auger electrons.

ICD is one of the important mechanisms to produce low energy electrons after Auger decay!

Prediction of ICD after ICD Auger decay in Ne_2

R. Santra and L.S. Cederbaum, PRL **90**, 153401 (2003).

Prediction of ICD after resonant after Auger decay in ArKr

K. Gokhberg, P. Koloren, A. I. Kuleff & L.S. Cederbaum, submitted

Controlling electron emission and thus radiation damage site specifically => principle of radiation therapy

First experiment of interatomic Coulombic decay after Auger decay in Ar_2

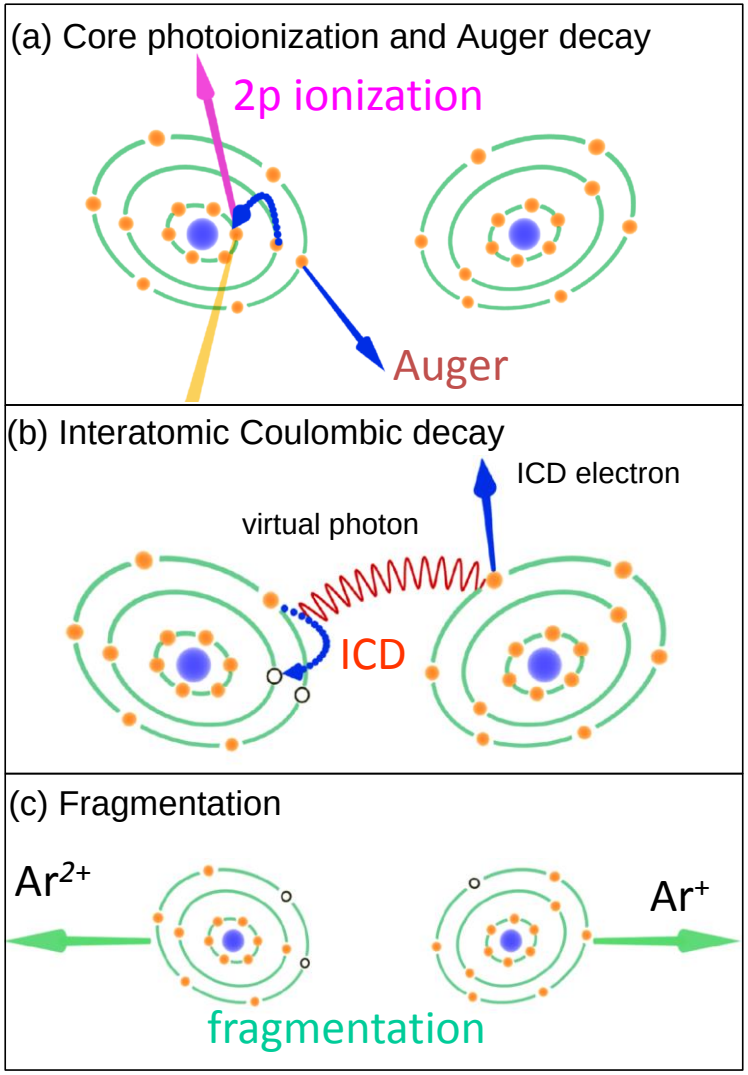

Y. Morishita, X.-J. Liu, N. Saito, T. Lischke, M. Kato, G. Pruemper, M. Oura, H. Yamaoka, J. Harries, Y. Tamenori, I.H. Suzuki, and K. Ueda Phys. Rev. Lett. **96**, 243402 (1)-(4) (2006)

K. Ueda *et al.* JESRP **155**, 113-118 (2007)

ArKr

Y. Morishita et al. J. Phys. B **41,** 025101 (2008)

K. Ueda et al. JESRP **166-167,** 3 (2008)

We detect ICD electrons in coincidence with Ar^{+} and Ar^{2+} using e-i-i coincidence momentum spectroscopy

Interatomic Coulombic decay after Auger decay in Ne_2

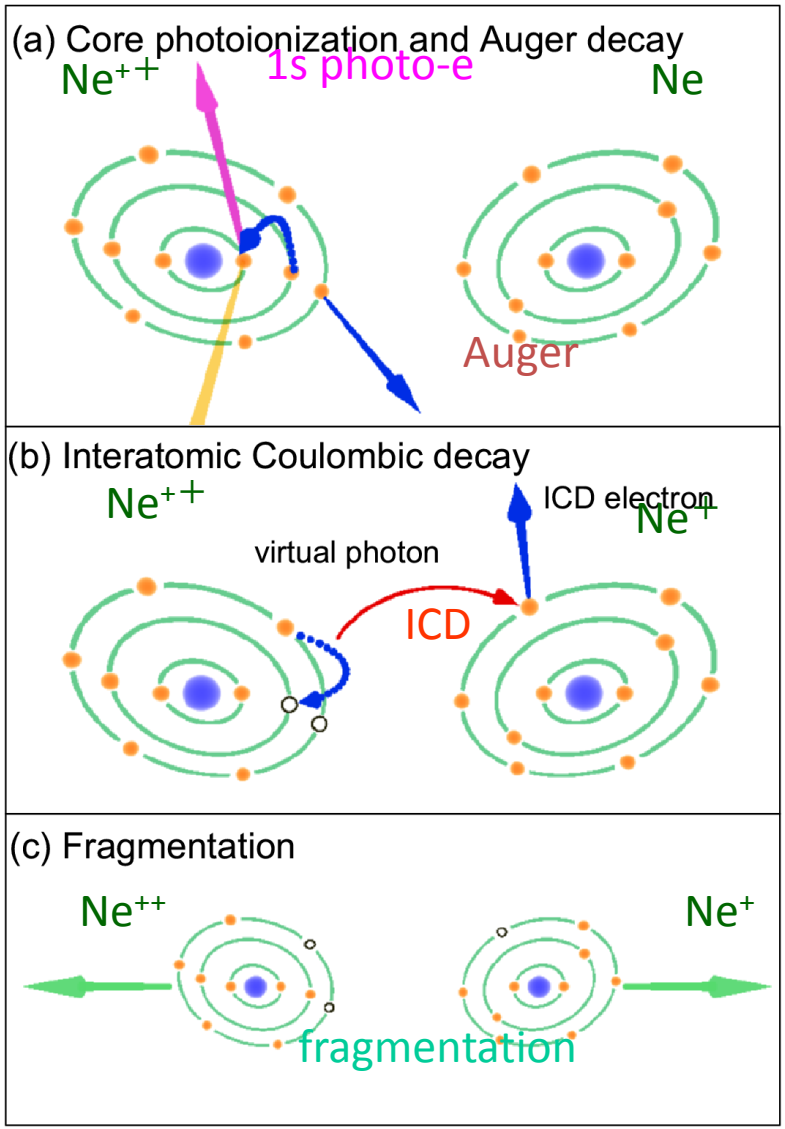

K. Kreidi, T. Jahnke, …… , R. Doener

X.J. Liu, Y. Morishita, …, K. Ueda

J. Phys. B. **41**, 101002 (2008)

Phys. Rev. A **78**, 043422 (2008)

Phys. Rev. Lett. **103**, 033001 (2009)

J. Phys.: Conf. Ser. **212**, 012007 (2010)

Phys. Rev. A **85**, 043421 (2012)

We detect ICD electrons in coincidence with Ne^+ and Ne^{2+}using e-i-i coincidence momentum spectroscopy

ICD after Ne 1s Auger decay in NeAr

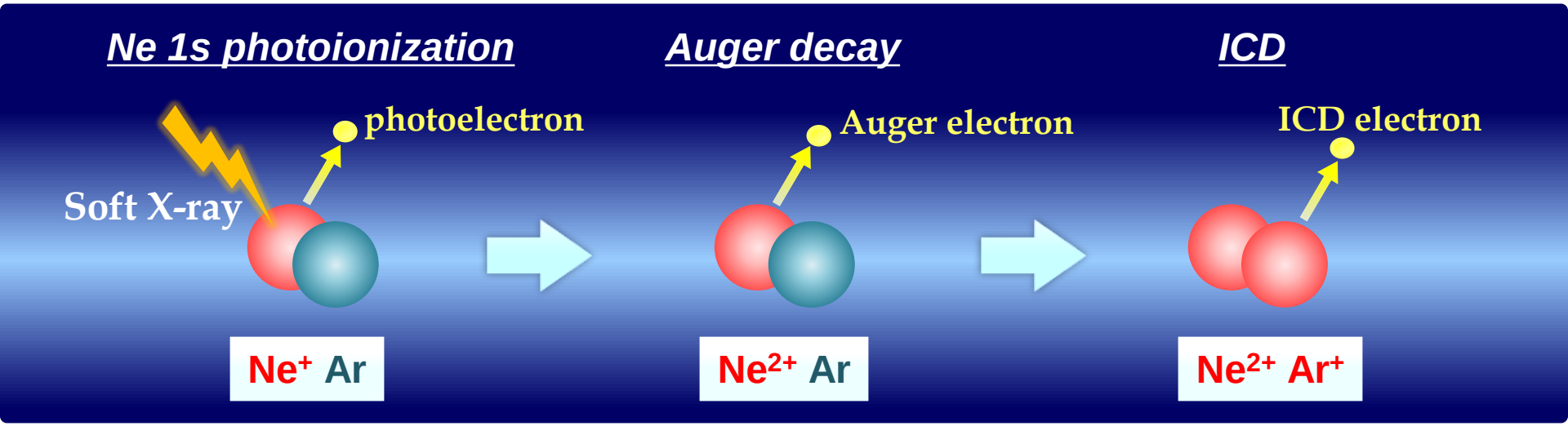

$h\nu$ = 889 eV

(the atomic Ne 1s ionization threshold: 870 eV)

Ion–ion coincidence TOF map

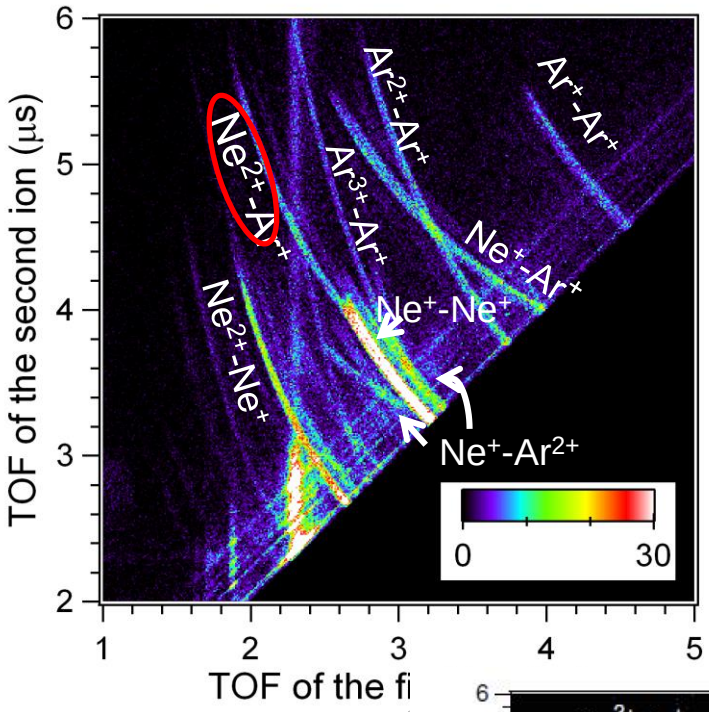

Homodimers (Ne-Ne, Ar-Ar) and heterodimers (Ne-Ar) are produced.

We can distinguish target dimers from others by using momentum conservation law.

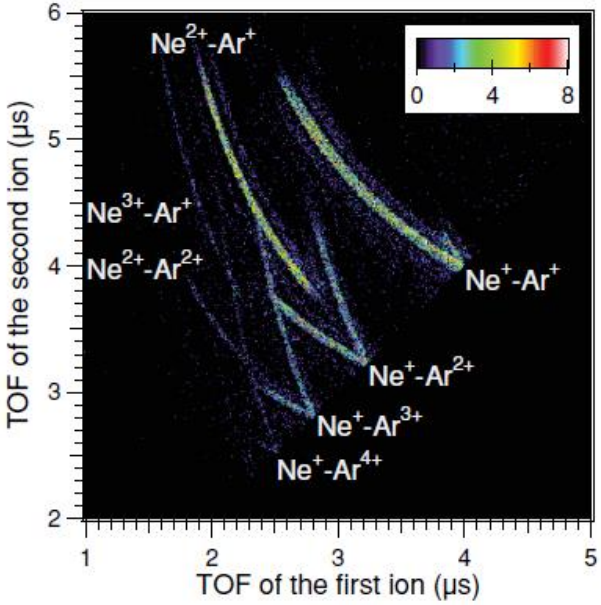

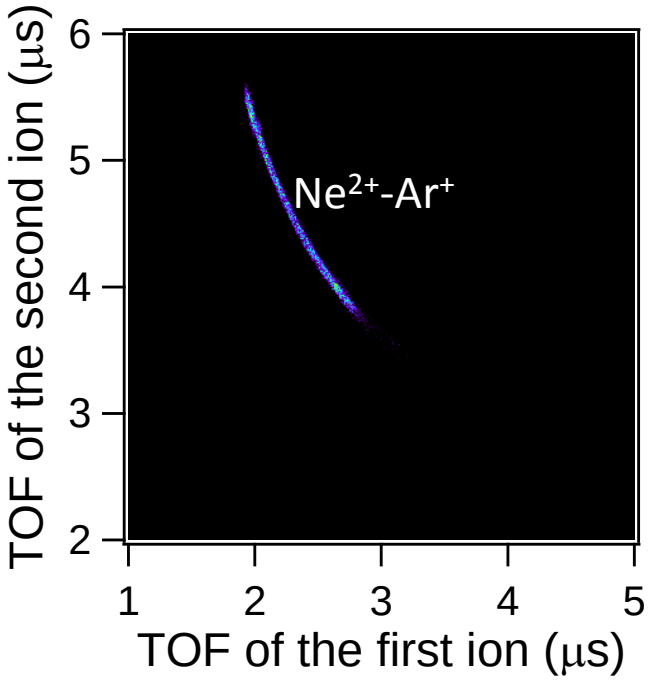

Ne^{2+}-Ar^{+} -electron coincidence events

Ne^{2+}-Ar^{+} coincident Electron spectrum

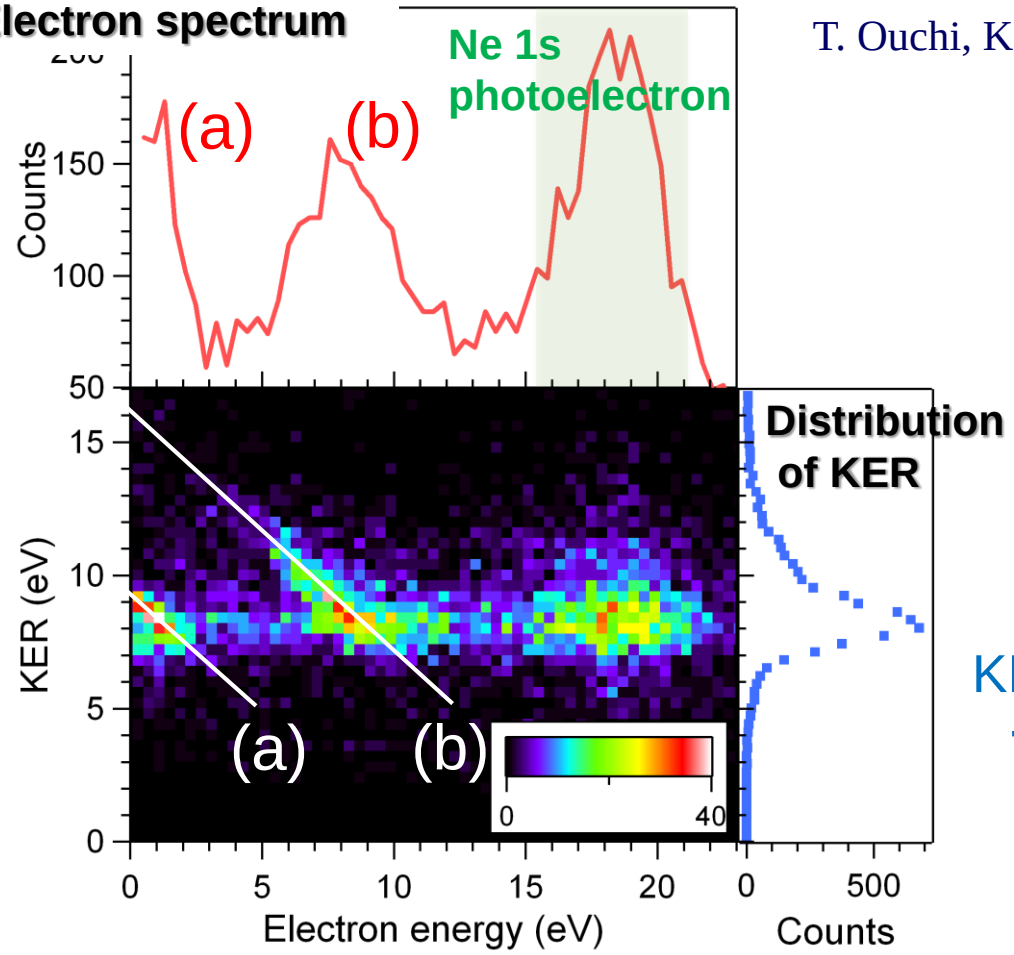

Ph.V. Demekhin *et al.*, *J. Chem. Phys.* **131**, 104303 (2009)
T. Ouchi, K. Sakai *et al.*, *Phys. Rev. A*, **80**, 053415 (2011)

Sum of the kinetic energies of the two fragment ions (KER; Kinetic Energy Release)

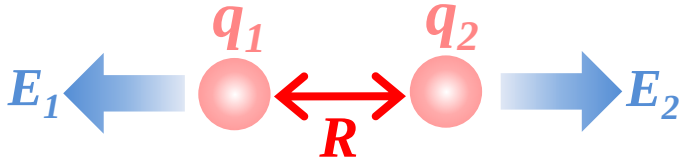

$$\mathrm{KER} = E_1 + E_2 = \frac{1}{4\pi\varepsilon_0} \times \frac{q_1 q_2}{R}$$

(Coulomb law)

KER peak ~ 8.2 eV
→ R = 3.5 Å

This distance coincides with the equilibrium distance of the neutral ground state of NeAr.

(a) ICD

$Ne^{2+}(2s^{-1}2p^{-1}\ {}^3P)$–Ar
→ $Ne^{2+}(2p^{-2}\ {}^3P)$–$Ar^{+}(3p^{-1})$

(b) ICD

$Ne^{2+}(2s^{-1}2p^{-1}\ {}^1P)$–Ar
→ $Ne^{2+}(2p^{-2}\ {}^1D)$–$Ar^{+}(3p^{-1})$

Extraction of the ICD lifetime from line shape

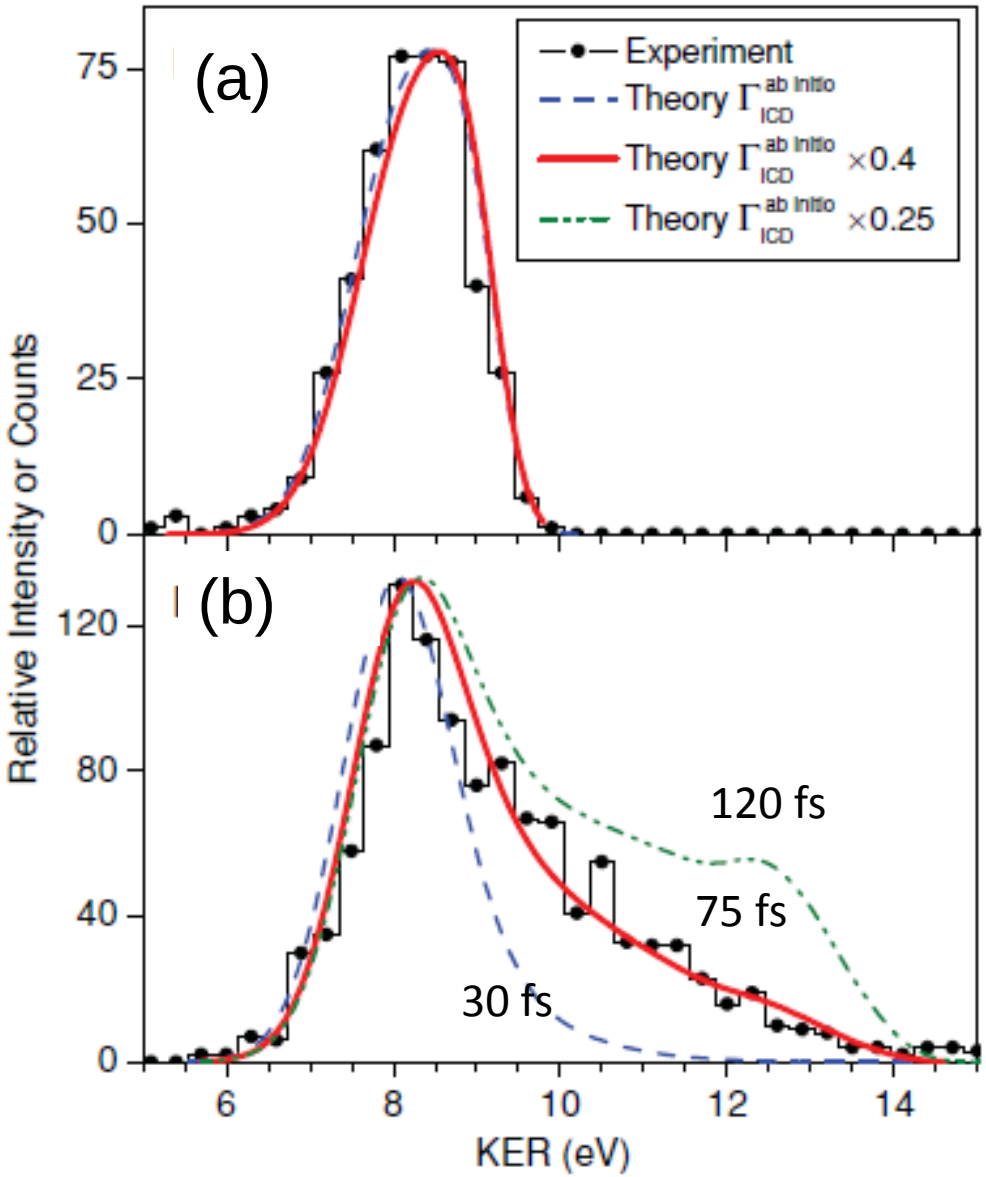

A long tail of Peak (b) comes from nuclear dynamics within ICD lifetime !

ICD lifetime of ~75 fs has been determined for the first time!

T. Ouchi, K. Sakai *et al.*, *Phys. Rev. A*, **80**, 053415 (2011).

Energy level diagram

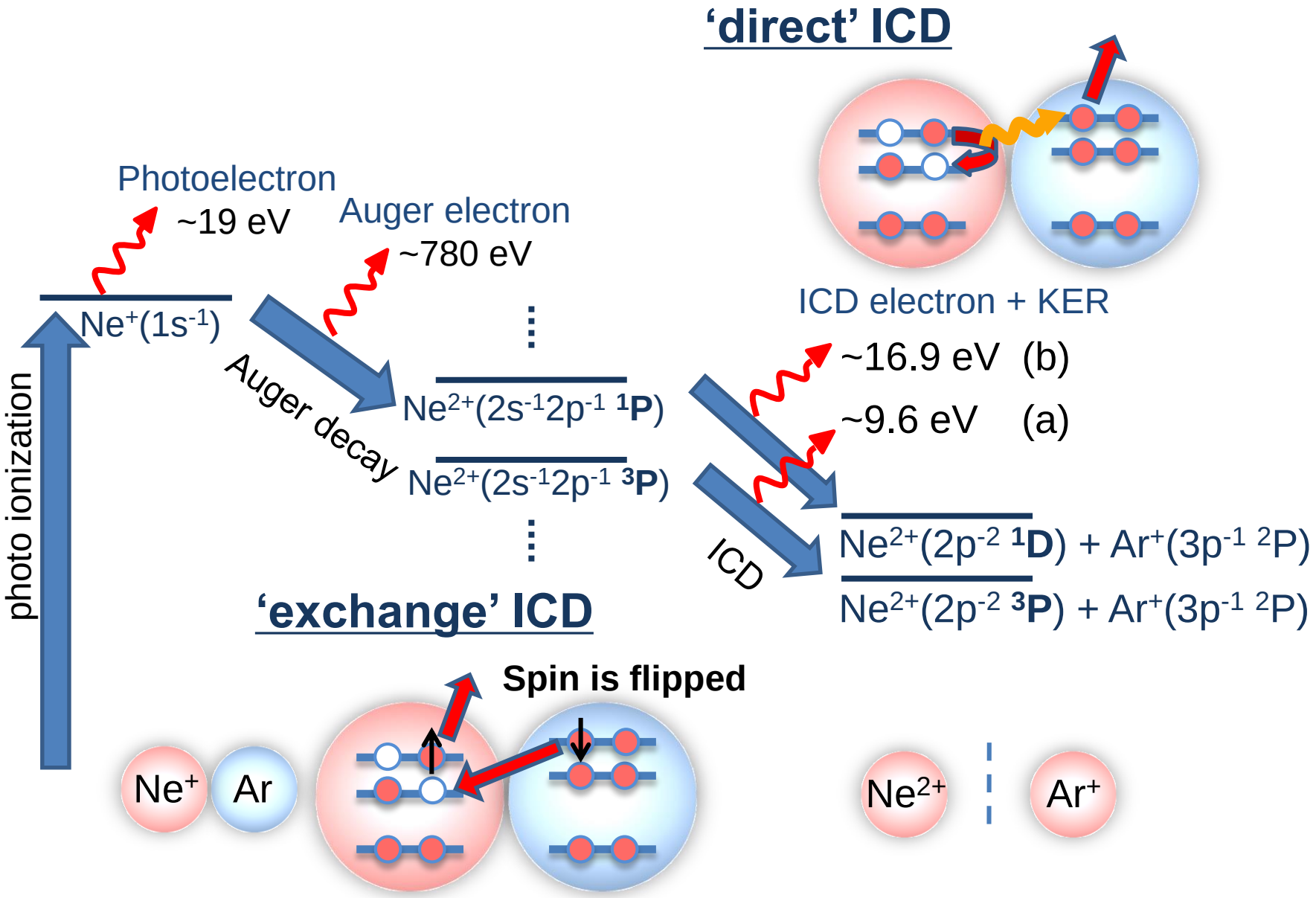

Kreidi *et al.* J. Phys. B. **41**, 101002 (2008)

ICD after resonant Auger decay

(1) Resonant excitation

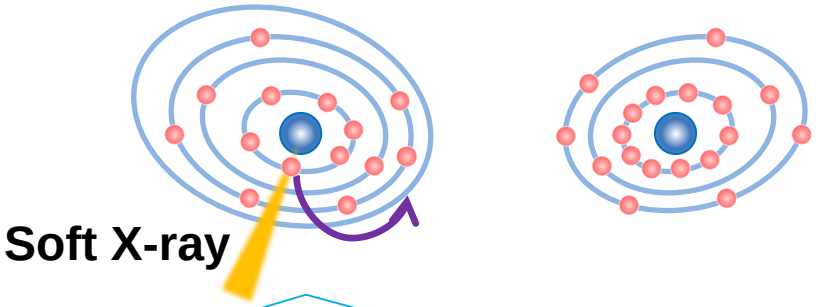

Promotion of an inner-shell electron to the unoccupied orbital

(2) Resonant Auger decay

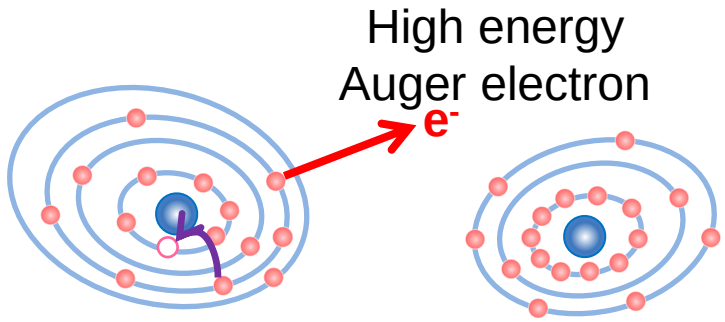

Creation of an inner-valence hole

(3) ICD

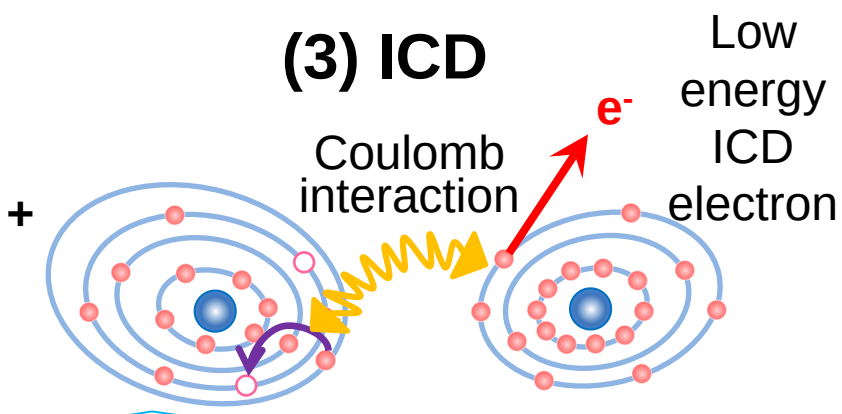

Ionization of the adjacent atom via ICD

(4) Coulomb explosion

Dissociation via Coulomb repulsion

We detect ICD electrons in coincidence with two singly-charged ions.

Theory: Kirill Gokhberg, Premysl Koloren, Alexander I. Kuleff & Lorenz S. Cederbaum (submitted)

Photo-excitation energies

Total ion yield spectrum

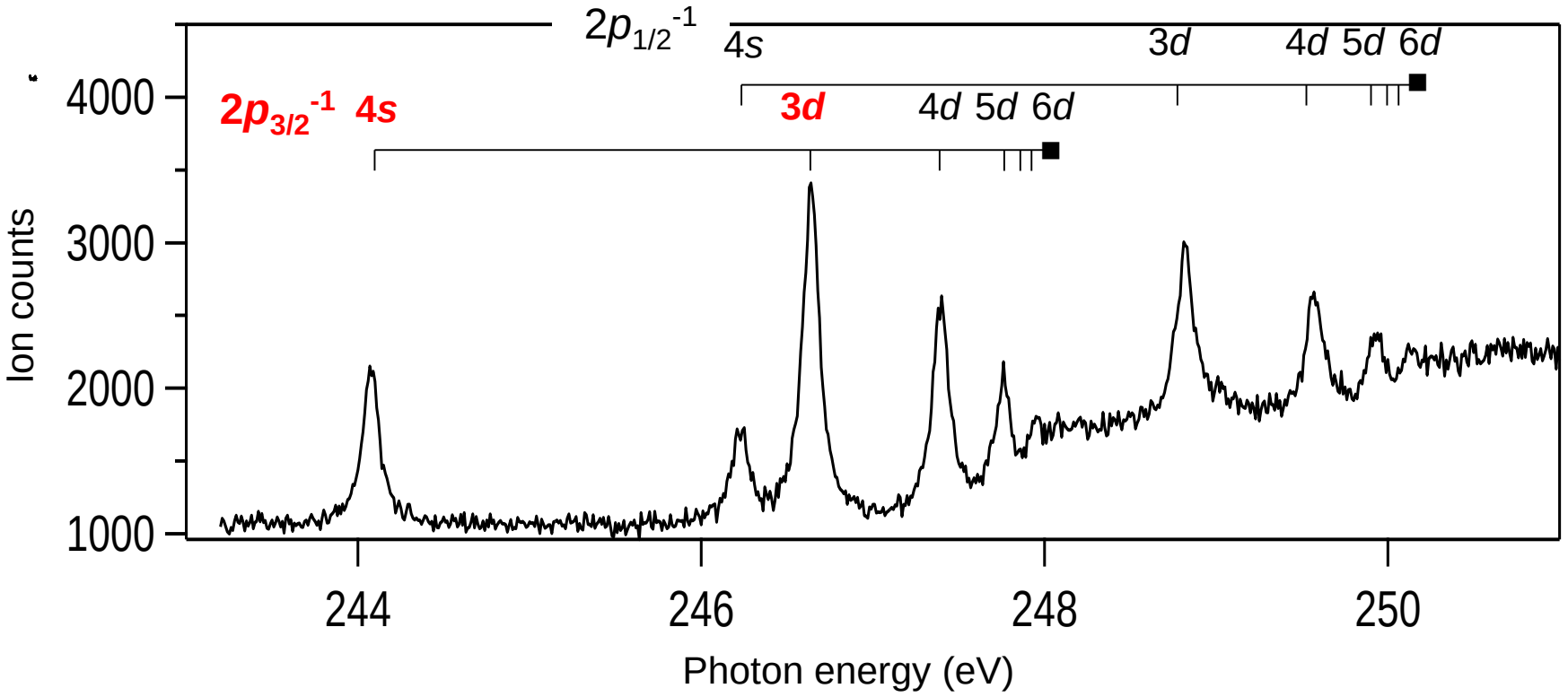

Ar $2p_{3/2} \rightarrow 4s$: 244 eV

Ar $2p_{3/2} \rightarrow 3d$: 247 eV

Ar^+-Kr^+ - electron coincidence events at Ar 2p → 4s excitation

Electron spectrum coincident with Ar^+-Kr^+

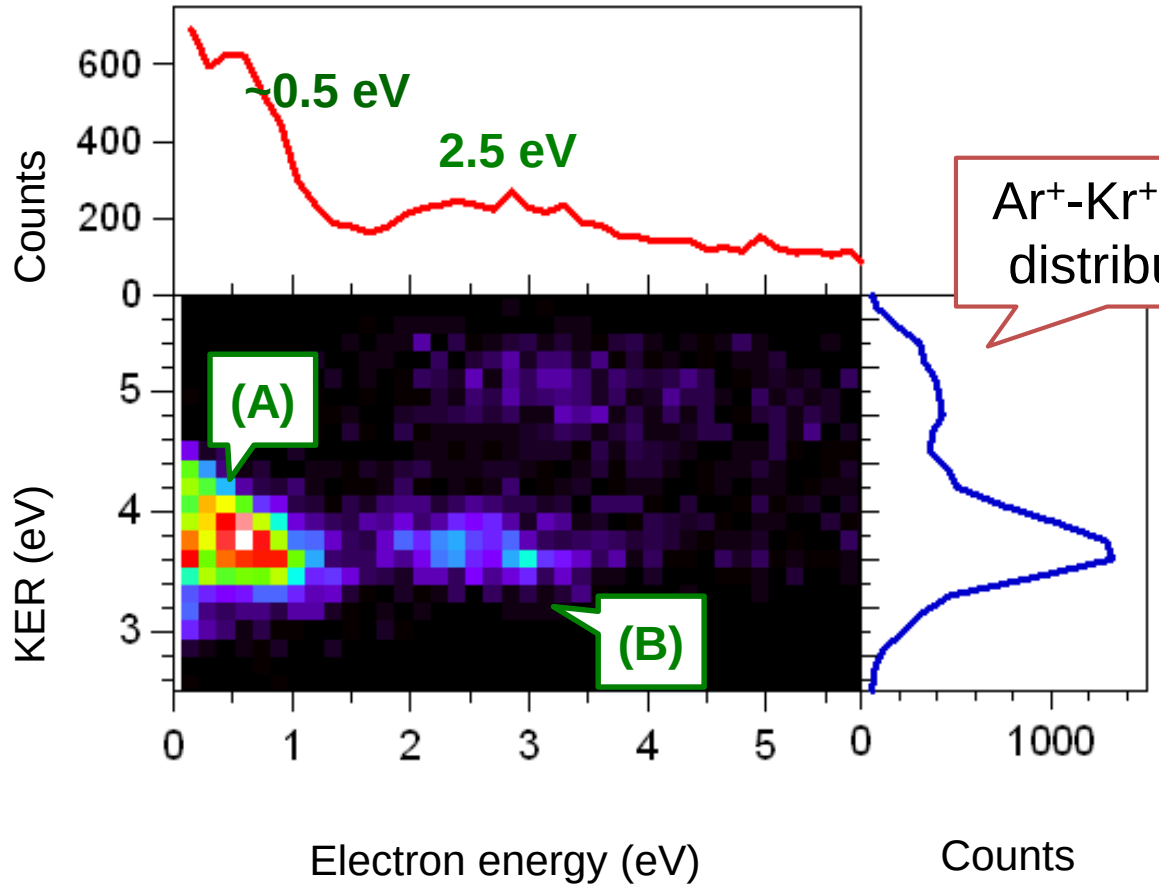

Ar^+-Kr^+ KER distribution

KER = 3.7 eV (*R* = 3.9 Å)

(A) KER = 3.7 eV <–> electron energy ~ 0.5 eV
(B) KER = 3.7 eV <–> electron energy ~ 2.5 eV
Both ICDs take place at *R* = ~3.9 Å(equilibrium bond length)

ICD after Ar 2p → 4s excitation in ArKr [244 eV]

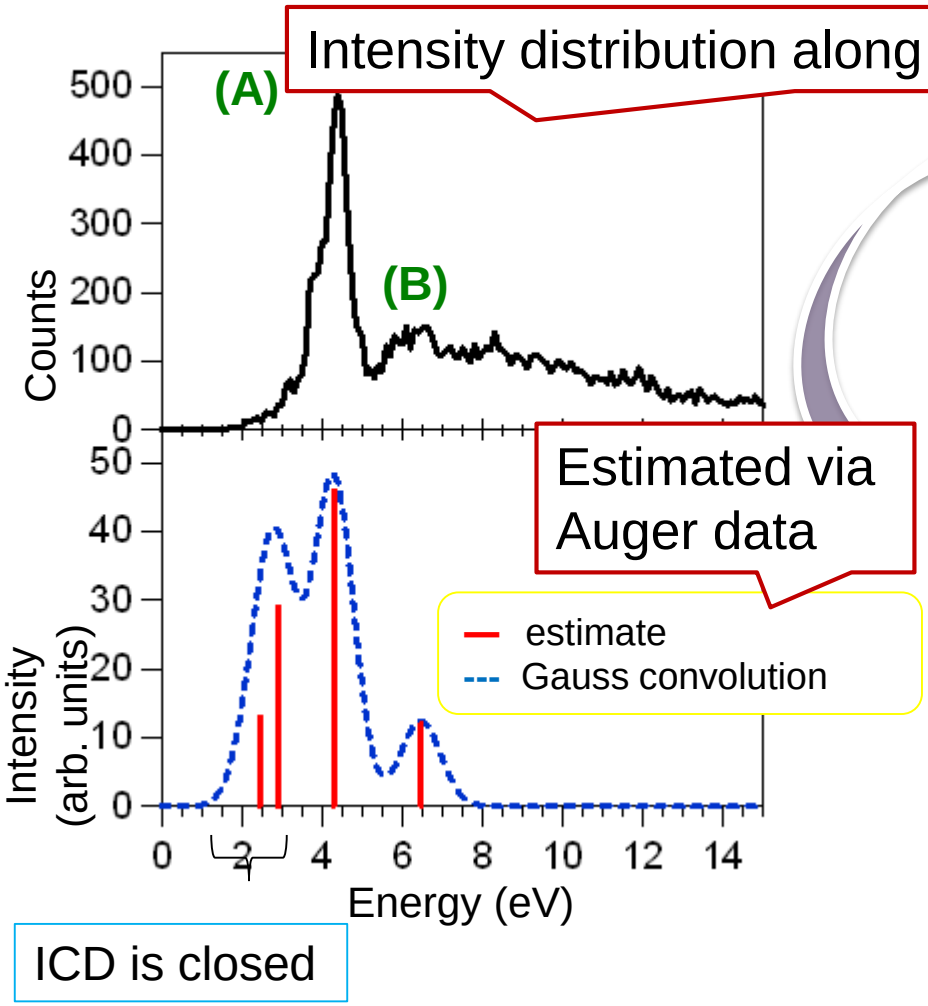

Energies are calculated as

E = Auger final state energy

- $Ar^+(3p^{-1})Kr^+(4p^{-1})$ ICD final state energy

Intensities are estimated from branching ratios of Auger transitions

	Auger final state	Energy (eV)	Intensity (%)
(A)	$3p^4\ (^1D/^3P)3d\ ^2D$	4.16	46
(A)	$3p^4\ (^1D)4s\ ^2D$	4.42	
(B)	$3p^4(^1S)4s\ ^2S$	6.46	12

[2] M. Meyer, *et al.*, *Phys. Rev. A*, **49** 3685 (1994).

(A) $Ar^+ (3p^{-2}(^1D/^3P)3d\ ^2D), 3p^{-2}(^1D)4s\ ^2D), –Kr \rightarrow Ar^+ (3p^{-1})\text{-}Kr^+ (4p^{-1})$

(B) $Ar^+ (3p^{-2}(^1S)4s\ ^2S)–Kr \rightarrow Ar^+ (3p^{-1})\text{-}Kr^+ (4p^{-1})$

ICD may take place at ~60 % probability….

Ar^+-Kr^+ - electron coincidence events at Ar 2p → 3d excitation

Electron spectrum coincident with Ar^+-Kr^+

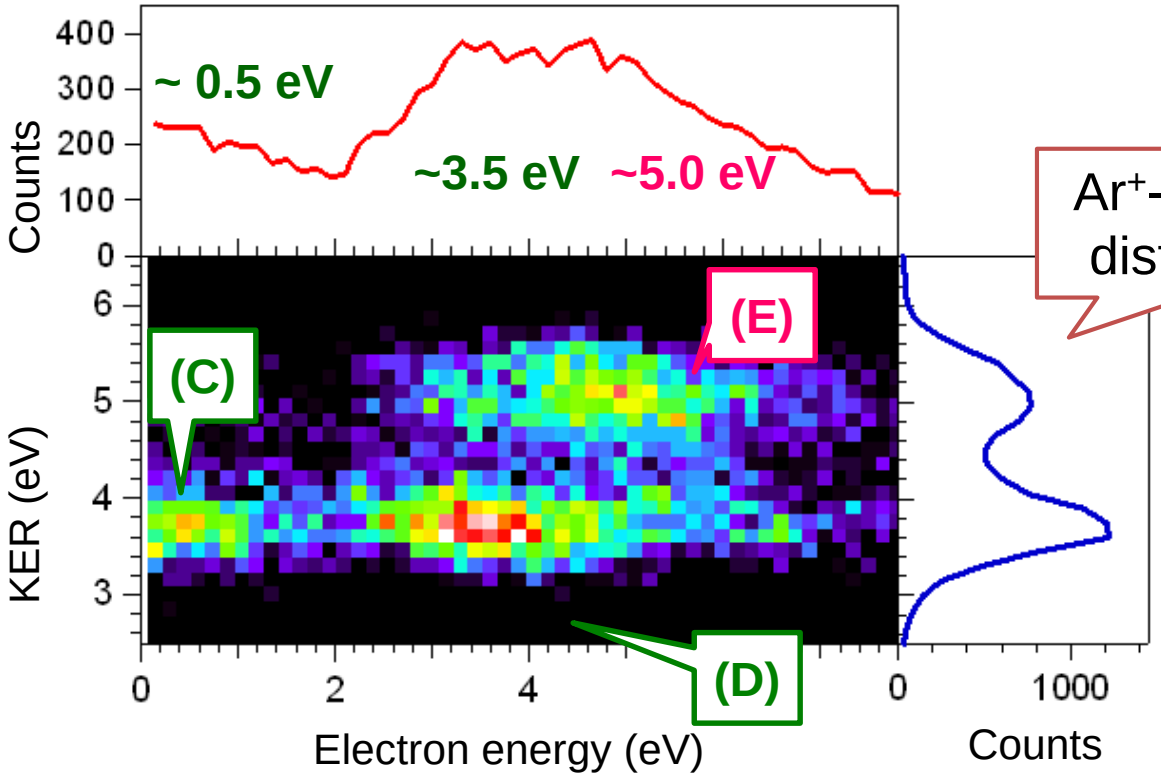

Ar^+-Kr^+ KER distribution

KER = 5.0 eV (*R* = 2.9 Å)

KER = 3.7eV (*R* = 3.9 Å)

(C) KER = 3.7 eV <–> electron energy: ~ 0.5 eV

(D) KER = 3.7 eV <–> electron energy : ~ 3.5 eV

ICD takes place at *R* = ~3.9 Å (equilibrium bond length)

(E) KER = 5.0 eV <–> electron energy : ~ 5 eV

ICD takes place at *R* = ~2.9 Å (Van-der Waals wall)

ICD after Ar 2p → 3d excitation in ArKr [247 eV]

Intensity distribution along KER + electron energy

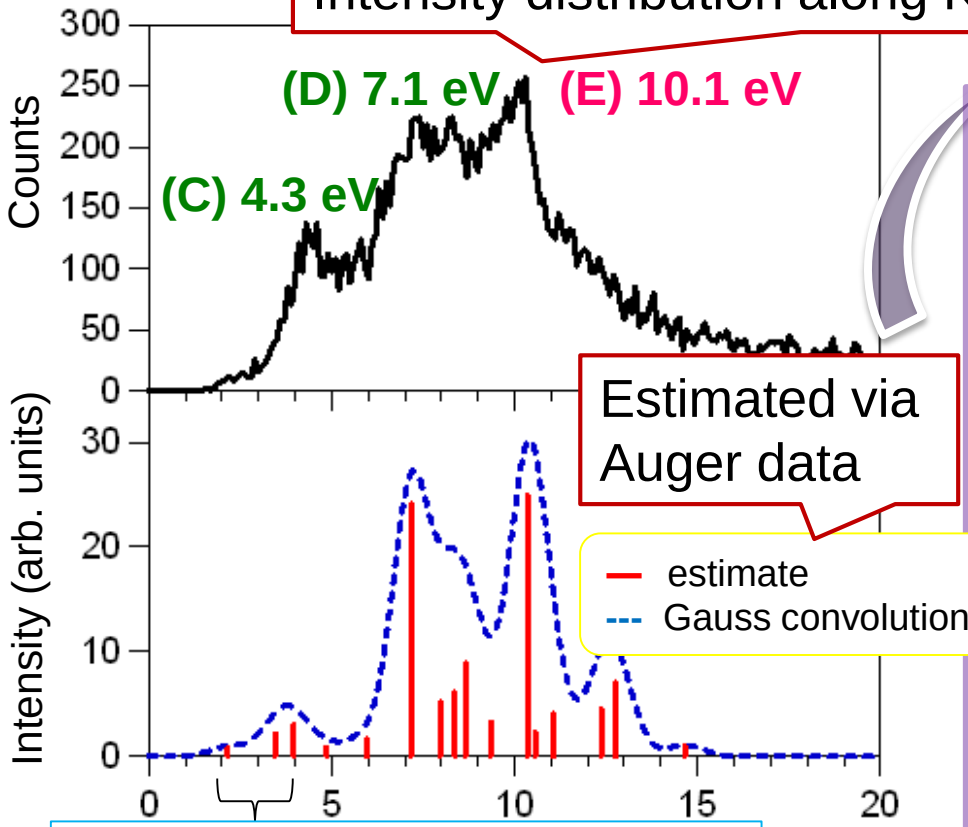

ICDへのチャンネルが閉じている

Energies are calculated as

E = Auger final state energy
- $Ar^+(3p^{-1})Kr^+(4p^{-1})$ ICD final state energy

Intensities are estimated from branching ratios of Auger transitions

	Auger final state	Energy (eV)	Intensity (%)
(C)	$3p^{-2}(^3P)3d$ $^4P + ^2F + ^2D + 4s\ ^2D$	3.96	3.01
(D)	$3p^4(^1D)3d\ ^2D + ^2P$	6.88	24.08
(E)	$3p^4(^1D)4d$ $^2G + ^2P + ^2D + ^2F$	10.08	24.91

[3] M. Meyer *et al.*, *Phys. Rev. A* **43**, 177 (1991).

(C) $Ar^+ (3p^{-2}(^3P)3d\ ^4P + ^2F + ^2D + 4s\ ^2P)$-Kr → $Ar^+ (3p^{-1})$-$Kr^+ (4p^{-1})$

(D) $Ar^+ (3p^{-2}(^1D)3d\ ^2D)$–Kr → $Ar^+ (3p^{-1})$-$Kr^+ (4p^{-1})$

(E) $Ar^+ (3p^{-2}(^1D)4d\ ^2D)$–Kr → $Ar^+ (3p^{-1})$-$Kr^+ (4p^{-1})$

ICD may take place at ~97 % probability….

ICD after Ar 2p → 3d excitation in Ar2 [247 eV]

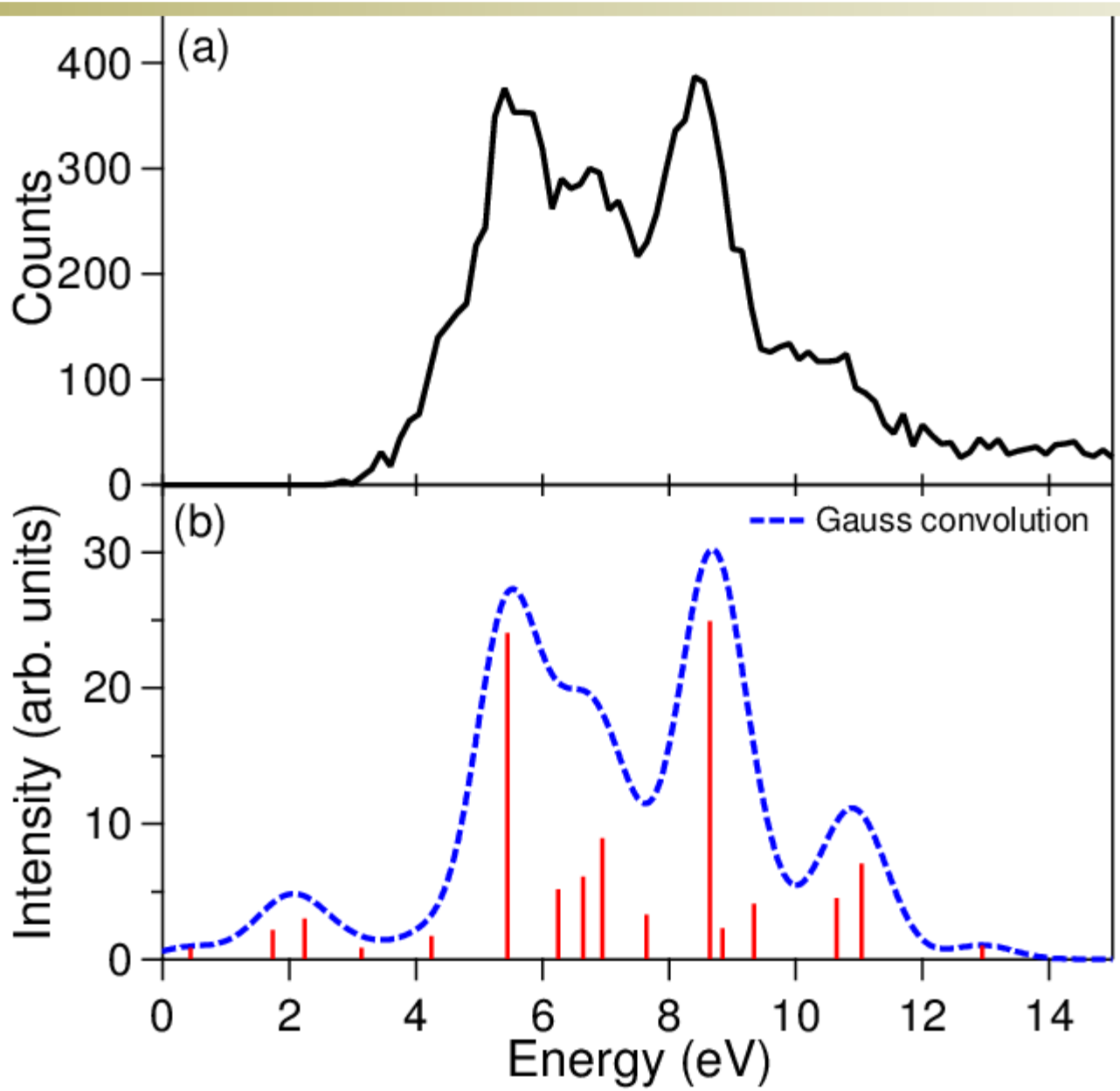

ICD electron energy spectra

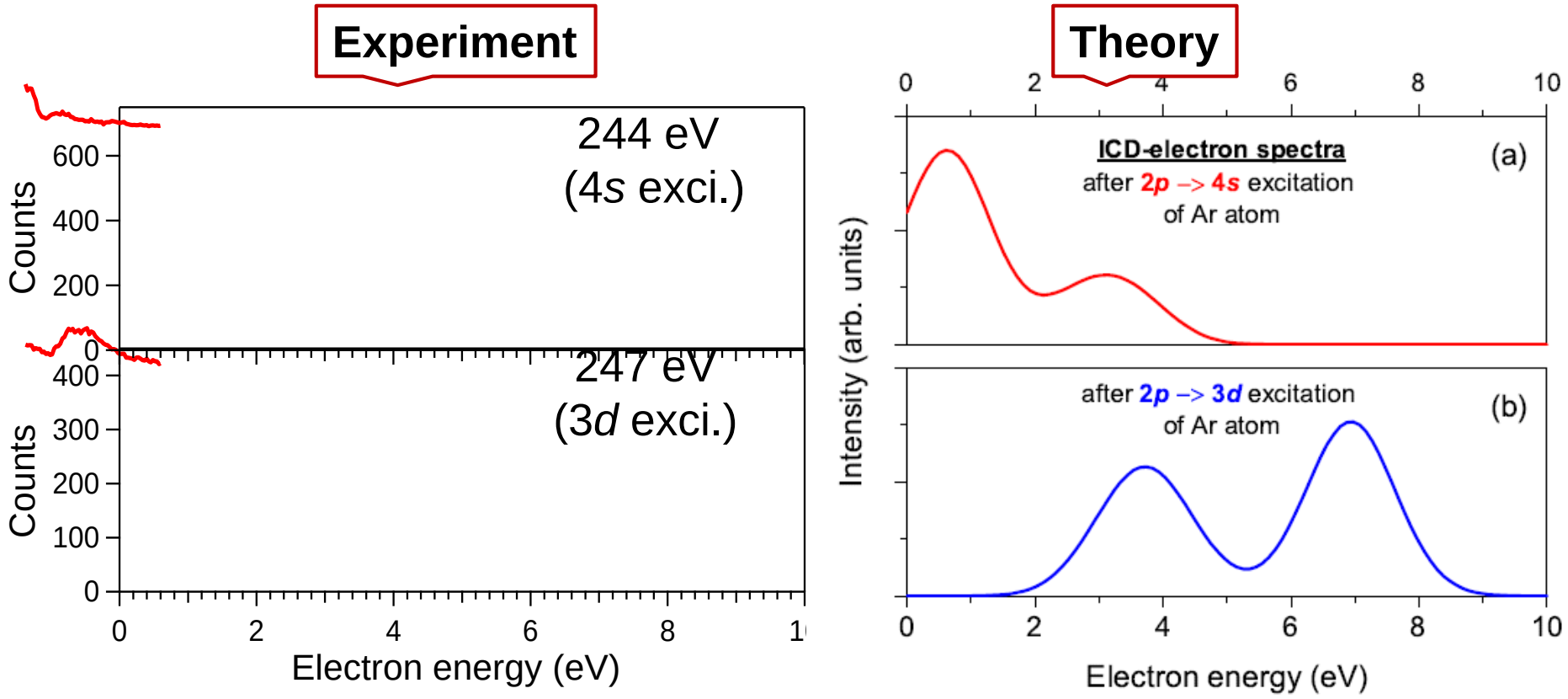

Resonant-Auger-induced ICD

Gokhberg et al.

One can generate low-energy electron site specifically.

One can control the energy of electrons via photo-excitation energy.

One can control the radiation damage site specifically (radiation therapy!)

ICD gangs in Germany and Japan !

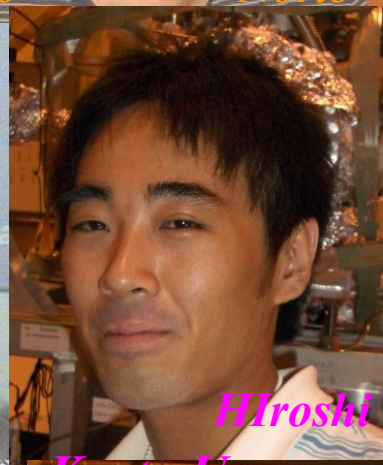

EUV-X FELs in the world

Swiss FEL (2017), Korean FEL, Shanghai FEL, etc., are coming!

Single-shot X-ray imaging by XFEL

Before **During ~10 fs** **After ~50 fs**

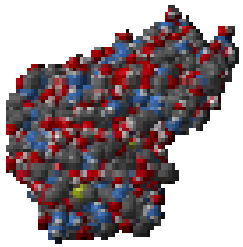

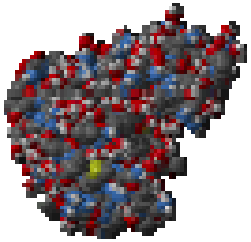

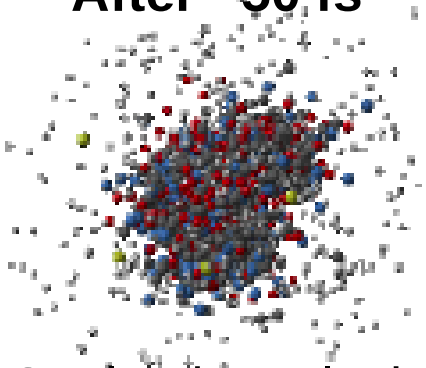

Coulomb explosion

Diffraction pattern

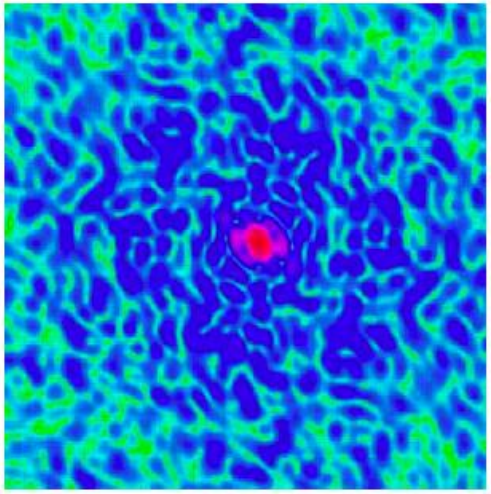

3D reconstruction possible from many views

Needs more photons….

Radiation damage….

R. Nertze *et al*., Nature **406**, 752 (2000).

Serial femtosecond x-ray crystallography: phasing

Femtosecond X-ray Protein Nanocrystallography ,Chapman et al., Nature 470, 73–77 (2011).

*High-Resolution Protein Structure Determination by Serial Femtosecond Crystallography, Boutet et al. Science **337**, 362 (2012).*

*Natively Inhibited Trypanosoma brucei Cathepsin B Structure Determined by Using an X-ray Laser, Redecke et al. Science **339**, 227 (2013).*

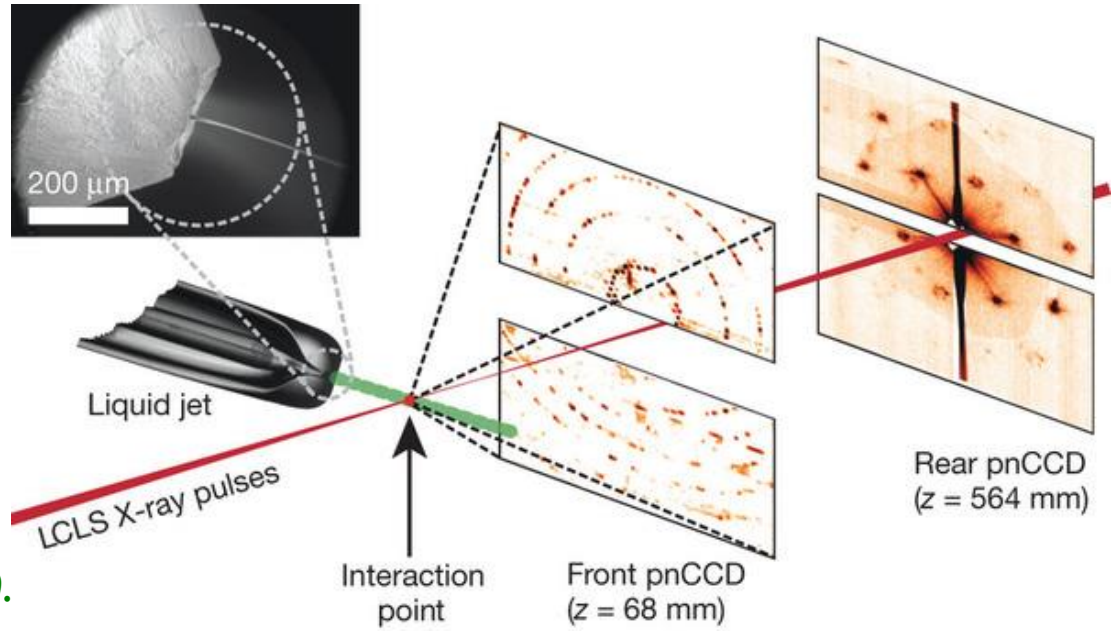

Phasing of the serial femtosecond x-ray crystallography has been dependent on molecular replacements…

*If the structure is completely unknown, phasing approaches make use of anomalous dispersion in the scattering signals from specific **heavy** atoms.*

Multi-wavelength anomalous diffraction at high X-ray intensity
*S.-K. Son, H. N. Chapman, and R. Santra, Phys. Rev. Lett. **107**, 218102 (2011).*
However…..
De novo protein crystal structure determination from X-ray free-electron laser data
T.R.M. Barends et al., Nature (2013) doi:10.1038/nature12773
Conventional phasing method based on anomalous dispersion worked !

Characteristic properties of FEL pulses

Intense 10^{14} W/cm^2 (EUV) - 10^{20} W/cm^2 (X)

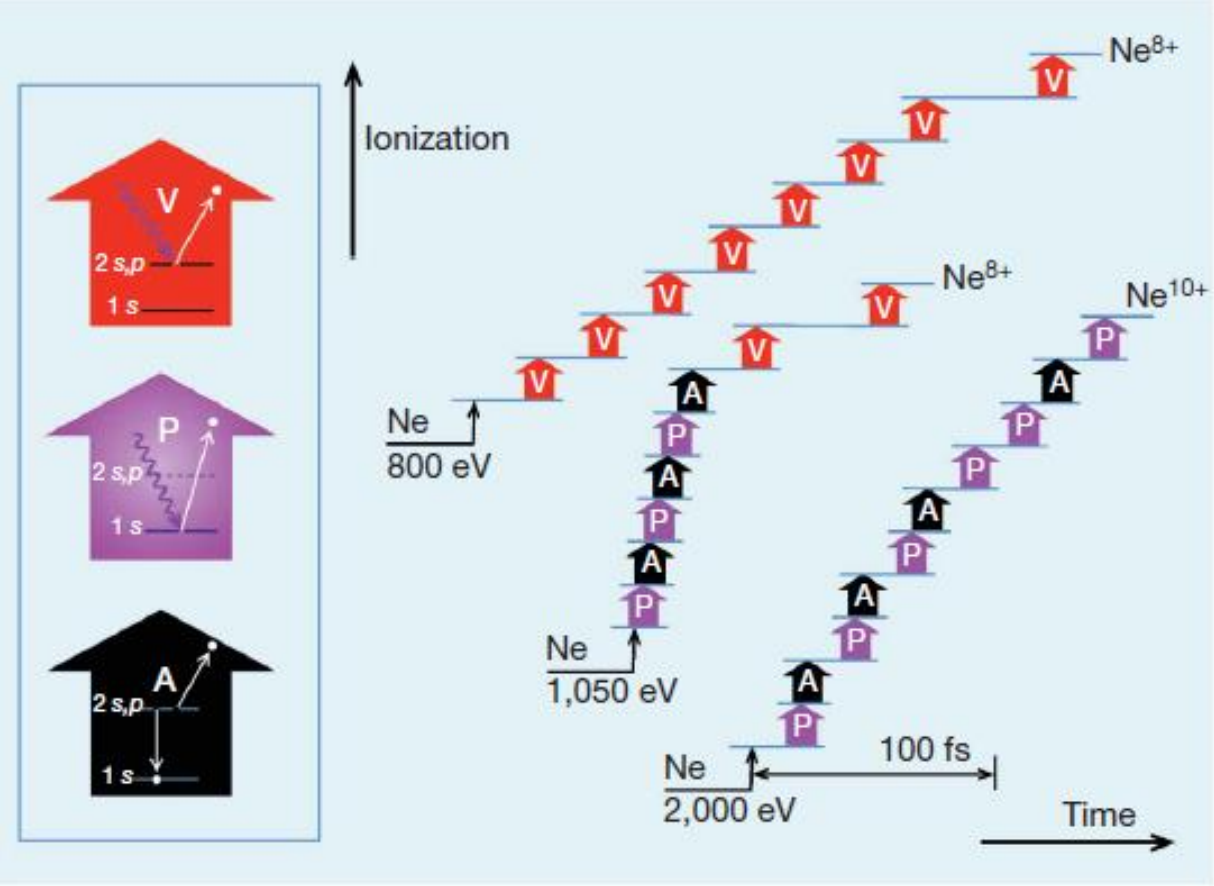

Femtosecond electronic response of atoms to ultra-intense x-rays
*L. Young et al., Nature **466**, 56 (2010).*

One LCLS pulse at 2 keV can remove all ten electrons from the neon atom.

The pulse is so intense that it causes electronic damage to the sample.

Non-linear X-ray atomic Physics

Ultra-Efficient Ionization of Heavy Atoms by Intense X-Rays

*B. Rudek, S-K. Son, L. M. Foucar, S. W. Epp, B. Erk, R. Hartmann, M. Adolph, R. Andritschke, A. Aquila, N. Berrah, C. Bostedt, J. Bozek, N. Coppola, F. Filsinger, H. Gorke, T. Gorkhover, H. Graafsma, L. Gumprecht, A. Hartmann, G. Hauser, S. Herrmann, H. Hirsemann, P. Holl, A. Hömke, L. Journel, C.Kaiser, N. Kimmel, F. Krasniqi, K-U. Kühnel, M. Matysek, M. Messerschmidt, D. Miesner, T. Möller, R. Moshammer, K/ Nagaya, B.Nielsson, G. Potdevin, D. Pietschner, C. Reich, D. Rupp, R.Santra, G. Schaller, I. Schlichting, C. Schmidt, F. Schopper, S. Schorb, C-D. Schröter, J. Schulz, M. Simon, H. Soltau, L. Strüder, **K. Ueda**, G. Weidenspointner, J. Ullrich, A. Rudenko, and D. Rolles*

Nature Photonics Nature Photonics 6, 858 (2012).

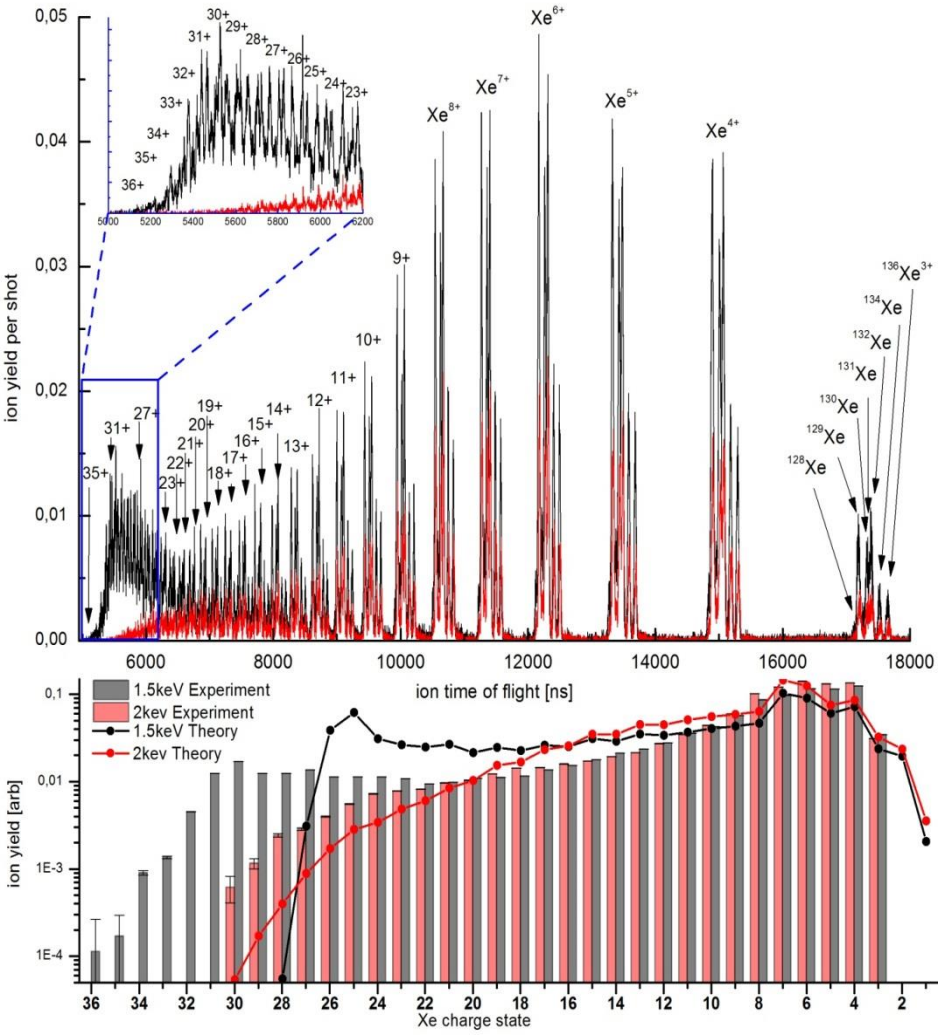

Characteristic properties of FEL pulses

ultra-short (10 – 1 fs)

Attosecond dynamics

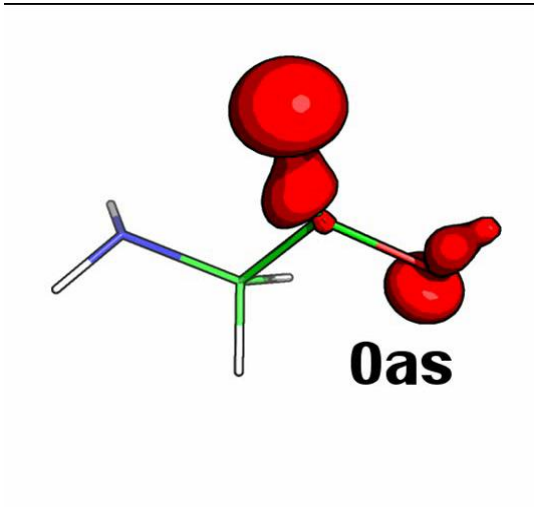

0 – 0.5 fs

Femtosecond dynamics

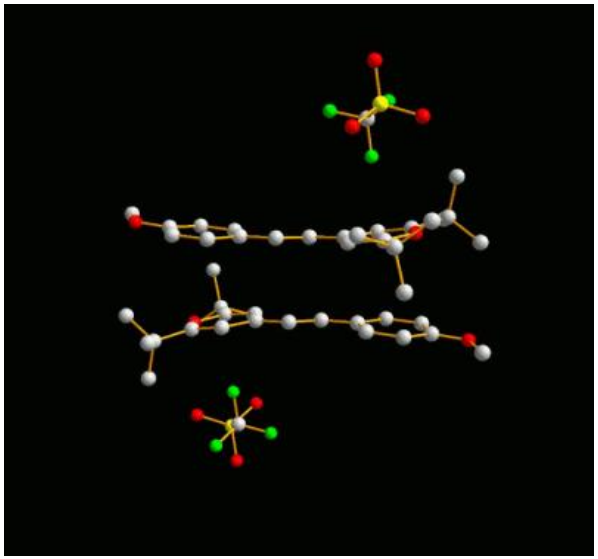

0 – 10 ps

Mili-second mechanics

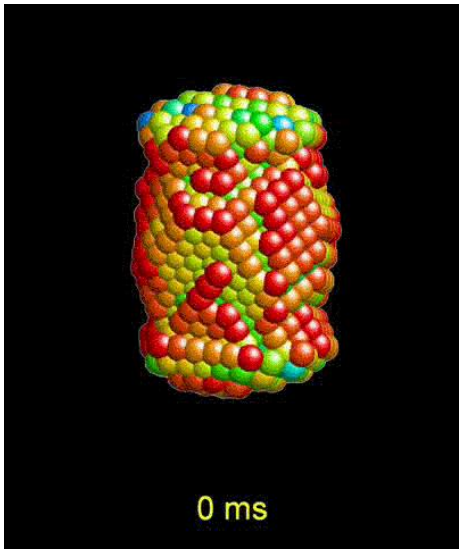

0 – 200 ms

Courtesy of Simone Techert

Characteristic properties of FEL pulses

ultra-short (10 – 1 fs)

Attosecond dynamics

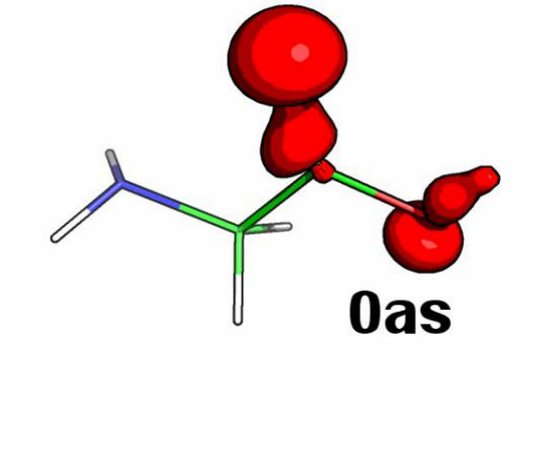

0 – 0.5 fs

Femtosecond dynamics

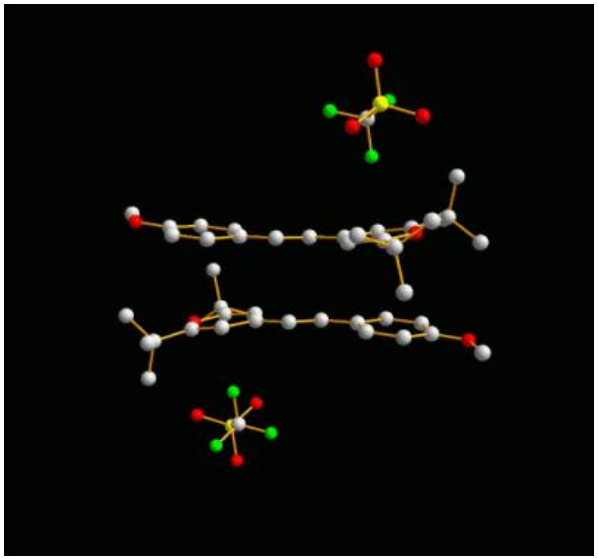

0 – 10 ps

Catching atomic motion and electron (hole) wave-packet in reaction (molecular vs electron movie)

SACLA XFEL (lased on 7 June 2011)

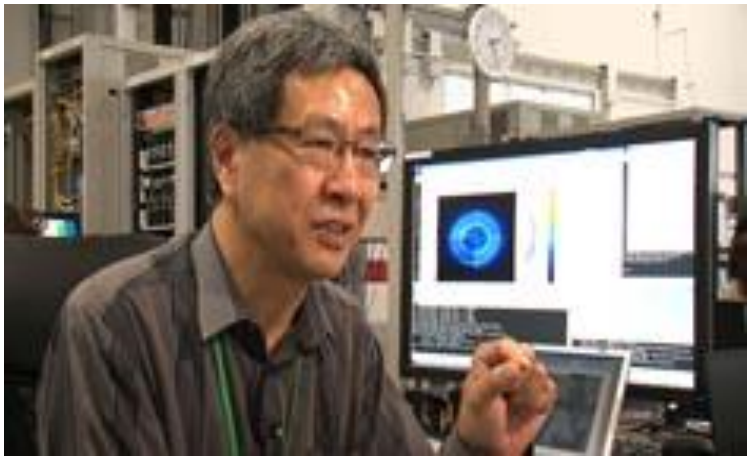

on air!

SCSS test accelerator : EUV-FEL (20-24 eV)

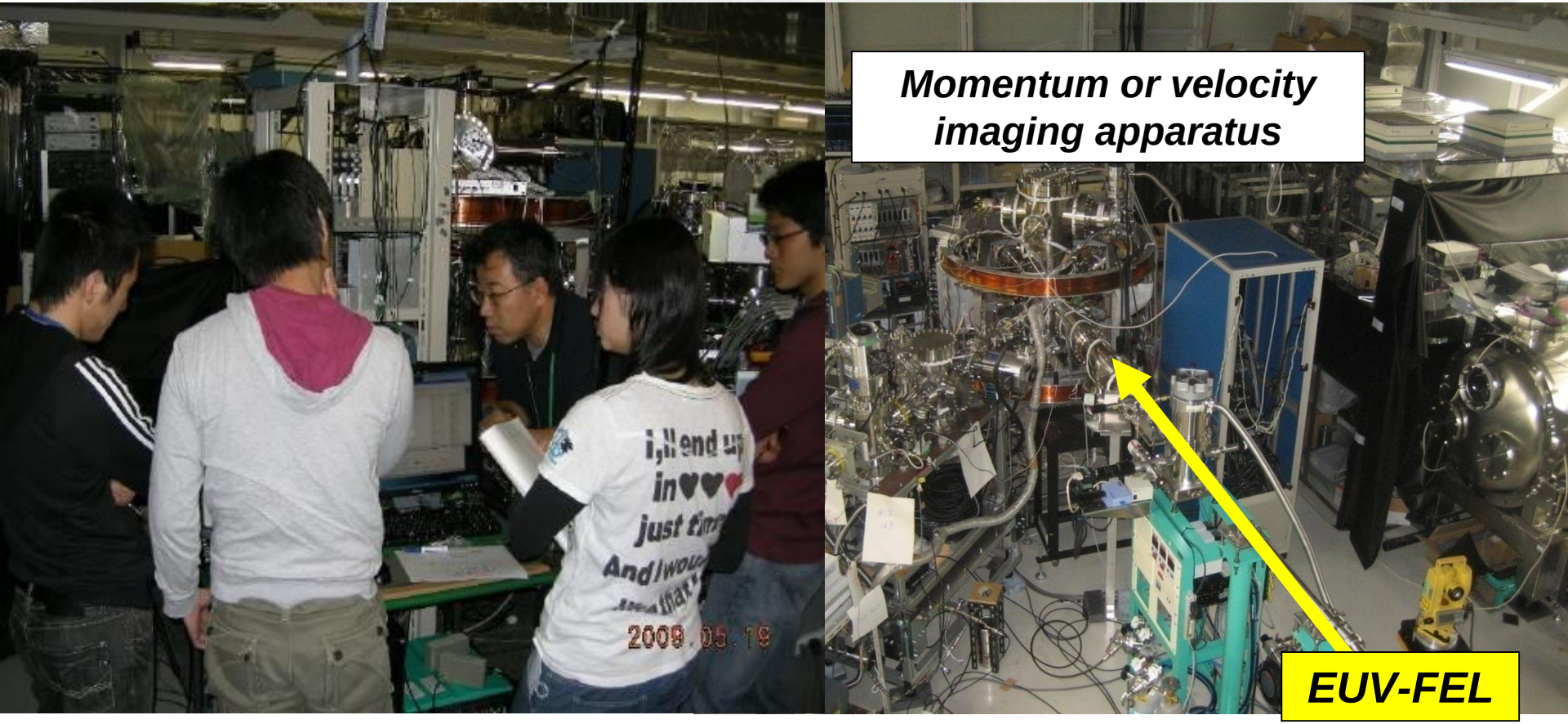

Multiple ionization of rare gas atoms and clusters: with M. Yao's group

VMI: with help of M. Vrakking's group

Autocorrelation: with J. Ullrich's group

Multi-photon ionization of atoms

● Second-order autocorrelation of **SCSS** EUVFEL pulses via time-resolved two-photon single ionization of He

– Characteristics of SASE-FEL

● Photoelectron angular distributions for two-photon Ionization of He atoms by **SCSS** EUVFEL pulses

– Potential of coherent control via seeded FEL

● Deep inner-shell multi-photon absorption of Ar and Xe atoms by **SACLA** XFEL pulses

– Relevance to the electronic radiation damage

Second-order autocorrelation of EUV FEL pulses via time resolved two-photon single ionization of He

R. Moshammer, Th. Pfeifer, A. Rudenko, Y.H. Jiang, L. Foucar, M. Kurka, K.U. Kuhnel, C.D. Schroter, J. Ullrich, O. Herrwerth, M.F. Kling, X.-J. Liu, K. Motomura, H. Fukuzawa, A. Yamada, K. Ueda, K. L. Ishikawa, K. Nagaya, H. Iwayama, A. Sugishima, Y. Mizoguchi, S. Yase, Yao, N. Saito, A. Belkacem, M. Nagasono, A. Higashiya, M. Yabashi, T. Ishikawa, H. Ohashi, H. Kimura, and T. Togashi, *Optics Express **19**, 21698 (2011).*

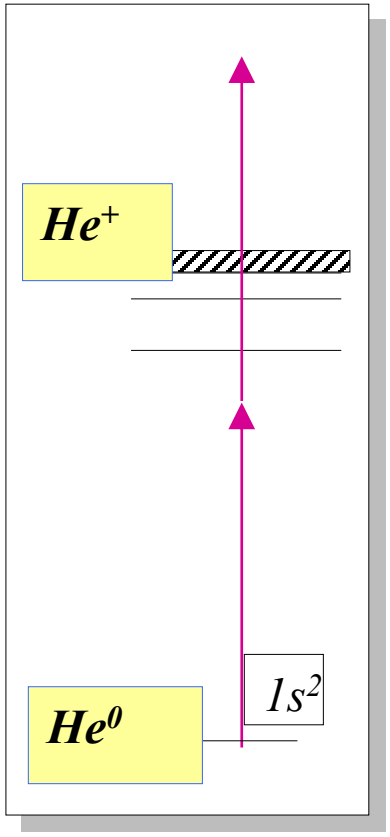

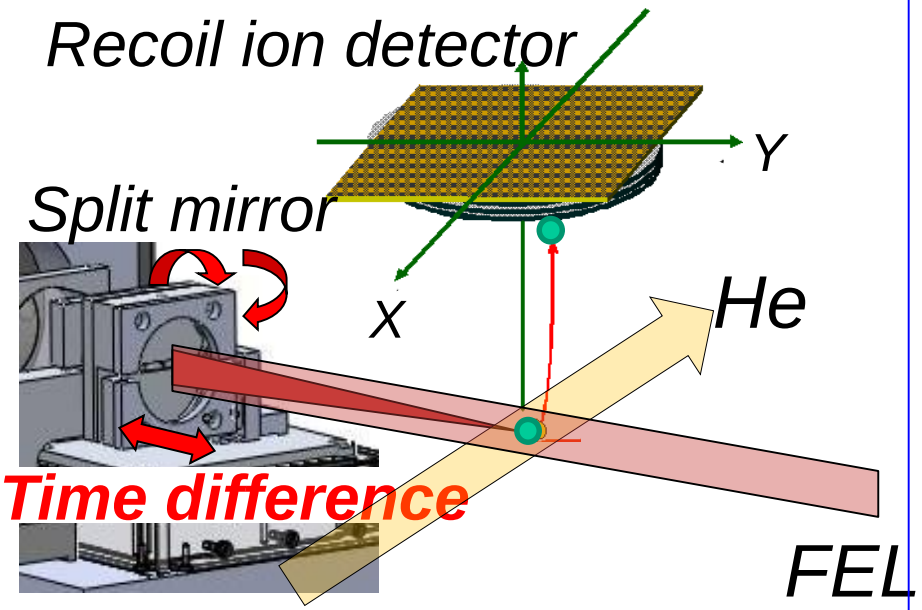

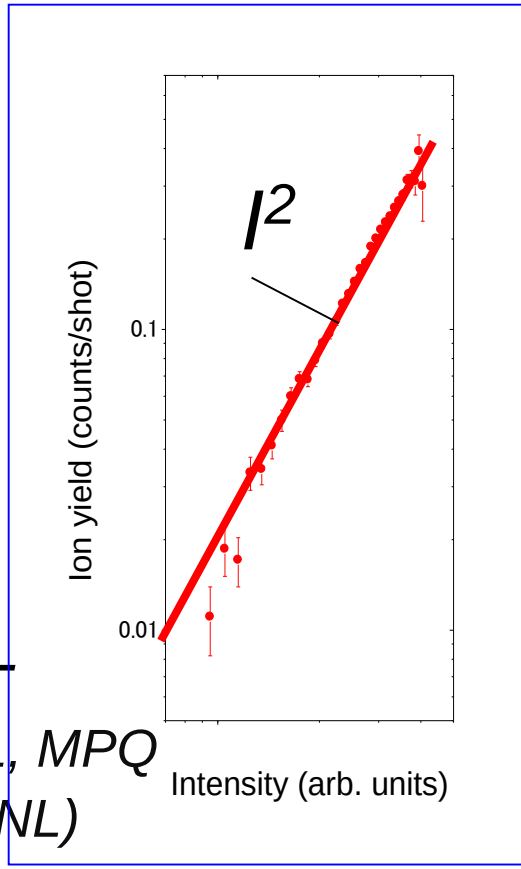

Split mirror assembly: MPI-K, ASG-CFEL, MPQ

Mirror: Mg/Si multilayer (f=600 mm, LBNL)

Autocorrelation measurement with He two photon ionization

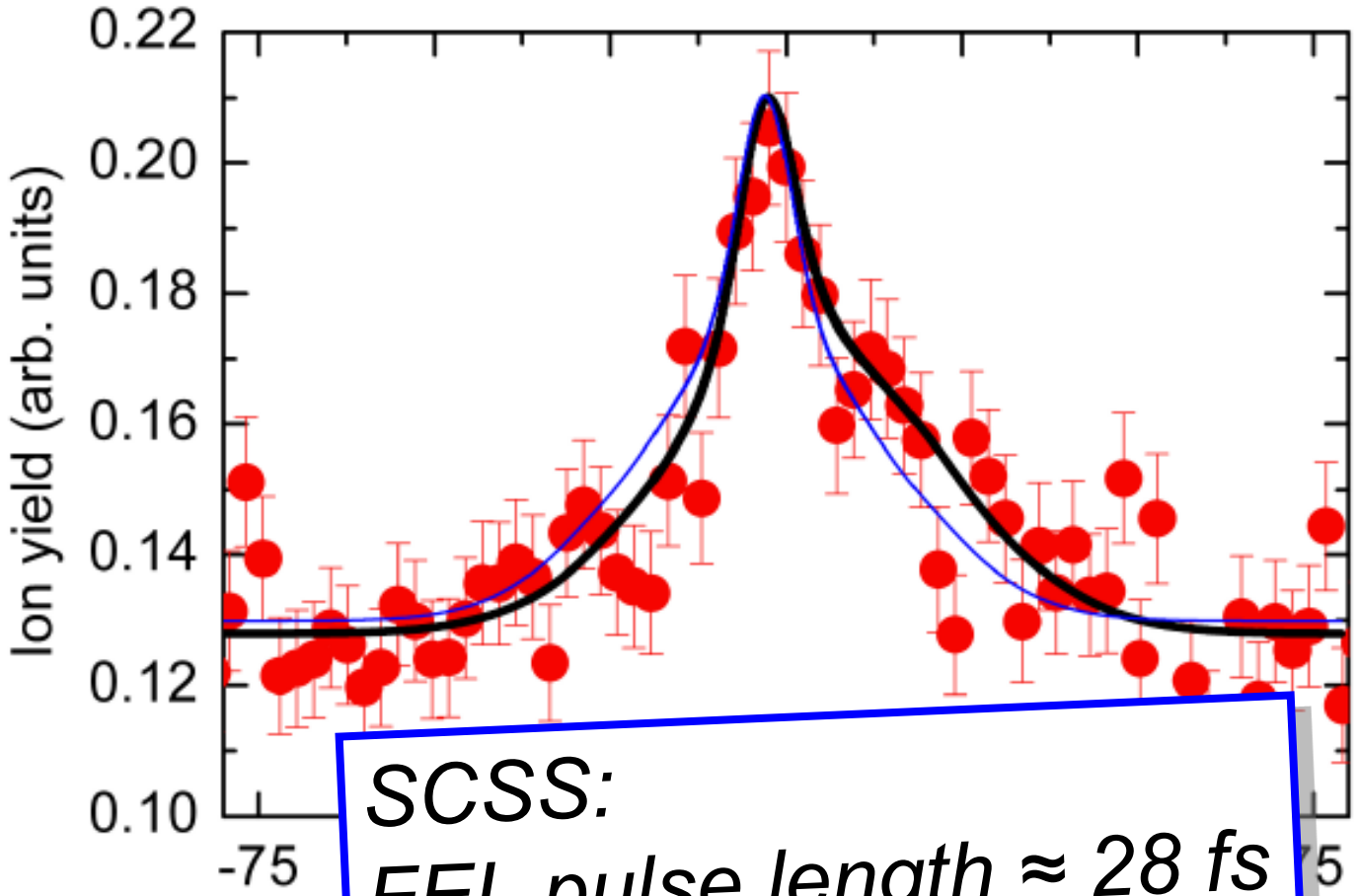

SCSS:
FEL pulse length ≈ 28 fs
coherence length ≈ 8 fs
Pulse-front tilt ≈ 5 fs

Optics Express ***19****, 21698 (2011).*

SCSS Sample Pulse Shapes

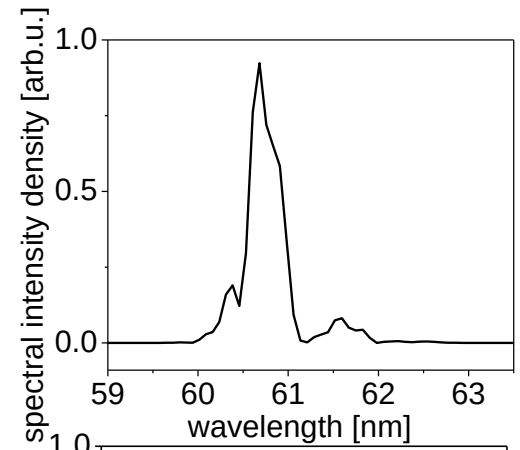

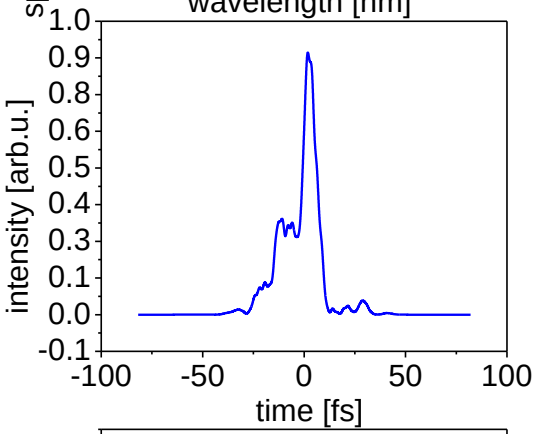

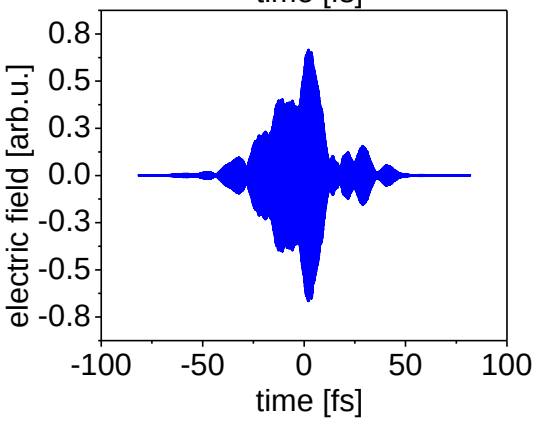

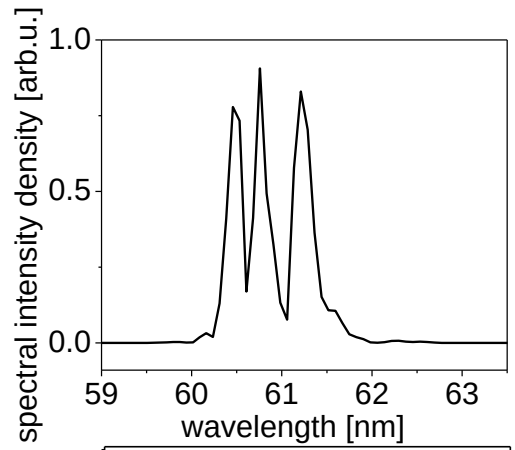

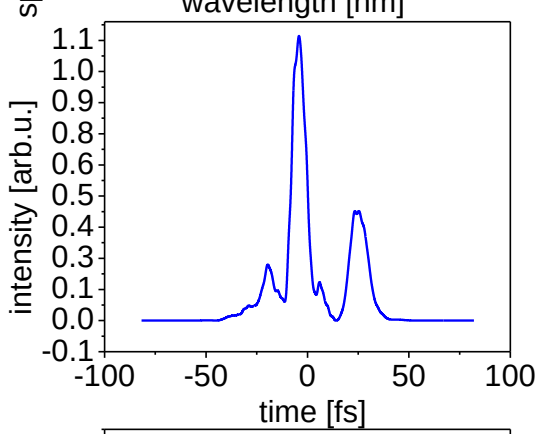

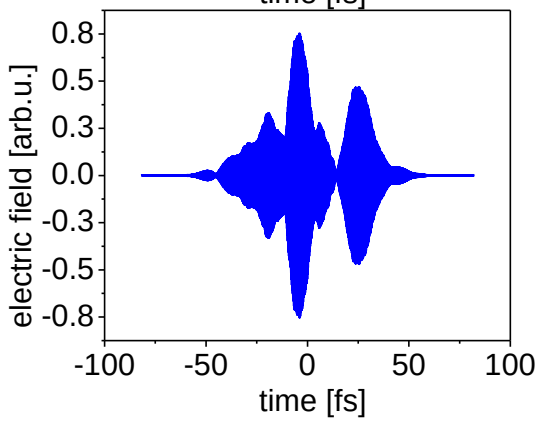

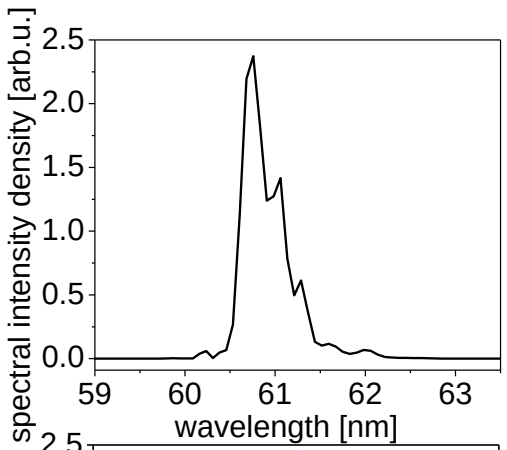

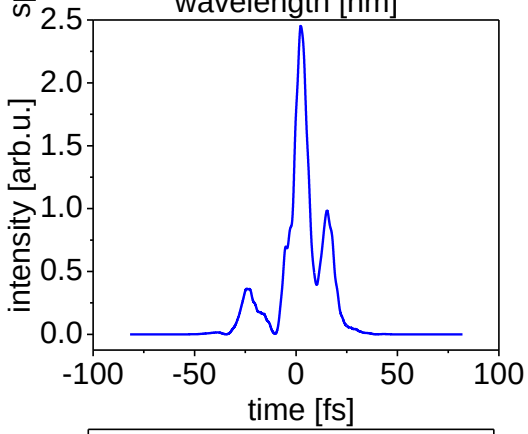

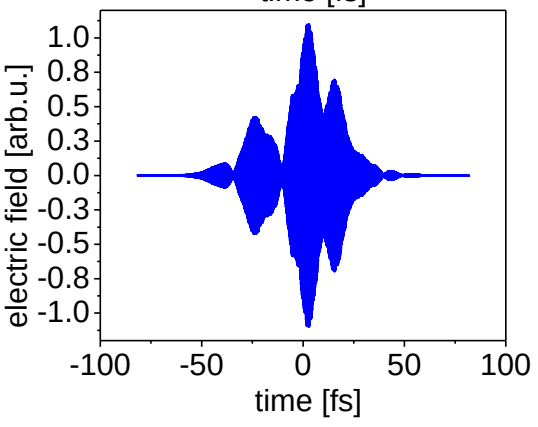

Experimental evidence for competition between the resonant and non-resonant two-photon ionization

R. Ma, K. Motomura, ***K.L. Ishikawa****, H. Fukuzawa, A. Yamada,* ***K. Ueda****, K. Nagaya, S. Yase, Y. Mizoguchi,* ***M. Yao****, A. Rouzee, A. Hundermark,* ***M. Vrakking, P. Johnsson****, M. Nagasono, K. Tono, T. Togashi, Y. Senba, H. Ohashi, M. Yabashi, and* ***T. Ishikawa***

Photoelectron angular distribution for two-photon single ionization of He

Direct numerical simulation of the two-electron time-dependent Schrödinger equation (TDSE)

vs

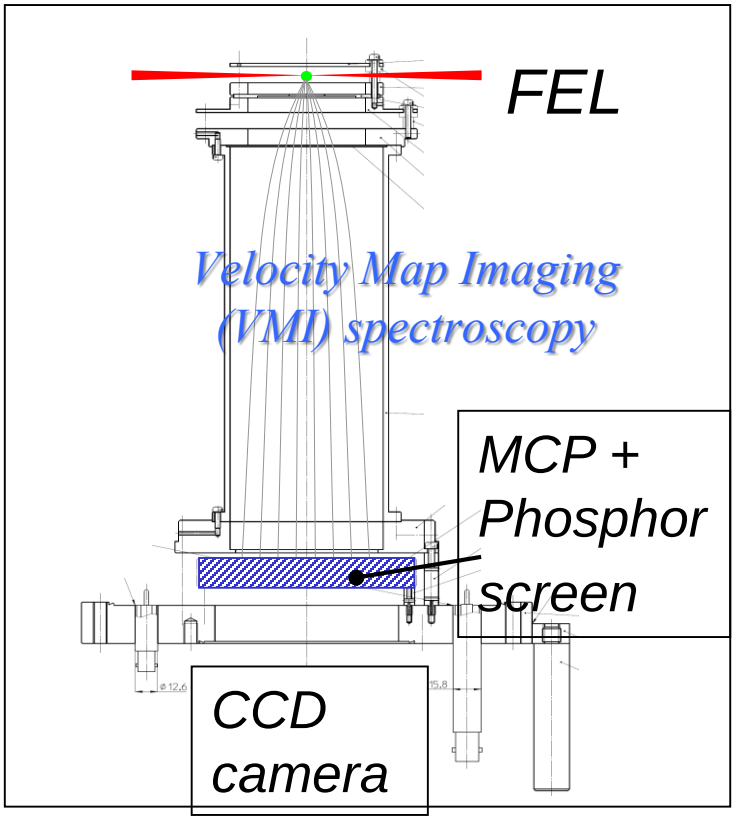

Excitation energies for two-photon ionization of He

Photon energy range available at SCSS test accelerator

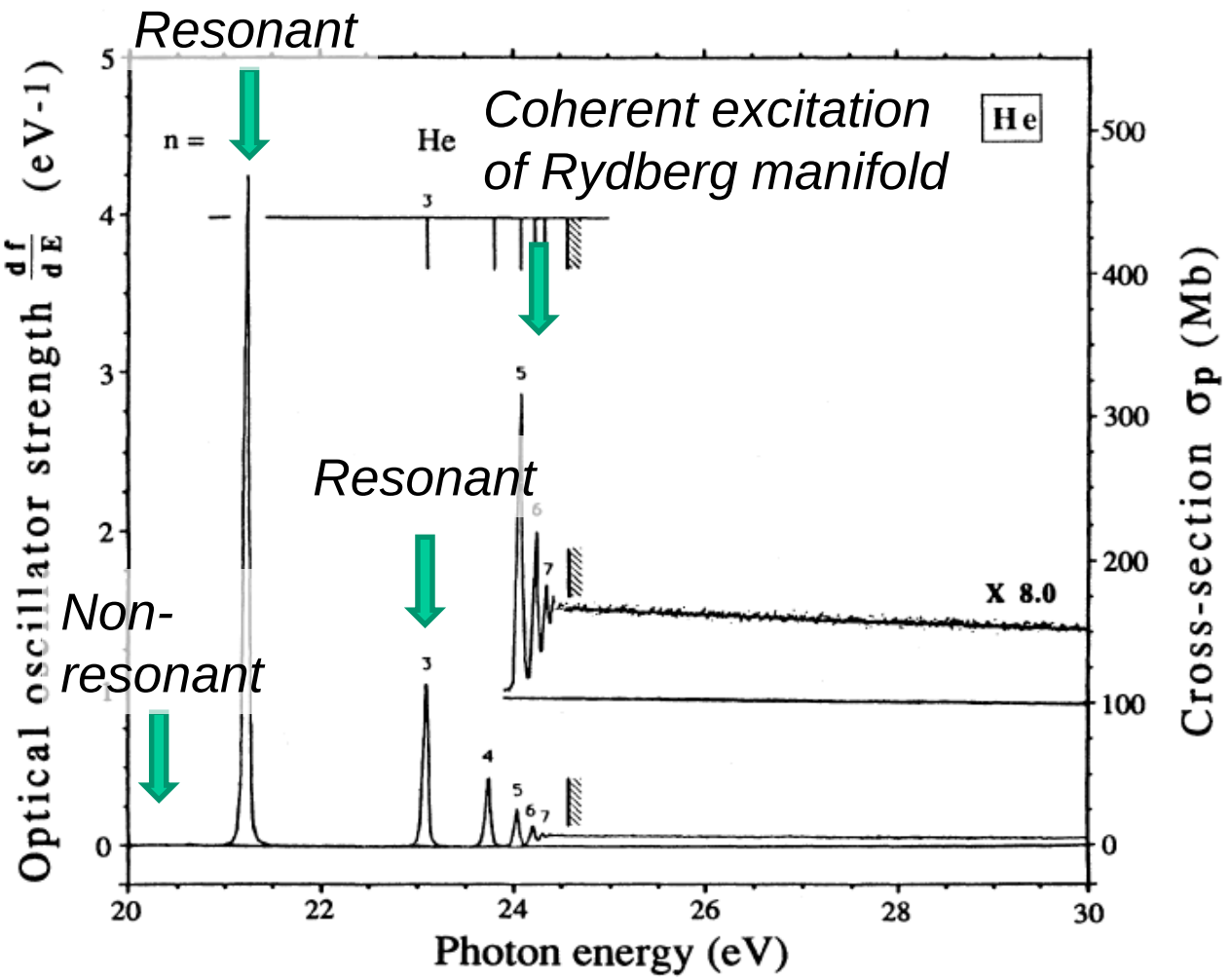

*W. F. Chan et al., Phys. Rev. A **44**, 186 (1991).*

Photoelectron angular distribution for two-photon ionization of He

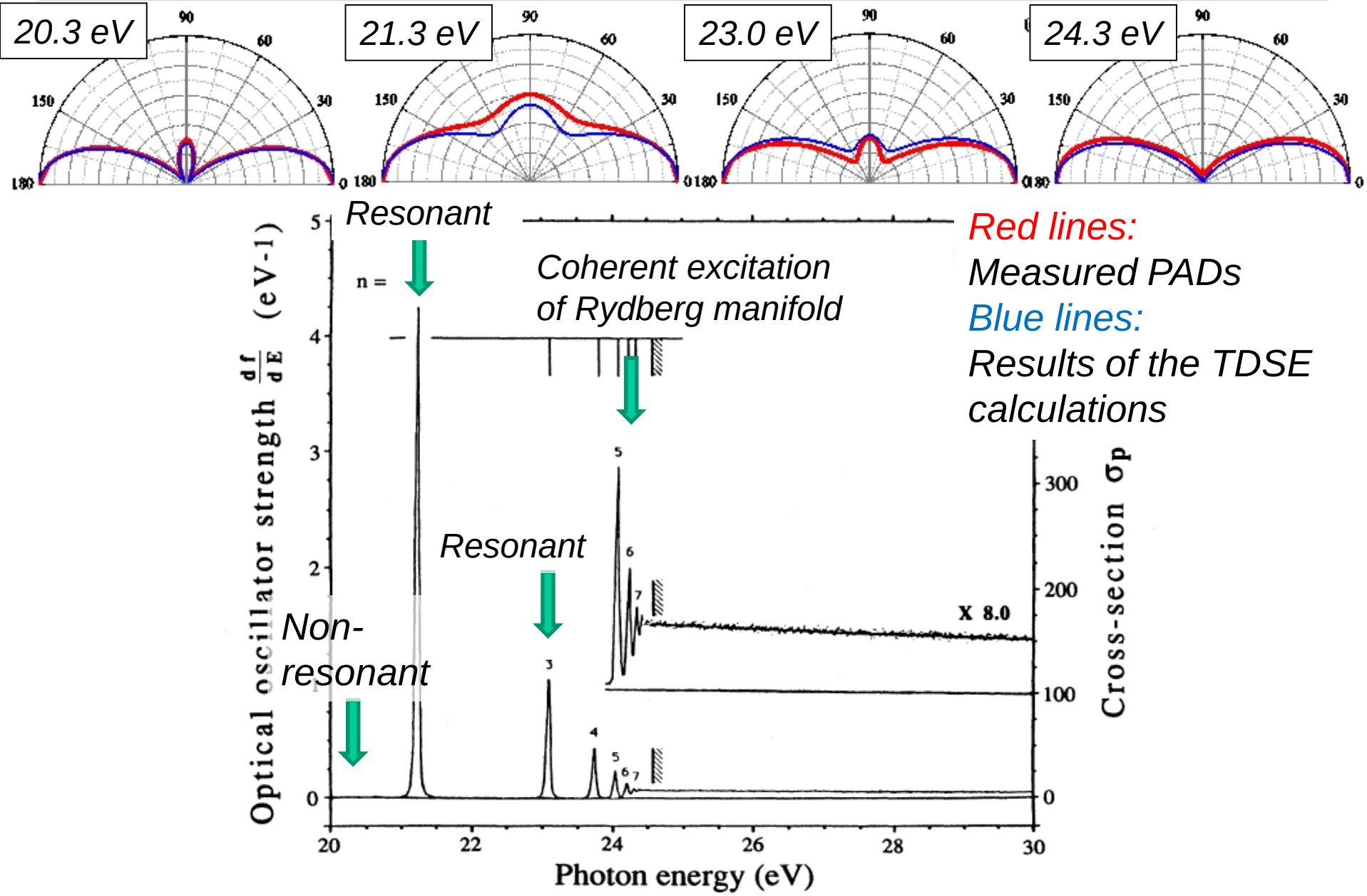

R. Ma, K. Motomura, K. L. Ishikawa, H. Fukuzawa *et al*., submitted.

Photoelectron angular distribution for two-photon ionization of He

$$I(\theta) = \frac{\sigma}{4\pi}\left[1 + \beta_2 P_2(\cos\theta) + \beta_4 P_4(\cos\theta)\right]$$

The outgoing photoelectron wave is a superposition of s and d waves.

Anisotropy parameters

$$\beta_2 = \frac{10}{W^2+1}\left[\frac{1}{7} - \frac{W}{\sqrt{5}}\cos\delta\right], \quad \beta_4 = \frac{18}{7(W^2+1)}$$

see:
*K. L. Ishikawa and K. Ueda, Phys. Rev. Lett., **108**, 033003 (2012).*

$W = |c_0 / c_2|$: *Amplitude ratio*, $\delta = \delta_0 - \delta_2$: *Phase difference*

c_l : *complex amplitude of a final state with an angular momentum l*
δ_l : *phase of each partial wave*

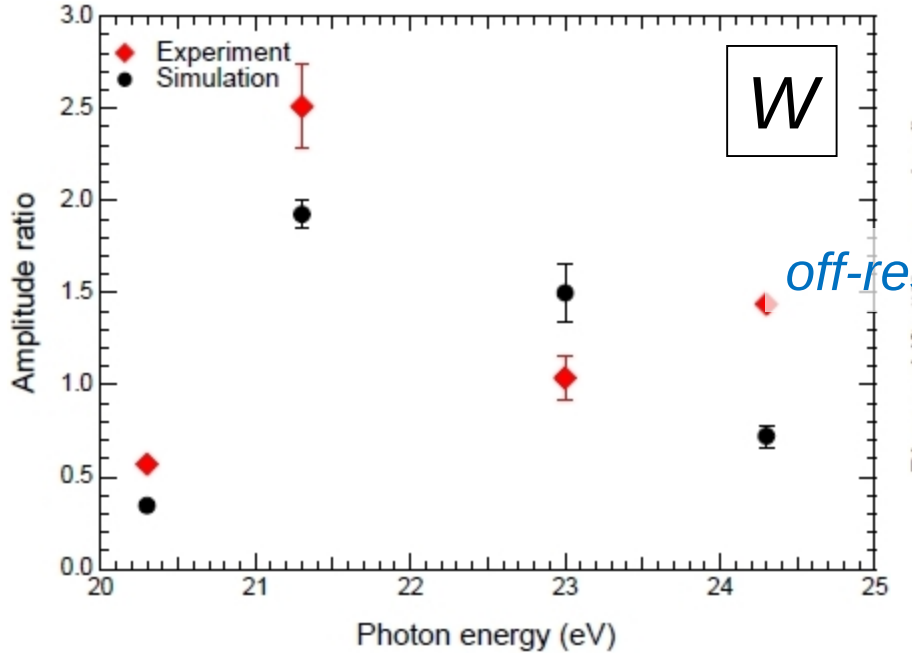

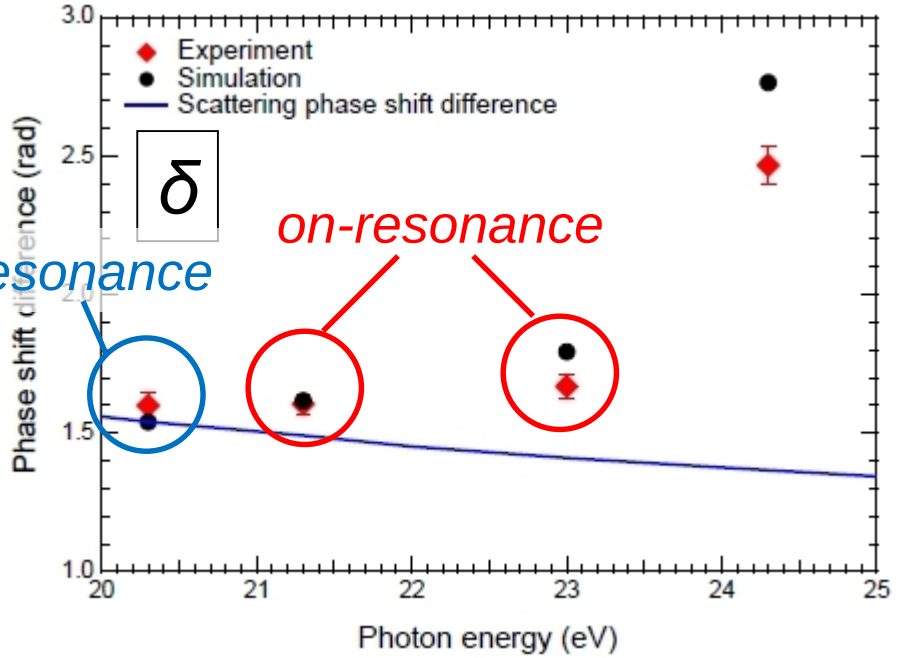

Deviation from scattering phase shift difference

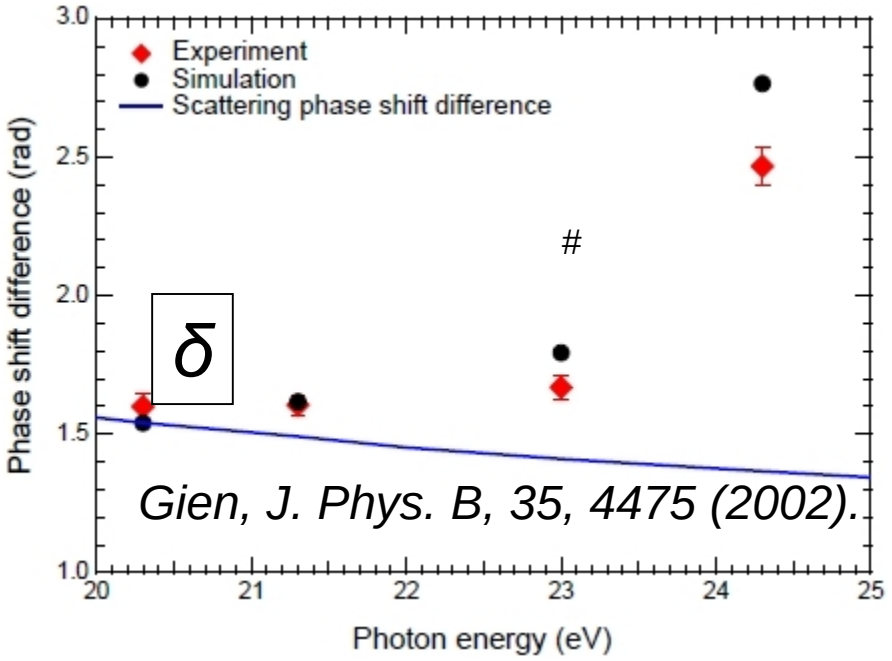

Gien, J. Phys. B, 35, 4475 (2002).

The excitation laser is a short pulse with finite width in both energy and time!
Taking it into account, we have

$$\delta = \delta_{SC} + \mathrm{Arg}\, c_0 / c_2$$

Additional phase shift

δ_{SC} : scattering phase shift difference

*K. L. Ishikawa and K. Ueda, Phys. Rev. Lett., **108**, 033003 (2012).*

$$c_f = \pi E_0^2 T^2 \sum_m \mu_{fm}\mu_{mi} \left[e^{-\Delta_m^2 T^2} - i\frac{2}{\sqrt{\pi}} F(\Delta_m T) \right]$$

$\Delta_m = \omega_m - (\omega_i + \omega)$ T: the pulse width

Deviation from δ_{SC} is evidence of competition between resonant and non-resonant paths

Tailoring continuum wavepacket controlling the additional phase shift by the short EUV pulses !

Dependence of W and δ on the pulse width of the Fourier transform limited pulse

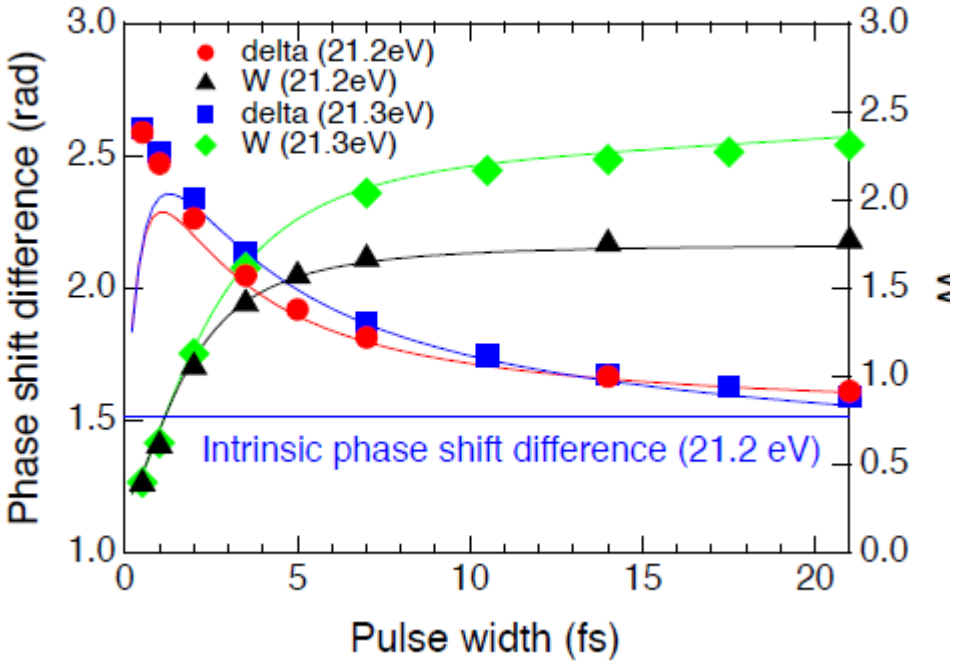

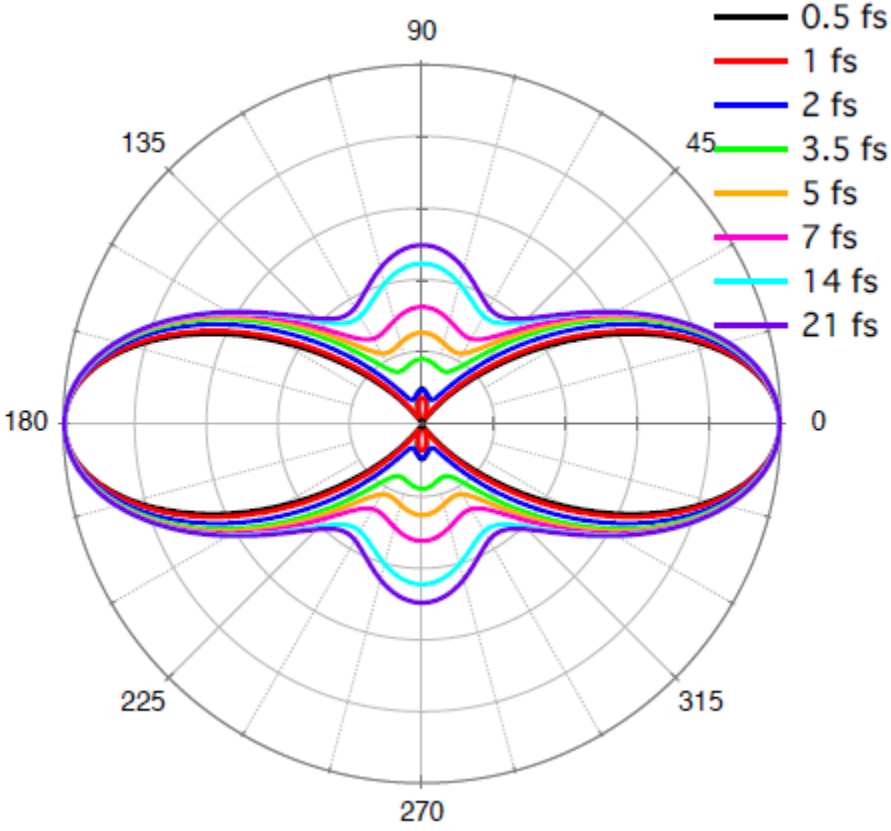

$$\frac{c_S}{c_D} = \frac{\mu_{Sr}}{\mu_{Dr}} \frac{\sqrt{\pi}Te^{-\Delta_r^2 T^2} - i[a_S + 2F(\Delta_r T)T]}{\sqrt{\pi}Te^{-\Delta_r^2 T^2} - i[a_D + 2F(\Delta_r T)T]}$$

$$\Delta_m = \omega_m - (\omega_i + \omega)$$

T: the pulse width

Chirping the pulse width from 500 as to 20 fs, we can control the contributions of direct and non-direct contributions

Tailoring the continuum wave packet (wave function)!

Ishikawa and Ueda, PRL ***108****, 033003 (2012).*

Multiple ionization of rare gas atoms irradiated by EUV free-electron laser pulses at 51 nm

K. Motomura, H. Fukuzawa, K. Papamihail, M. Kurka, A. Rudenko, L. Foucar, H. Iwayama, K. Nagaya, X.-J. Liu, H.-U. Kühnel, G. Prümper, P. Labropoulos, J. Ullrich, K. Ueda, N. Saito, H. Murakami, M. Yao, A. Belkacem, R. Feifel, M. Nagasono, A. Higashiya, T. Togashi, H. Ohashi, and H. Kimura, M. Yabashi, and T. Ishikawa

Ar^{7+} > 434 eV
> 18 photons

Kr^{8+} > 508 eV
> 21 photons

Mirror:
Mg/Si multilayer
f=250 mm,
made by LBNL

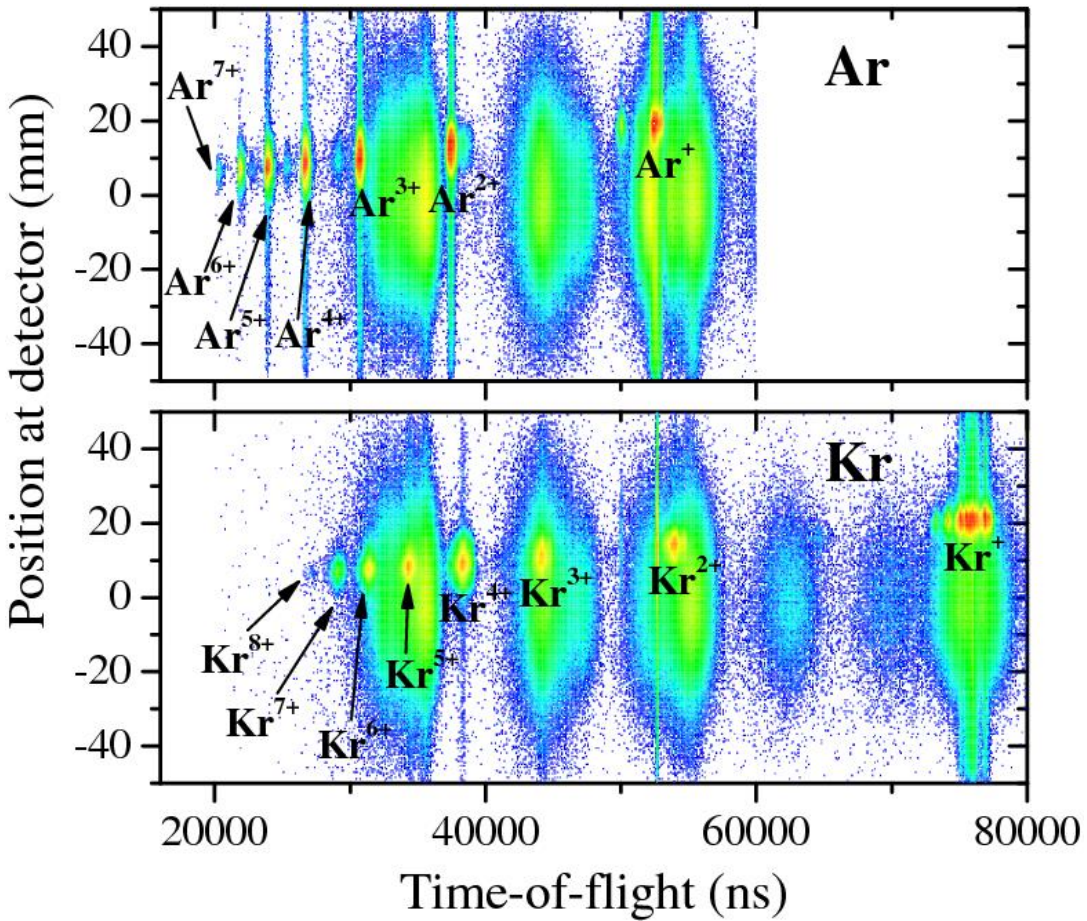

SACLA XFEL

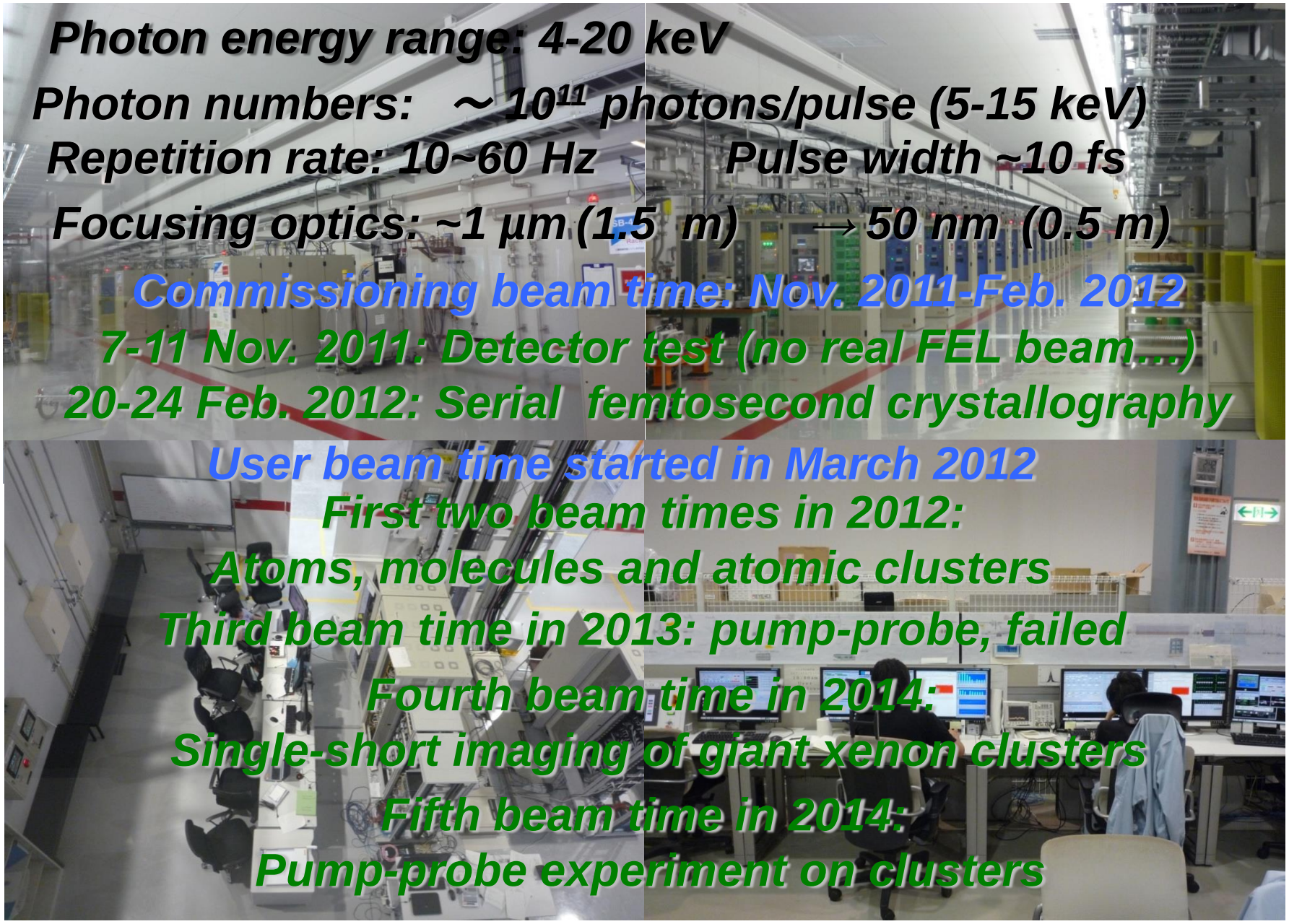

Photon energy range: 4-20 keV

Photon numbers: ~ 10^{11} photons/pulse (5-15 keV)

Repetition rate: 10~60 Hz Pulse width ~10 fs

Focusing optics: ~1 μm (1.5 m) → 50 nm (0.5 m)

Commissioning beam time: Nov. 2011-Feb. 2012

7-11 Nov. 2011: Detector test (no real FEL beam…)

20-24 Feb. 2012: Serial femtosecond crystallography

User beam time started in March 2012

First two beam times in 2012:

Atoms, molecules and atomic clusters

Third beam time in 2013: pump-probe, failed

Fourth beam time in 2014:

Single-short imaging of giant xenon clusters

Fifth beam time in 2014:

Pump-probe experiment on clusters


Multi-photon, multiple ionization of
Atoms, Molecules and Rare-gas clusters
Single-shot imaging of Nano-clusters
Pump-probe experiments for
Atoms, Molecules and Rare-gas clusters
Aiming at probing
Ultrafast electron and structure dynamics

Experimental configuration @ SACLA BL3 EH3

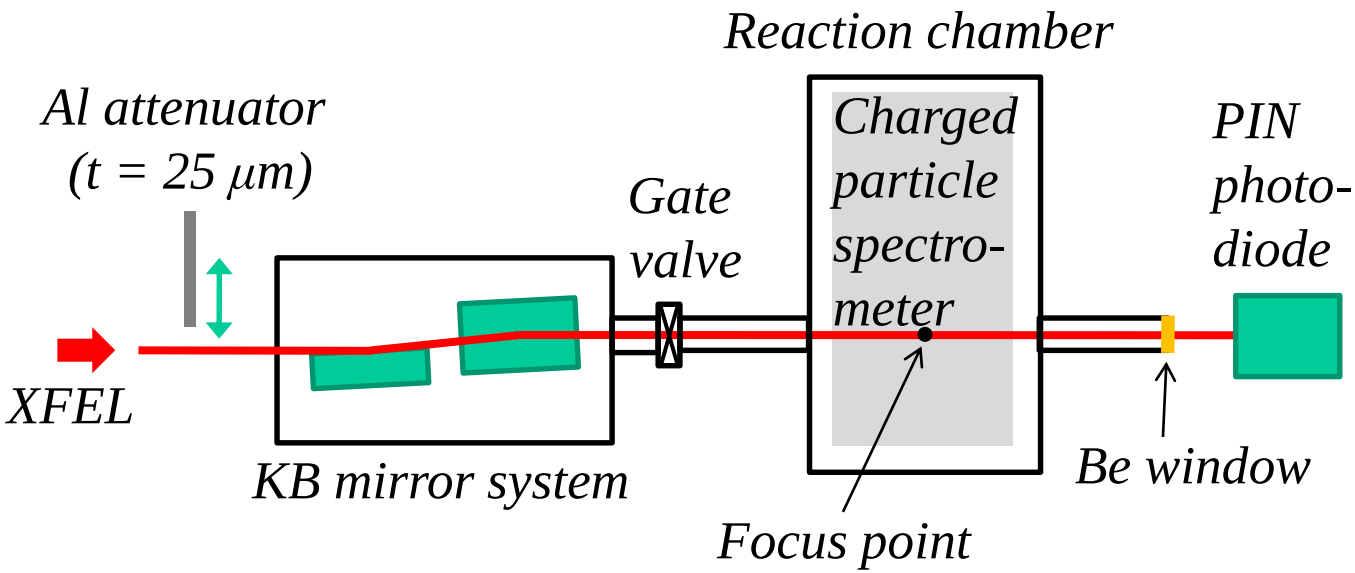

XFEL pulses

Photon energy: *5 and 5.5 keV*
(Wavelength: 0.25 and 0.22 nm)
Band width: *~60 eV (FWHM)*
Repetition: *10-30 Hz*
Pulse energy before KB mirror:
~240 μJ (~3 ×10^{11} photons) @5.5keV
Fluctuation of pulse energy:
±25% (50% FWHM)

@Focus point

Focus size: *1-2 μm (FWHM)*
Peak fluence:
~47 μJ/μm^2 (atoms, clusters),
~26 μJ/μm^2 (molecules)

Sample gas were introduced as a pulsed super sonic gas jet to the focus point.

I. Deep inner-shell multiphoton absorption by intense x-ray free-electron laser pulses

H. Fukuzawa, S.-K. Son, K. Motomura, S. Mondal, K. Nagaya, S. Wada, X.-J. Liu, R. Feifel, T. Tachibana, Y. Ito, M. Kimura, T. Sakai, K. Matsunami, H. Hayashita, J. Kajikawa, P. Johnsson, M. Siano, E. Kukk, B. Rudek, B. Erk, L. Foucar, E. Robert, C. Miron, K. Tono, T. Togashi, Y. Inubushi, T. Sato, T. Katayama,T. Hatsui, T. Kameshima, M. Yabashi, M. Yao, R. Santra, and K. Ueda (PRL **110**, 173005 (2013) & JPB **46**, 164024 (2013).

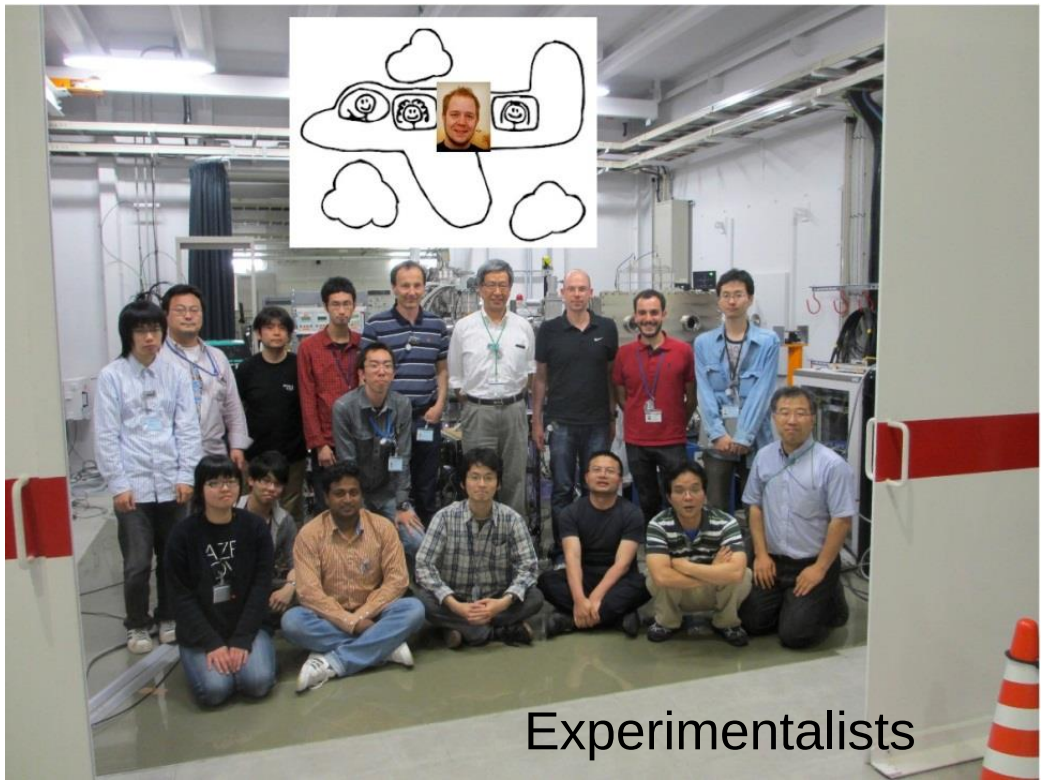

Experimentalists

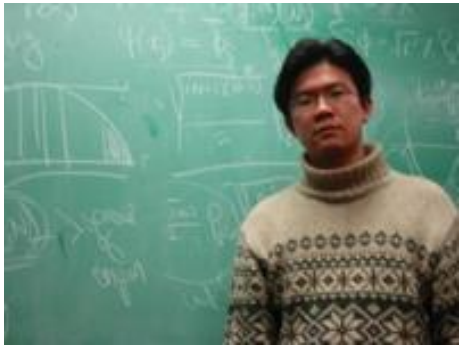

Theorists

Time of Flight spectrum of argon ions

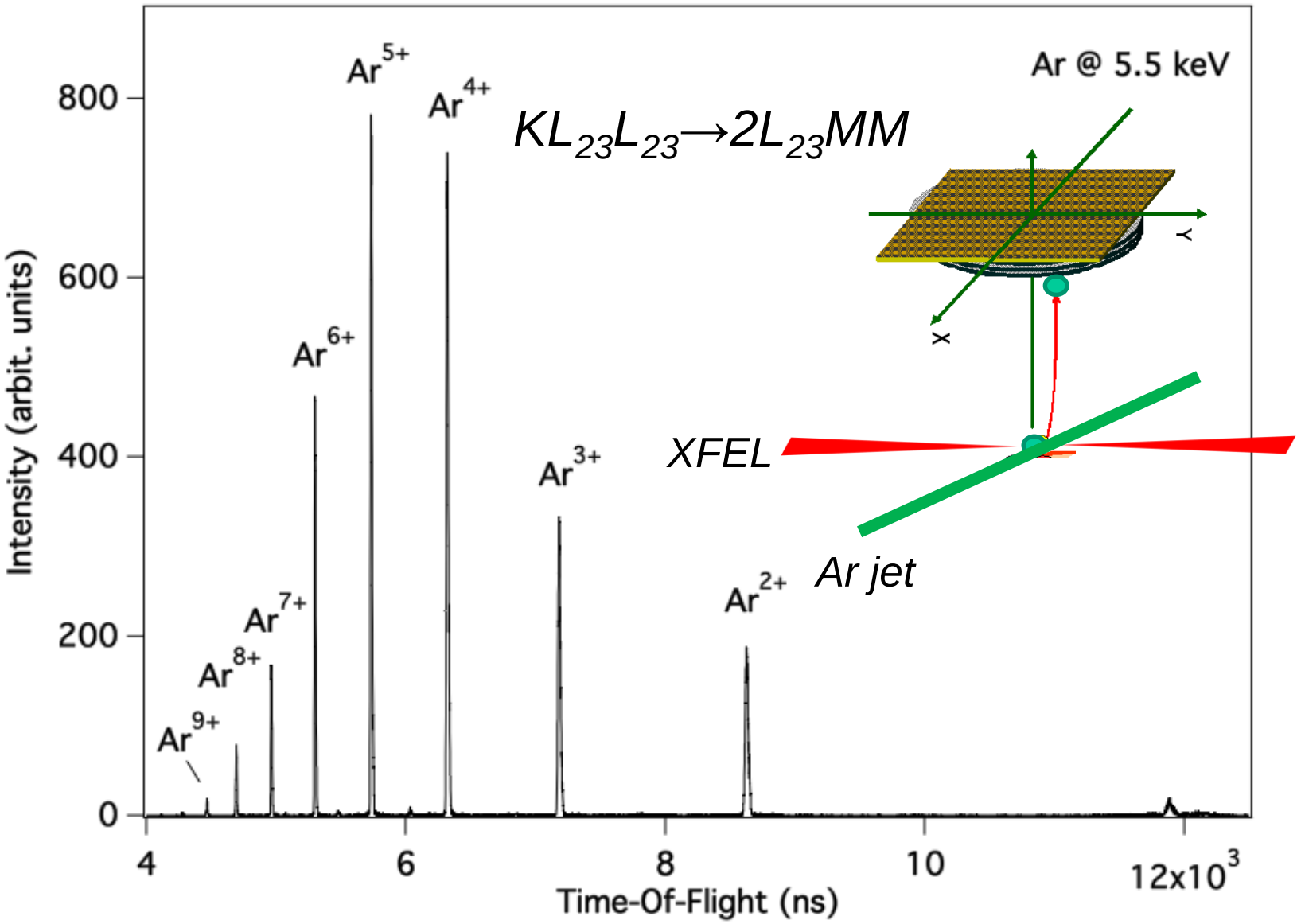

XFEL fluence dependence for Ar^{n+} yields

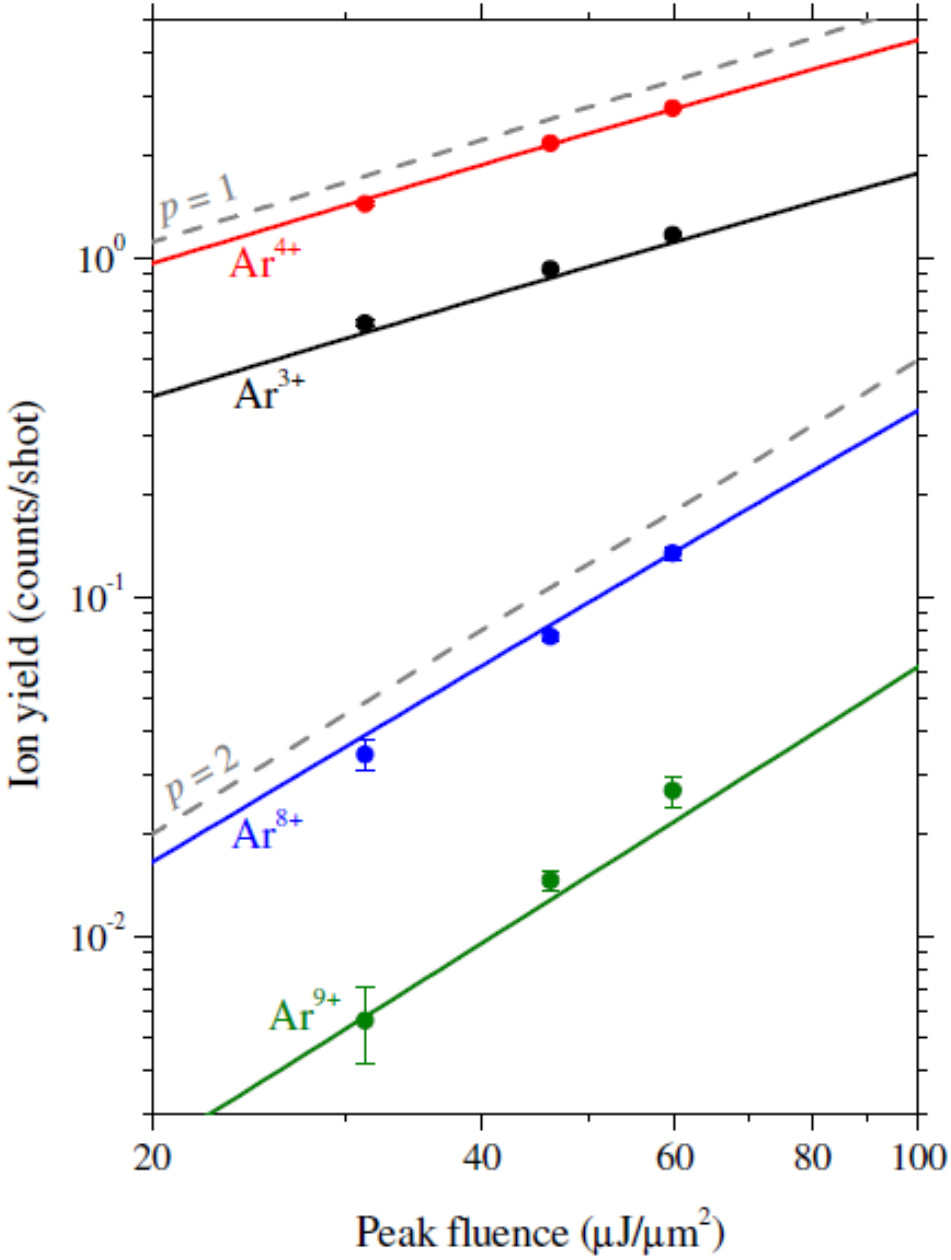

Ar^{4+}: *single photon K-shell ionization*
→ $KL_{23}L_{23}$ *Auger* → $2L_{23}MM$ *Auger*

Ar^{3+}: *single photon K shell absorption*
→ $KL_{23}M$ *Auger* → $L_{23}MM$ *Auger*

Ar^{8+}, Ar^{9+}: *sequential two photon K shell ionization*

Bench mark ab initio calculation reproduces fluence dependence and relative ratios.

In the theory, the pulse shape of Gaussian of 30 fs (FWHM), and Gaussian focal shape of 1 μm (FWHM) ×1 μm (FWHM) are assumed.

Charge state distribution of Ar: experiment and theory

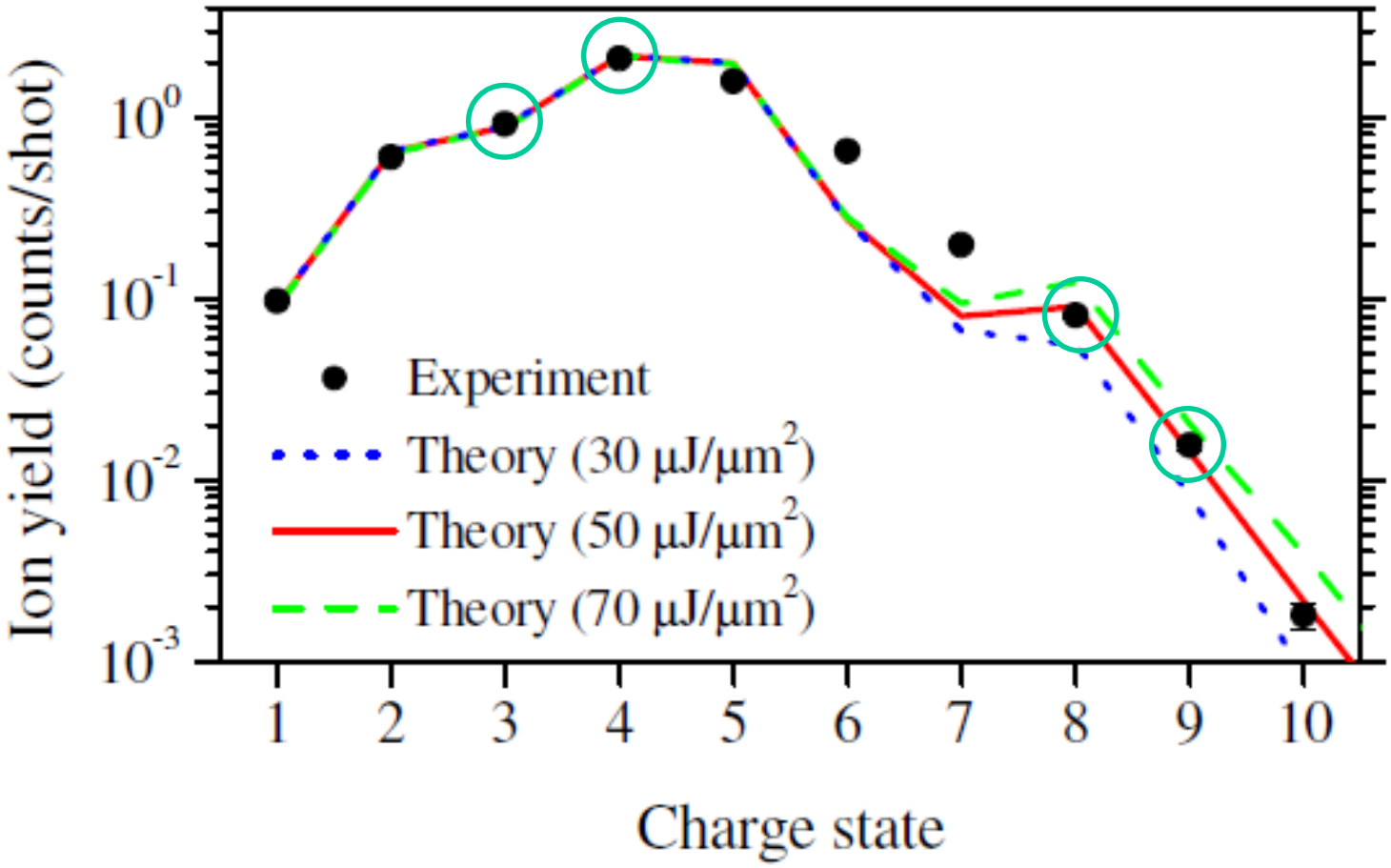

By comparison with theory, we obtained peak fluence of 50 μJ/μm^2 in the experiment!

Time of Flight spectrum of xenon ions

5.5 keV, 50 μJ/μm² at SACLA

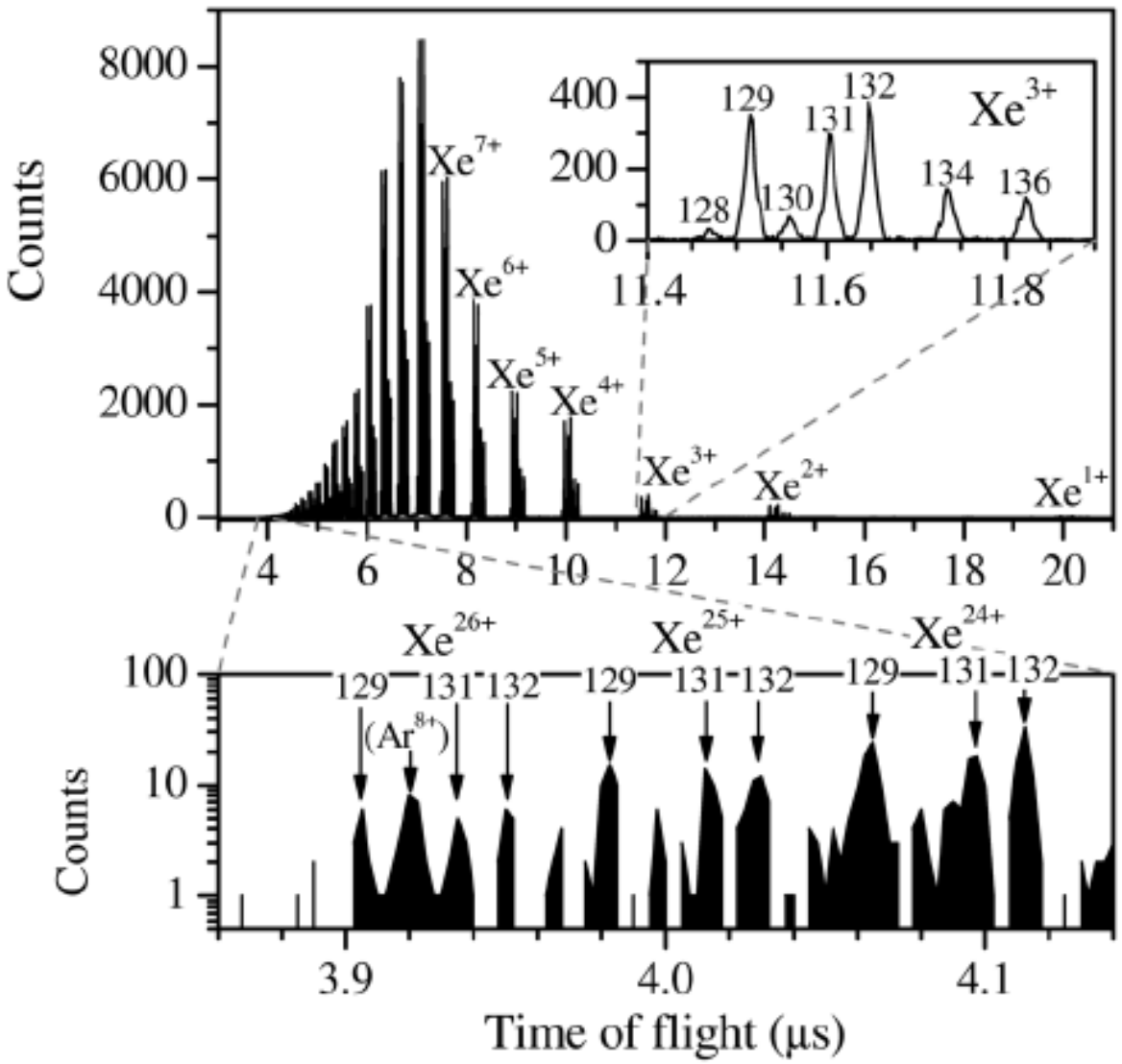

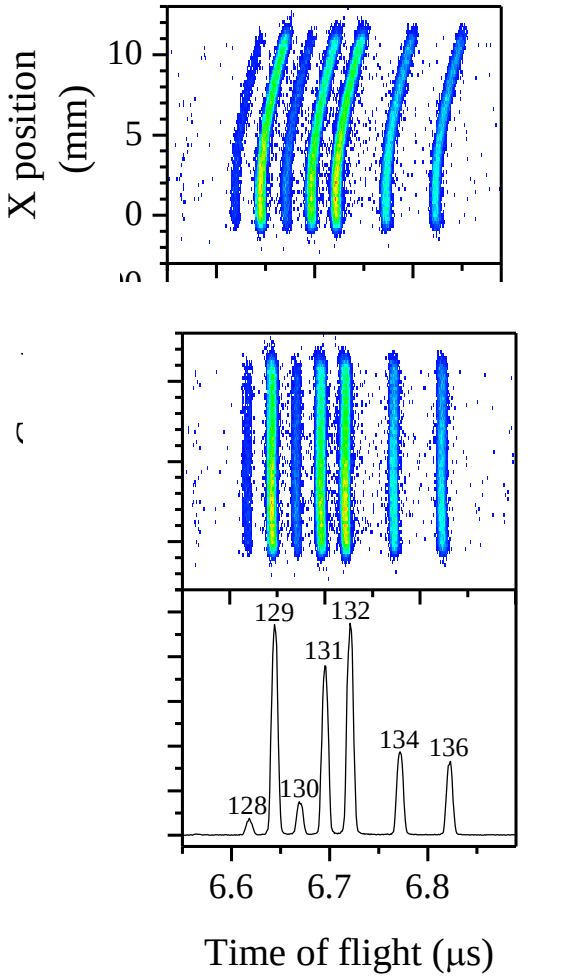

2D position resolved TOF improves the resolution!

High charge states Xe^{n+} with n up to 26 are produced!

XFEL fluence dependence for Xe^{n+} yields

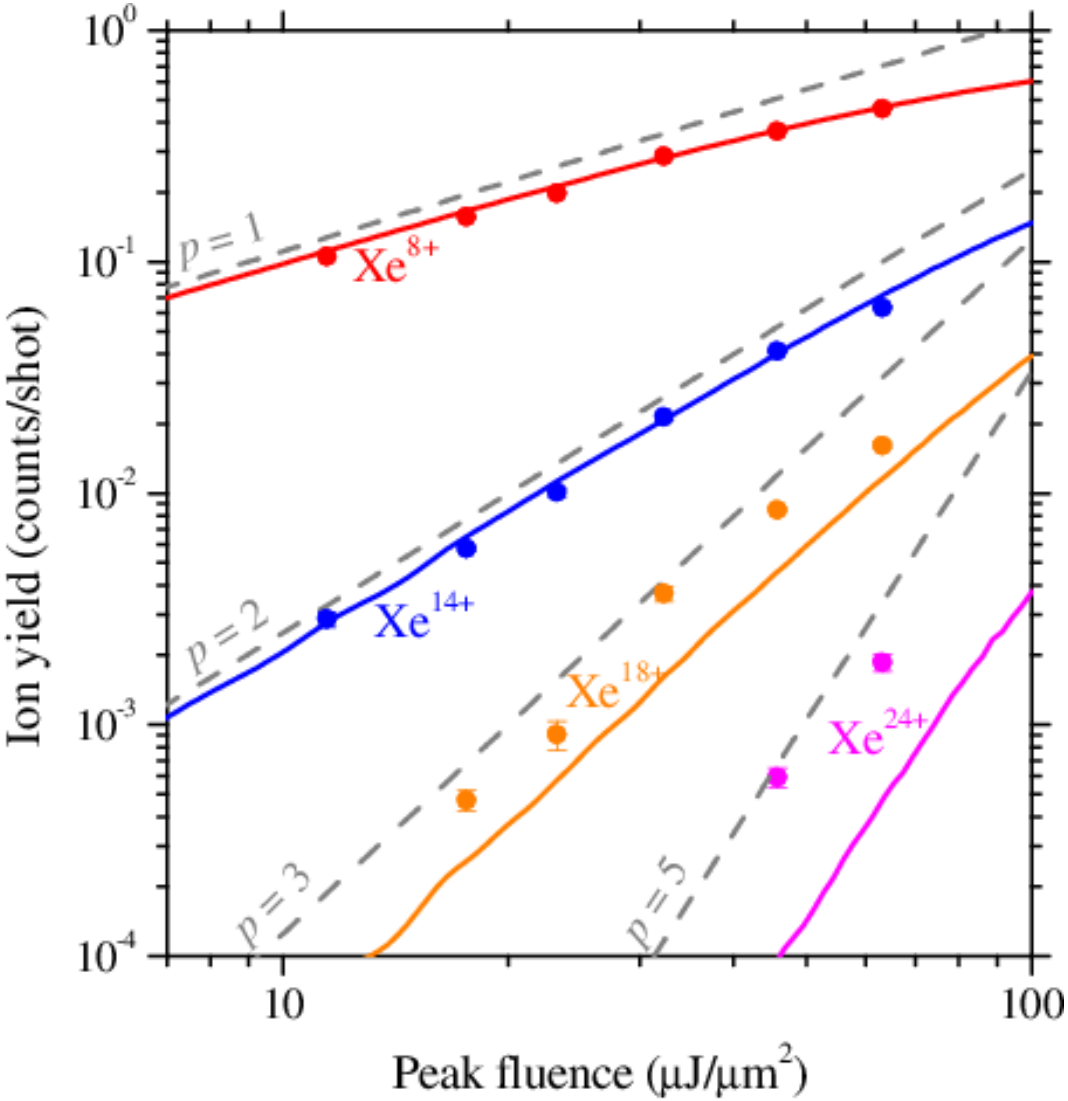

With help of ab initio calculations, we find that the observed high charge states ($n \geq 24$) are produced via five-photon absorption, evidencing the occurrence of multiphoton absorption involving deep inner shells.

Xenon ion charge distributions (exper. vs theory)

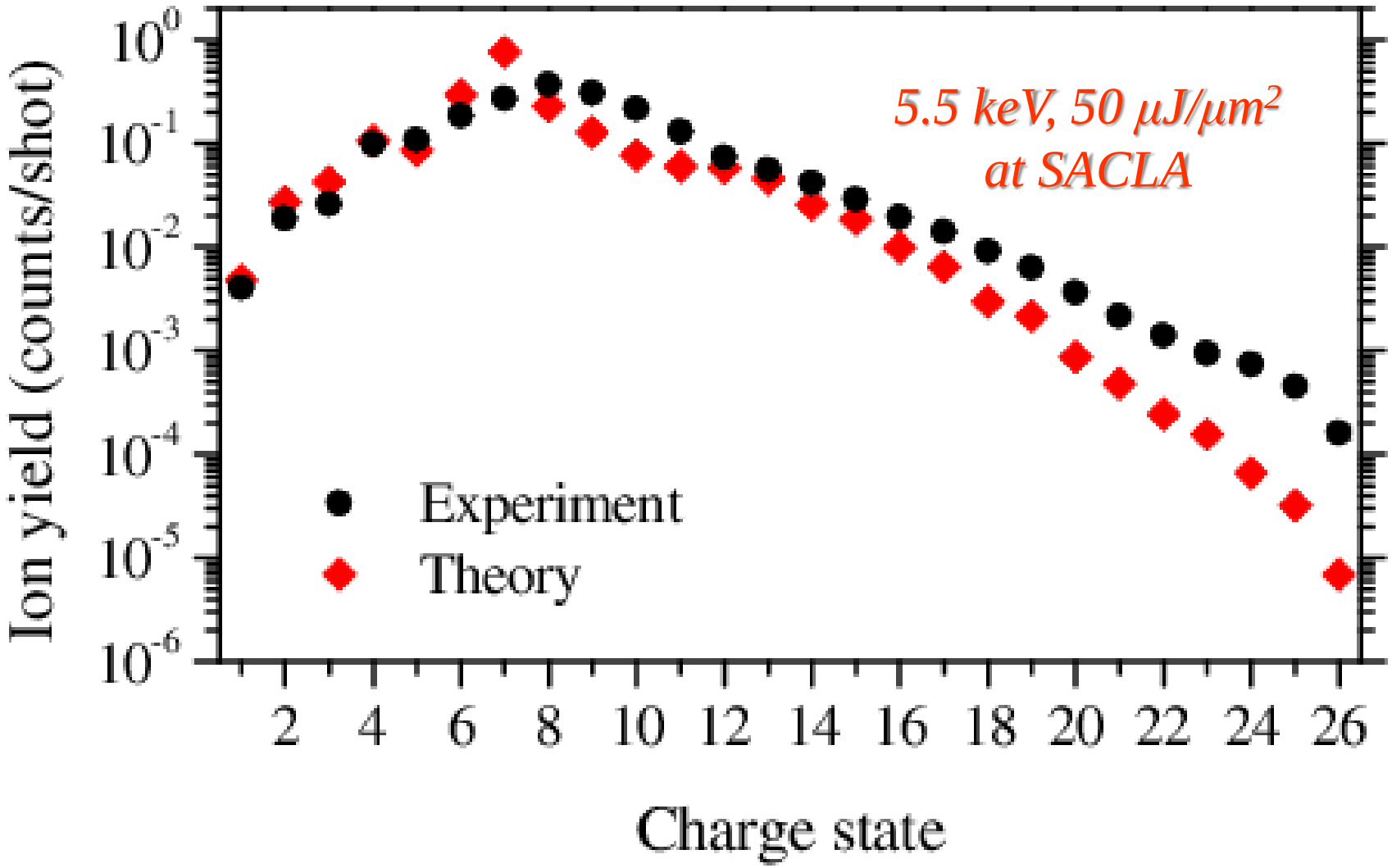

A newly developed theoretical model shows good agreement with the experiment!

An exemplary pathway of multiphoton multiple ionization

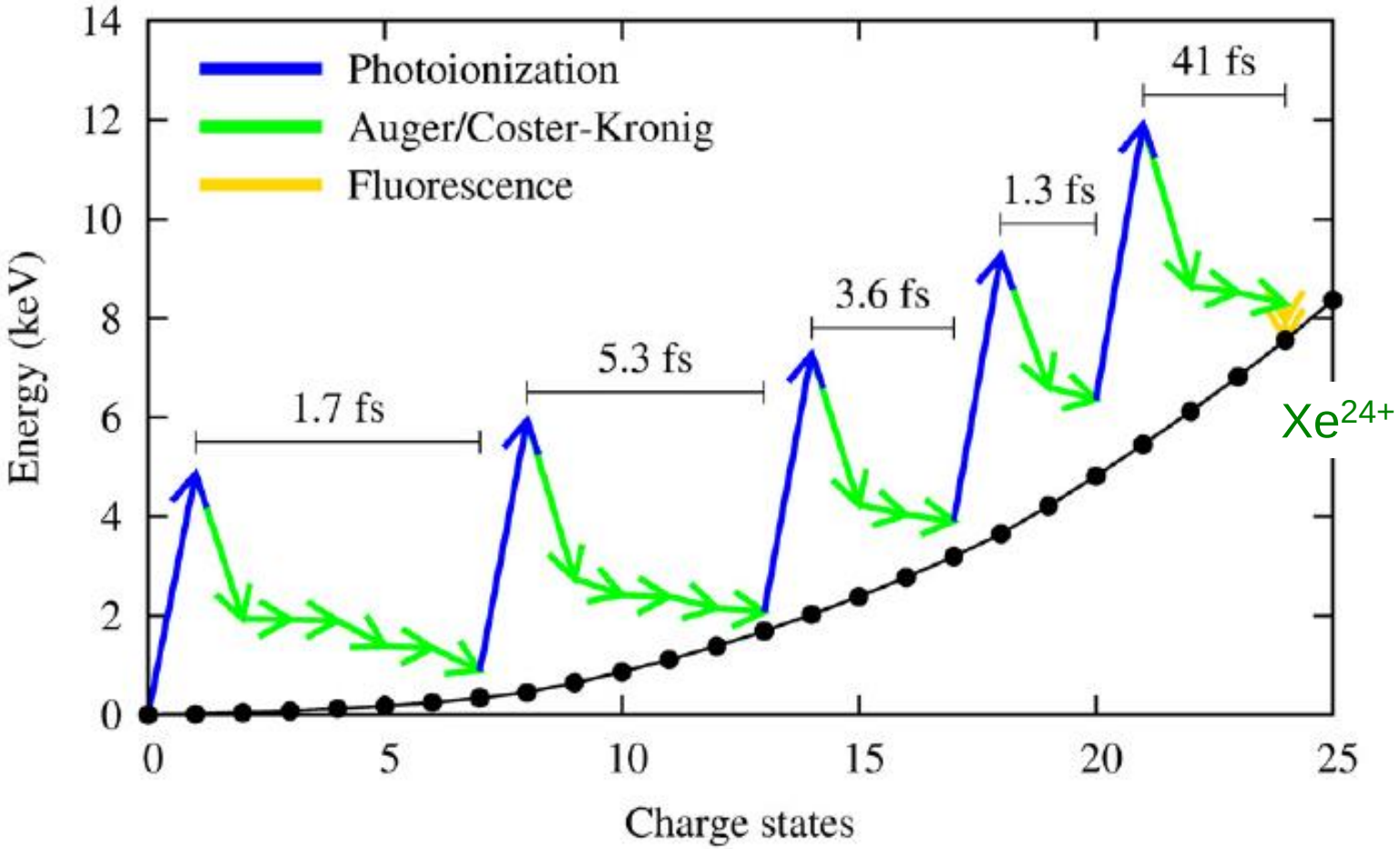

A newly developed theoretical model elucidates the complex pathways of sequential electronic decay cascades accessible in heavy atoms, *revealing that L shell ionization and sequential electronic decay cycles are repeated multiple times within the XFEL pulse duration of ~10 fs.*

*Fukuzawa, Son et al. PRL **110**, 173005 (2013)*

Relevance to other fields: Radiation damage

Radio-sensitizer

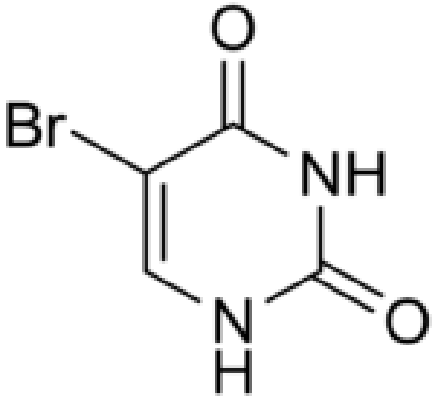

5Br-Uracil

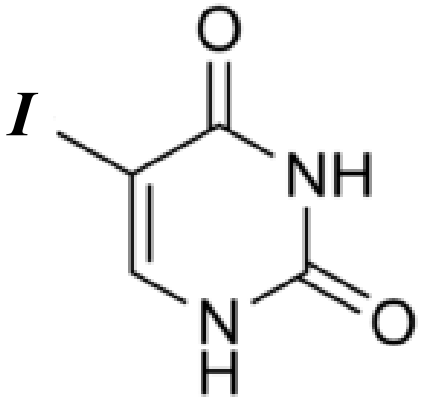

5I-Uracil

Anomalous X-ray scattering

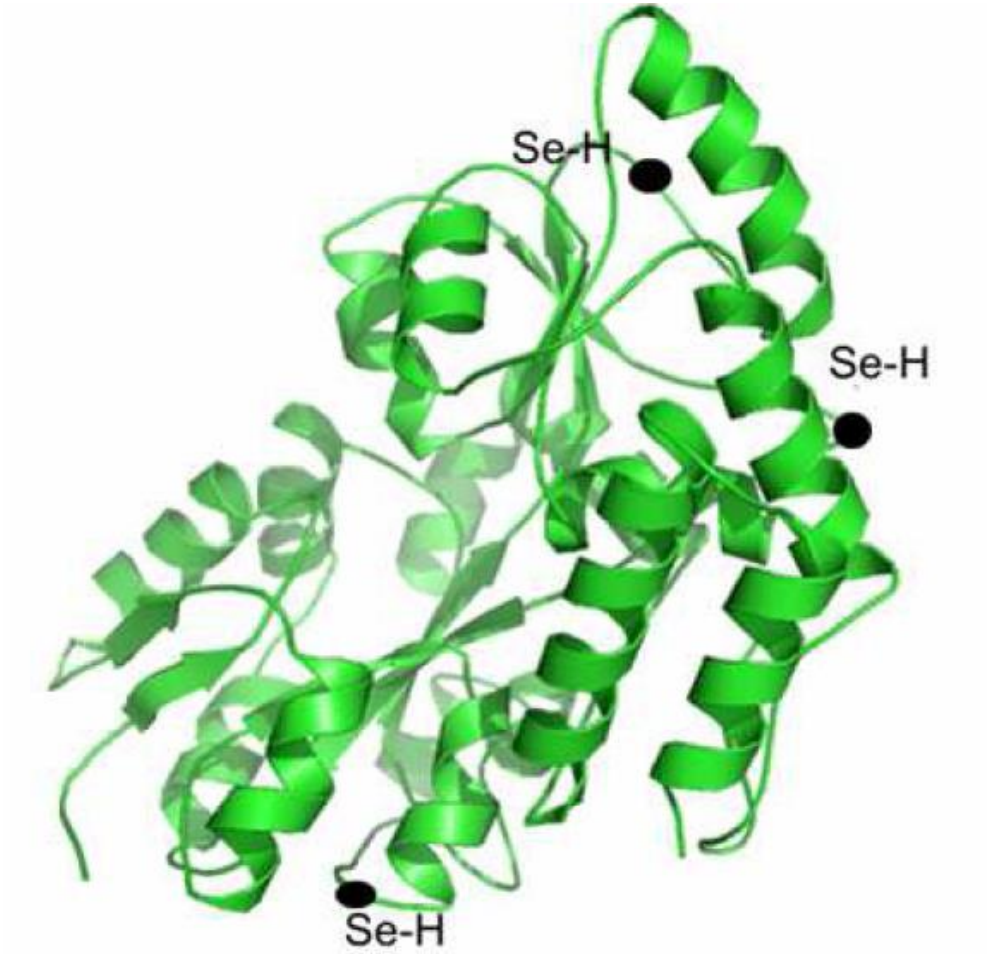

Multiwavelength anomalous diffraction at high X-ray intensity

S.-K. Son, H. N. Chapman, and R. Santra, Phys. Rev. Lett. 107, 218102 (2011).

The end

Thank you very much for your attention!